Effect of Suboptimal Temperature on Endogenous Antigen Presentation in Two Fish Species, *Oncorhynchus mykiss* and *Sander vitreus*

by

Quinn Harrison Abram

A thesis

presented to the University of Waterloo

in fulfillment of the

thesis requirements for the degree of

Master of Science

in

Biology

Waterloo, Ontario, Canada, 2019

Author's Declaration

The thesis consists of material all of which I authored or co-authored: see Statement of Contributions included in the thesis. This is a true copy of the thesis, including any required final revisions, as accepted by my examiners.

I understand that my thesis may be made electronically available to the public.

Statement of Contributions

Chapter 2 - C. Soulliere originally cloned and produced the recombinant rainbow trout IFN1. T. Rodriguez-Ramos developed and optimized the quantitative ELISA (qELISA) for rainbow trout IFN1 and assisted with the performance of the qELISA for the IFN1 secretion samples.

Chapter 3 - B.A. Katzenback and C.J. Kellendonk designed and validated the qRT-PCR primers used in this study.

Abstract

Winter months and the increasing frequency and magnitude of extreme low temperature events, occurring as a result of global climate change, subject teleosts such as rainbow trout and walleye to suboptimal temperatures, conditions that have been shown to generally impair their immune responses. Viruses provide an example of one type of pathogen that could take advantage of impairments in the host immune response at low temperatures. Most viruses produce double-stranded RNA (dsRNA) at some point in their viral life cycle, and recognition of the virally produced dsRNA results in the production of type I interferons (IFNs), cytokines that mediate the cellular antiviral response. Type I IFN signalling in mammals is involved in the regulation of the endogenous antigen presentation pathway (EAPP), an important antiviral pathway that participates in limiting the spread of infection. However, the relationship between IFN1 and the EAPP has not been fully studied in fish. Previous studies examining the effect of low temperatures on the EAPP have found varied results across teleost species, and have not examined the potential role of IFN1 in any impairment in EAPP function seen at such temperatures. In this thesis, the effect of suboptimal temperatures on the constitutive and inducible regulation of EAPP transcript levels and the role of IFN1 in regulating the EAPP were examined using the rainbow trout hypodermal fibroblast cell line RTHDF and the walleye skin fibroblast cell line WESk-11 as *in vitro* models, allowing for a comparison between two teleost species that diverged 206 million years ago. In contrast to previous work in the WESk-11 cell line, suboptimal temperatures did not impair constitutive regulation of the EAPP in the RTHDF cell line. Interferon-stimulated response elements (ISREs) were identified in the promoter regions of the pathway-specific members of the EAPP (*b2m*, *mhIa*, and *tapasin*) in rainbow trout for the

first time, suggesting that IFN1 is involved in the regulation of these genes in rainbow trout as it is in mammals. As such, the observed delays in IFN1 transcript up-regulation and secretion at suboptimal temperatures following stimulation with polyinosinic-polycytidylic acid (poly(I:C)), a synthetic dsRNA molecule, in the RTHDF cell line may provide a partial explanation for the impaired inducible EAPP transcript levels that were seen at these temperatures. Inducible regulation of EAPP transcript levels was also impaired in the WESk-11 cells following stimulation with poly(I:C), and in both the rainbow trout and walleye cell lines following infection with viral haemorrhagic septicaemia virus (VHSV) IVb, albeit to a greater degree in the walleye cells in both cases. Finally, VHSV IVb replication was greater at 20°C in the WESk-11 cells than the RTHDF cells, indicating that the WESk-11 cell line is more permissive to the virus, although some replication was observed in both cell lines at 4°C. These results suggest that the impairment of EAPP regulation at the suboptimal temperature in the rainbow trout and walleye cells may be indicative of a compromised cellular antiviral response that could allow for longer-lasting viral infections. Impaired antiviral responses in teleosts at suboptimal temperature could complicate the stocking of fish for recreational fisheries and conservation purposes, and contribute to diseases loss in the aquaculture industry, issues that could be exacerbated in the face of global climate change.

Acknowledgements

Firstly, I would like to thank my co-supervisors Dr. Brian Dixon and Dr. Barb Katzenback for their support and mentorship. Brian, you first took a chance on me as an eager honours thesis student with no lab experience, and I am grateful for the chance you gave me to enter and work in your lab, and the many opportunities, both in and outside of science, that you have given me since then. Your passion for fish and immunology is infectious (even if my immediate future path takes me in somewhat different directions), and your support and guidance have been instrumental in helping me navigate the treacherous cold waters of graduate school. Barb, I also owe you my gratitude in pushing me to become a better and more rigorous scientist as you accepted me into your lab as one of your first graduate students. Your always available feedback and advice has helped me become a stronger researcher and communicator, always pushing me to be and become better. Also, I thank you for all your support in helping me get through the "dark times" (as any graduate student knows) of my thesis when everything I touched seemed to fall apart and I was not sure where to turn next. I wouldn't be here today without the encouragement and support from both of you (and the very gracious editing of thesis chapters as the deadline to defend snuck up closer and closer) and am forever grateful for being lucky enough to have you as co-supervisors.

Secondly, I would like to thank my committee members, Dr. Stephanie DeWitte-Orr and Dr. Paul Craig for the invaluable guidance and input they have given me throughout this process. Stephanie, thank you for pushing me to expand my project to explore more of the interactions between dsRNA (even if it was poly(I:C)), type I interferons, and endogenous antigen presentation, an addition that has added a delightful piece to the puzzle of my thesis,

and helped spark a greater interest in viruses and their interactions with the host immune system. Paul, thank you for your valuable feedback and questions regarding my experimental design and fish in general. I thoroughly enjoyed your course and the discussions that arose in it regarding animal physiology (and the Thursday morning "snacks"). Also, I am grateful for your support outside of research in supporting our biology graduate social and athletic events and all the opportunities to meet and have free lunches (food is always appreciated in graduate school) with seminar speakers.

I would also like to thank a number of individuals who have directly assisted with aspects of this thesis: Dr. Niels Bols for providing the cell lines used, Dr. Tania-Rodriguez-Ramos for her assistance with the IFN1 qELISA, Dr. Nathan Vo and Dr. John Pham for their assistance and advice regarding *in vitro* studies and VHSV IVb infection, Dr. Lindy Whitehouse for her guidance regarding the statistical analysis of qRT-PCR data, and Dr. Andrew Doxey for his help with identifying promoter elements.

Thank you to all the previous members of the Dixon (Aaron, Tania, Shawna, George, Mark, Lindy, Sarah, Nathan) and Katzenback (Max, JV, Nat) labs for your support and friendship over the past three years. Also, thanks to the many other friends I've made along the way who have made this such an enjoyable ride (Éric, Mitch, Heather, Ben, Mike, Matt, Emilie, Rebecca, Ashley, Mark, Pat, Karsten, Therese, Nilanth, Ivan, Nathan, Nikhil, Monica to name a few but there are many more …) and such an amazing department to work in everyday. Thank you to my parents Angela and Jonathon for their continuing love and support, and my brother Brett for tolerating me. Lastly, thank you to Tina for being with me every step of the way, I couldn't have done this without your support.

Dedication

To the memory of Daniel Terpstra, one of the strongest and most inspirational people I've known.

Table of Contents

List of Figures

List of Tables

List of Abbreviations

ACBA	Arctic charr bulbous arteriosus cell line
Ag	antigen
ATF-2	activating transcription factor 2
β2m	beta-2-microglobulin
CD8	cluster of differentiation 8
cDNA	complementary deoxyribonucleic acid
CNX	calnexin
CRT	calreticulin
Dir	direction of primer
DNA	deoxyribonucleic acid
DNase I	deoxyribonucleic nuclease
dNTP	deoxyribonucleotide triphosphate
dsRNA	double-stranded ribonucleic acid
EAPP	endogenous antigen presentation pathway
ECL	enhanced chemiluminescence
EDTA	ethylenediaminetetraacetic acid
EF1a	elongation factor 1 alpha
Eff%	percent efficiency of specified primer set
EPC	epilthelioma papulosum cyprinid cell line
ER	endoplasmic reticulum
ERp57	endoplasmic reticulum resident protein 57
FBS	fetal bovine serum
GAPDH	glyceraldehyde-3-phosphate dehydrogenase
IgG	immunoglobulin G
IFN	interferon
IFNAR	interferon alpha receptor
IP5B11	mouse anti-VHSV nucleocapsid protein antibody
IRF-3	interferon regulatory factor 3
ISG	interferon-stimulated gene
ISGF-3	interferon-stimulated gene factor 3
ISRE	interferon-stimulated response element
L-15	Leibovitz’s L-15 medium
MH	major histocompatibility
mhIa	major histocompatibility class I alpha gene
MHC	major histocompatibility complex
MDA-5	melanoma differentiation-associated protein 5
MOI	multiplicity of infection
Mx	myxovirus resistance protein
N	nucleocapsid

ND	not detected
NF-κB	nuclear factor kappa-B
NP-40	nonyl phenoxypolyethoxylethanol-40
OD	optical density
PBS	phosphate buffered saline
pfu	plaque forming units
PLC	peptide-loading complex
poly(I:C)	polyinosinic:polycytidylic acid
PRR	pattern recognition receptor
PVDF	polyvinylidene fluoride
qELISA	quantitative enzyme-linked immunosorbent assay
qRT-PCR	quantitative reverse transcriptase polymerase chain reaction
RIG-I	retinoic acid-inducible gene-I
RMA-S	mouse leukemia cell line
RNA	ribonucleic acid
rRNA	ribosomal ribonucleic acid
RTG-2	rainbow trout gonad cell line
RTHDF	rainbow trout hypodermal fibroblast cell line
rtIFN1	recombinant rainbow trout IFN1
RT-PCR	reverse-transcriptase polymerase chain reaction
RTS-11	rainbow trout spleen 11 cell line
SOB	super optimal broth
SR-A	type A scavenger receptor
TAP	transporter associated with antigen processing
TBS	tris-buffered saline
TBS-T	tris-buffered saline with Tween-20
$TCID_{50}$	median tissue culture infectious dose
TFR	transferrin
TLR-3	toll-like receptor 3
TLR-22	toll-like receptor 22
TMB	3,3’,5,5’-tetramethylbenzidine
UDG	uracil-DNA glycosylase
VHSV	viral haemorrhagic septicaemia virus
WDSV	walleye dermal sarcoma virus
We-cfin11f	walleye caudal fin fibroblast cell line
WESk-11	walleye skin fibroblast cell line

Chapter 1: Literature Review and Thesis Scope

Global climate change will impact teleost fish and their immunocompetency against pathogens. Increases and decreases in environmental temperature are known to modulate the immune responses of teleosts since their internal body temperature is the same as the temperature of their environment [1-4]. While climate change will lead to global warming overall, it will also lead to increased acute exposure of teleosts to suboptimal temperatures. In addition to the increasing frequency and magnitude of extreme weather events such as cold snaps as a result of climate change, fish already experience chronic exposures to such temperatures over the winter months in northern climates such as Canada [5-8]. Aquaculture is the fastest-growing sector for food production globally, with levels of production increasing steadily over the last 30 years, while the capture fishing industry has remained relatively constant [9]. Disease is the one of the largest issues facing the aquaculture industry and is estimated to have resulted in losses totalling in the tens of billions of dollars over the past 30 years due to mortalities and decreased fillet quality, with climate change threatening to exacerbate this problem [9]. In the face of a growing human population, which is expected to reach 9.5 billion by 2050, reduced food production and food security as a result of disease in both the aquaculture and capture fishery industries poses a significant challenge, and as such, studying the effects of changing temperatures, including suboptimal temperatures, on the immunocompetency of teleost fish is important in order to try to combat this threat [9].

1.1 Important Freshwater Teleost Species in Canada

1.1.1 Rainbow Trout

Rainbow trout (*Oncorhynchus mykiss*) is a freshwater teleost species of economic and ecological importance in Canada. They are a member of the order Salmoniformes and, while native to the west coast of North America, have been introduced across the continent [10, 11]. Rainbow trout are capable of surviving between 0°C and 27°C, with a mean optimum growth temperature of 15.7°C, and a final temperature preferendum, the temperature of choice when the fish is exposed to an infinite range of temperatures, of 15.5°C [12, 13]. The range of average seasonal water temperatures at one rainbow trout fish farm in British Columbia was determined to be 5°C to 17°C, and is 2°C to 20°C in the Great Lakes [7, 14]. Along with brook trout, rainbow trout are one of the most common freshwater fish farmed in Canada, with a yearly production value of 41.2 million dollars as of 2010 [15, 16]. Furthermore, the production of rainbow trout increased 12% in 2015 in Ontario, where most farming is done along the Great Lakes, with a farm gate value of 26.8 million dollars [16, 17]. The species is also widely stocked in Ontario waterways ranging from the Great Lakes and their tributaries to inlands lakes and ponds [11]. Compared to other salmonids in the same ecosystem, rainbow trout tend to be superior competitors, acting to suppress population levels of other salmonids [11]. Conservation of rainbow trout in Canada is important due to their role in the aquaculture industry and in ecosystem stability.

1.1.2 Walleye

Another teleost species of importance in Canada is walleye (*Sander vitreus*). They are native to all of North America east of the Rocky Mountains, with the exception of Atlantic Canada and Florida, and are members of the Order Perciformes and the Supraorder

Percomorpharia [10, 18]. Walleye prefer warmer environmental temperatures than rainbow trout, as they have a mean optimum growth temperature and a final temperature preferendum of 22.1°C and 22.5°C, respectively, and are able to survive between 0°C and 34°C [12, 18]. In the Great Lakes region of Ontario, walleye experience temperatures between 0°C and 25°C, with average seasonal temperatures of approximately 20°C and 2°C over the summer and winter months, respectively [7, 19]. As of 2010, walleye was the most-caught recreational fish species in Canada, accounting for 23% of the total catch that year in an industry estimated to be worth approximately 8.3 billion dollars [20]. Additionally, the Ontario Great Lakes region was home to the world's largest freshwater commercial fishery in 2014, valued at 305 million dollars, and the species contributing the most value to this industry was walleye [21]. Every year, over 1 billion walleye are stocked in lakes across North America for the purposes of sport fishing and conservation, and this sector is conservatively estimated to be worth 1.5 million dollars annually in farm-gate revenues in Ontario alone [17, 18]. From an ecological perspective, walleye is a top predator in many ecosystems, making them able to exert considerable influence on lower trophic levels [18, 22]. Resultantly, fluctuations in walleye populations can have a large impact on prey fish populations in the same ecosystem [18]. Along with rainbow trout, failure to conserve walleye populations would have detrimental impacts on the Canadian commercial and recreational fishing industries and on the stability of lake ecosystems.

1.2 Suboptimal Temperatures and Teleosts

One potential issue facing teleost species is acute and prolonged exposure to suboptimal temperatures, which for the purposes of this thesis are defined as temperatures below the thermal preferendum of the fish *in vivo* and below the optimal growth temperature

of the cell line *in vitro*. Acute exposure to low temperatures will increase as a result of global climate change, since even though there will be warming on a global scale, there will also be an increase in the incidence and magnitude of extreme temperature events such as cold snaps due to growing climate variability [5, 6, 8]. An example of such an event occurred in the Gulf of Mexico in 2010, where over a two-week period, air and water temperatures dropped 12°C and 6°C respectively, resulting in widespread mortality of fish and other marine species [23]. Additionally, teleosts face prolonged exposure to suboptimal temperatures over the winter months, particularly in Canada, where the average winter water temperature is often below 5°C [7, 14, 19]. As a result, rainbow trout and walleye in Canada live over winter at temperatures that are on average 10°C and 17°C below their thermal preferendum, respectively [12]. Combined, these acute and prolonged exposures to suboptimal temperatures could prove problematic for teleost species such as rainbow trout and walleye.

The reason exposure to suboptimal temperatures poses a problem for teleosts is due to their poikilothermic nature. As poikliotherms, fish are unable to internally regulate their body temperature, which is therefore the same as their external environment, and as a result, they have zones of thermal tolerance with upper and lower limits for survival, as well as preferential temperatures [3, 24]. Consequently, the water temperature of their external environment influences their immune system and, in general, suboptimal temperatures have been shown to delay and/or suppress immune responses in teleosts, both at the innate and adaptive levels [1-3]. As a result, when fish are exposed to suboptimal temperatures, their fitness may be reduced which can lead to greater risk of disease [25].

1.3 Suboptimal Temperatures and Disease

While suboptimal temperatures can negatively impact the ability of the teleost immune system to ward off pathogens, they also impact the ability of the pathogen to cause disease. The right combination of host, pathogen, and environmental conditions must be present for disease to occur (**Figure 1.1**), and as a result, temperature influences both host susceptibility and pathogen virulence [25, 26]. As with hosts, pathogens have their own ranges of thermal tolerances and preferences, with temperature able to influence a number of factors, including, but not limited to, the rate of replication of the pathogen, environmental persistence, rates of transmission, and overall virulence [25]. Furthermore, the impact of temperature on these factors differs by pathogen, with some pathogens better equipped to cause infection at low temperatures than others [25]. Two examples of viruses that illustrate this link between environmental temperature and disease are walleye dermal sarcoma virus (WDSV; *Section 1.3.1*) and viral haemorrhagic septicaemia virus (VHSV; *Section 1.3.2*).

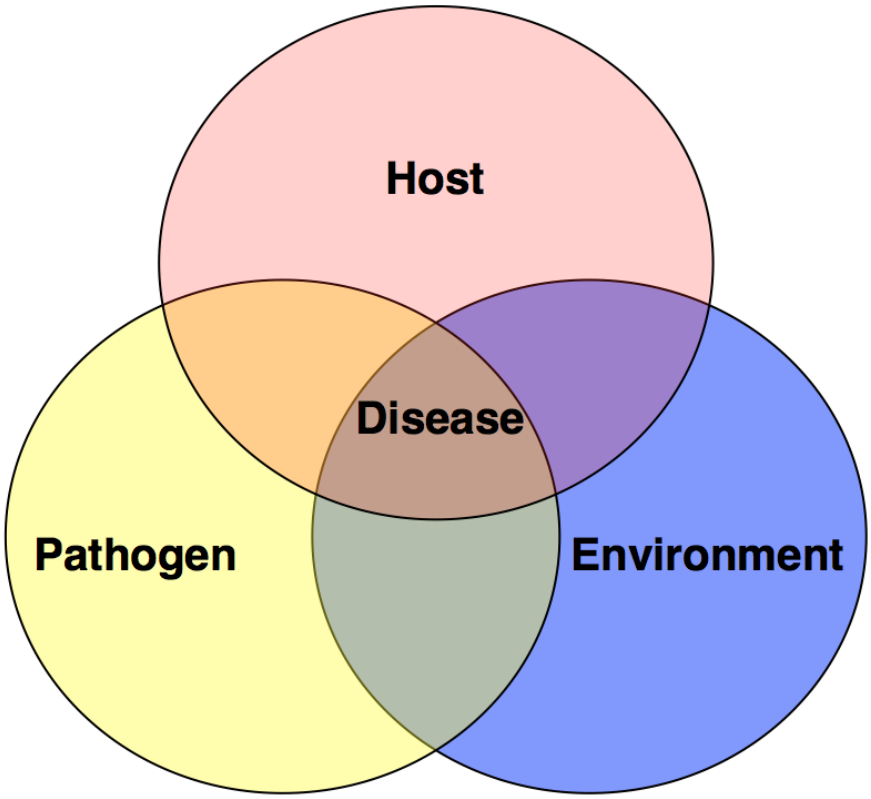

Figure 1.1 Venn diagram showing interaction of factors that contribute to occurrence of disease. The right environmental conditions for a pathogen to infect a susceptible host must be present in order for disease to occur.

1.3.1 Walleye Dermal Sarcoma Virus (WDSV)

WDSV, the causative agent of walleye dermal sarcoma, provides a strong example of how the influence of environmental temperature on the immune system impacts the incidence of disease in teleosts. WDSV is a positive-sense single-stranded RNA retrovirus and causes randomly distributed tumours on the skin of infected walleye, which are composed of interwoven bundles of fibroblast cells [27, 28]. Dermal sarcomas have been reported on walleye across Canada and the northern United States, with prevalence ranging between 20% and 30% in the Great Lakes basin [28-30]. The tumours have economic consequences for fisheries and vendors selling the fish, as the unappetizing appearance of the lesions can

negatively impact fish value [31]. Development and regression of the tumours follows a seasonal cycle, with tumours regressing in the spring as environmental temperatures rise, coinciding with the walleye-spawning season [27, 31, 32]. During this period, horizontal transmission is believed to occur as viral particles are released during tumour regression, either through direct contact of walleye during spawning or through exposure to water containing infectious virus [27, 33]. Following infection, a very low prevalence of lesions is observed over the summer months, with tumours beginning to appear more commonly in the late fall, as water temperatures decrease, implying that the retrovirus may be able to integrate into the genome and remain latent until water temperatures decrease sufficiently [27, 33, 34]. These tumours persist over the winter, before regressing again in the spring to begin a new transmission cycle [27, 31-33]. Contributing to the idea that environmental temperature plays a role in the observation of the tumours, studies have shown that tumour development is greatest at temperatures below 10°C, while temperatures above 15°C cause the highest amount of tumour regression [29, 32]. Furthermore, resolution of tumours leads to lifelong resistance against subsequent exposures to the disease, leading to the hypothesis that impairment of the immune system by exposure to suboptimal temperatures is a factor in the seasonal cycle of tumour development [1, 27, 31].

1.3.2 Viral Haemorrhagic Septicaemia Virus (VHSV)

Another example of a virus that is impacted by environmental temperatures is VHSV, a negative-sense single stranded RNA virus, member of the Rhabdoviridae family, and the causative agent of viral haemorrhagic septicaemia [35]. The disease affects numerous Northern Hemisphere freshwater and marine fish species, including rainbow trout and walleye, and causes symptoms including haemorrhagic septicaemia, pale gills, swollen

abdominal regions, lethargic behaviour, and bulging, sometimes bleeding, eyes [13, 36]. VHSV entry is believed to occur through either the gill or skin epithelium, based on previous studies that have shown replication of the virus in cells from these tissues [37, 38]. The life cycle of VHSV is believed to be similar to that of other members of the *Rhabdoviridae*, which begins with the virus entering the host cell via receptor-mediated endocytosis [35]. Then, following fusion of the viral envelope and host endosomal membranes, the viral nucleocapsid is released into the cytosol, where viral genes are sequentially transcribed, starting with the N (nucleocapsid) gene [35]. Finally, new virions are packaged and then bud off from the host cell membrane [35]. VHSV is known to have five distinct genotypes that differ in geographic range and virulence [39]. Genotype IVb, isolated from the Great Lakes, does not cause significant mortality in either rainbow trout or walleye at moderate doses, defined as less than or equal to 10^6 PFU/mL, although both fish species can be readily infected with the virus, and may participate in viral transmission in the wild [13, 36, 39, 40]. However, VHSV IVb has caused large-scale mortality events in other freshwater fish species, such as the freshwater drum and the round goby, with most instances of infection occurring between 4°C and 14°C [41, 42]. Additionally, the virus is able to remain viable in 4°C freshwater for close to 40 days outside the host, which is almost twice as long than at 10°C or 15°C, extending the window in which the virus can infect a new host [43]. In cell culture, propagation of VHSV IVb is optimal at 14°C, with successful infections able to occur as low as 1°C in some cases [44]. As with WDSV, environmental temperature seems to play a role in the interaction of VHSV and its host, but the virus has also been shown to directly modulate the host immune system, suppressing activation of important host antiviral pathways such as type I interferon (IFN) induction [45, 46].

1.4 dsRNA-Induced Type I IFNs

Double-stranded RNA (dsRNA) is known to be a potent inducer of type I IFNs in mammals, the cytokine mediators of the antiviral response [47]. At some point in the viral life cycle, most mammalian viruses produce dsRNA as either a replication intermediate, a product of convergent transcription, or as part of the genome itself [48]. dsRNA molecules greater than 40 bp act as a pathogen-associated molecular pattern (PAMP) that can be recognized by pattern recognition receptors (PRRs) involved in innate immunity, with endosomal and cytoplasmic ssRNA and DNA also recognized as common viral PAMPs [49-52]. Extracellular dsRNA is internalized by type A scavenger receptors (SR-As) via clathrin-mediated endocytosis, where it can be sensed by TLR3 in endosomes, or, following escape into the cytosol, by cytosolic PRRs such as RIG-I and MDA5 that also sense intracellular dsRNA [53-57]. Sensing of dsRNA leads to the activation of interferon regulatory factor (IRF) 3 and 7 transcription factors that induce type I IFNs gene expressions as well as activation of nuclear factor kappa-light-chain enhancer of activated B-cells (NF-κB), and c-Jun and ATF-2, which combine to form AP-1, transcription factors involved in the regulation of pro-inflammatory immune responses. (**Figure 1.2**) [47, 58]. Secreted type I IFNs act in a paracrine or autocrine fashion through recognition by the IFN α receptor (IFNAR), resulting in the translocation of the transcription factor interferon-stimulated gene factor-3 (ISGF-3), which is a complex of STAT1, STAT2, and IRF9, into the nucleus and the activation of NF-κB (**Figure 1.3**) [47, 59-61]. ISGF-3 binds to the interferon-stimulated response element (ISRE; consensus sequence: 5’ GAAA(A)NNGAAA 3’) in promoter regions, resulting in the up-regulation of genes known as interferon stimulated genes (ISGs), including all the members of the mammalian endogenous antigen presentation pathway (EAPP) [61, 62].

Through the action of these ISGs, a cellular antiviral state is created in host cells and impairs viral replication by interfering with host and viral processes, such as transcription and translation, and the promotion of a pro-apoptotic state [61, 63].

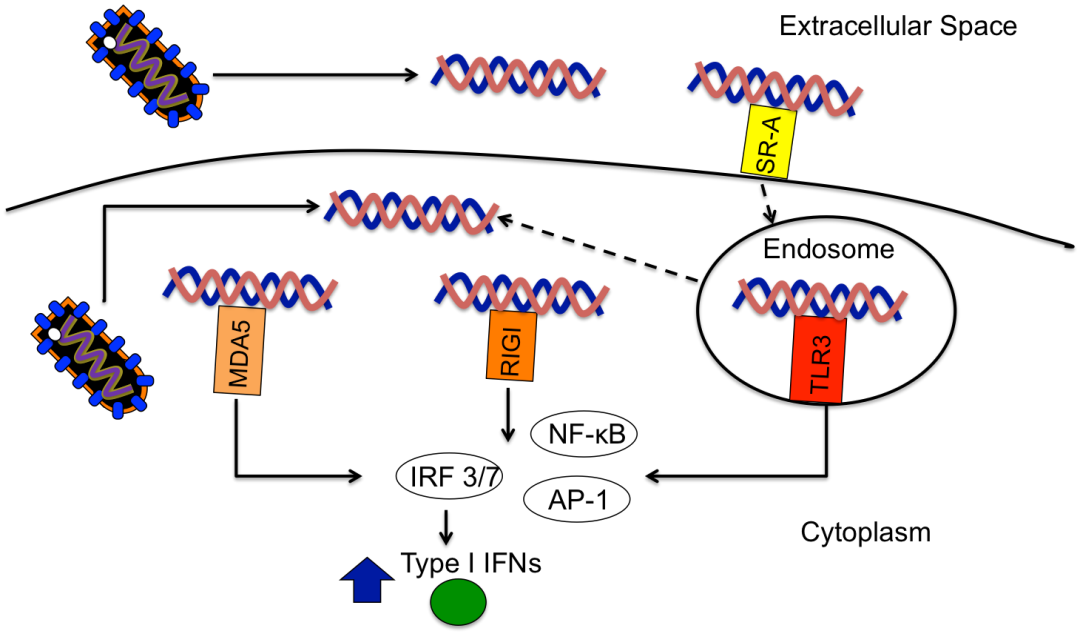

Figure 1.2 Induction of type I IFNs through sensing of dsRNA. dsRNA produced by viruses extracellularly or intracellularly can be sensed by host cells. Extracellular dsRNA is internalized by SR-As via clathrin-mediated endocytosis, where it can be sensed by TLR3 in endosomes. This dsRNA can also escape the endosome into the cytosol, where cytosolic PRRs such as MDA5 and RIG-I sense dsRNA, as well as intracellularly produced dsRNA. Sensing of dsRNA results in the activation of NF-κB and AP-1, transcription factors involved in the regulation of immune responses, as well as the activation of interferon-regulatory factors (IRF) 3 and 7 which induce expression of type I interferons (IFNs; green circle in figure), the cytokine mediators of the antiviral response.

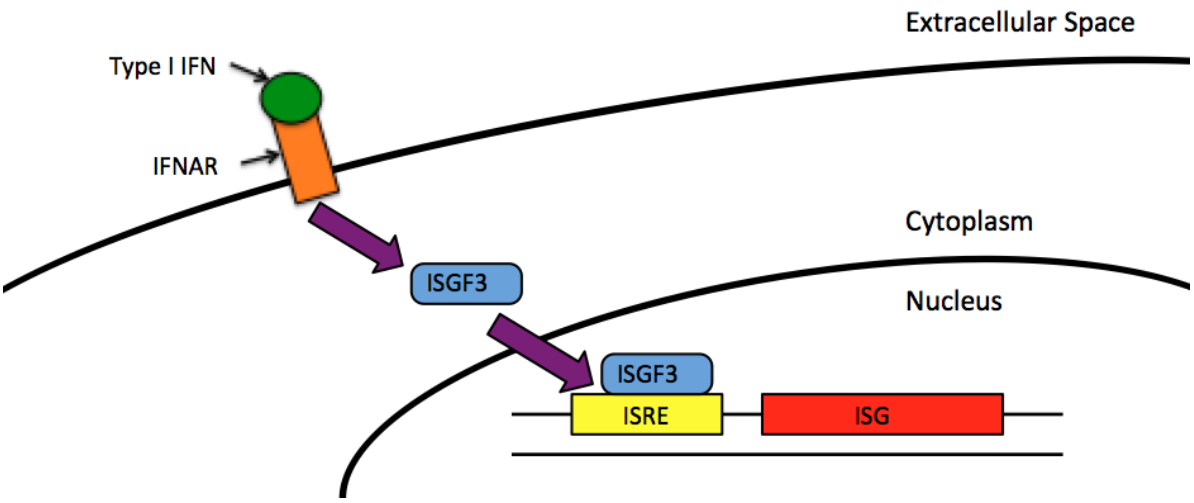

Figure 1.3 Up-regulation of ISGs following type I IFN receptor signalling in mammals. Secreted type I interferons (IFNs) are bound by their receptor (IFNAR), initiating a signalling cascade that results in the transcription factor interferon-stimulated gene factor-3 (ISGF3), typically a complex of STAT1, STAT2, and IRF9, translocating to the nucleus. ISGF3 can then bind to interferon-stimulated response elements (ISREs) in the promoters of interferon-stimulated genes (ISGs), resulting in an up-regulation in gene expression.

The induction of type I IFNs though sensing of dsRNA in teleosts is relatively similar to that of mammals. Teleosts have SR-As that contain similar structural domains to their mammalian counterparts and seem to be involved in internalization of dsRNA [64-66]. As in mammals, teleost TLR3 is an endosomal sensor of dsRNA, but there is also a teleost-specific TLR, TLR22, that is surface-expressed and is involved in dsRNA recognition [67-70]. Additionally, while cytosolic dsRNA-sensing PRRs such as RIG-I and MDA-5 have been identified in some teleosts, there may be some exceptions in certain species, such as RIG-I, which has not yet been identified in rainbow trout [68, 71]. Following sensing, the downstream signalling resulting in production of type I IFNs and activation of NF-κB also seems to be relatively well conserved in teleosts [68, 69, 72]. However, there are two groups of type I IFNs in teleosts, based on the presence of either two (group I) or four (group II) cysteine residues in the mature peptide, with up to six subgroups (a-f) depending on the

species [73]. Three group I type I IFNs (IFN1, IFN2, and IFN5) and two group II members (IFN3, and IFN4) have been identified in rainbow trout, while type I IFNs have yet to be identified in walleye [74-76]. Interferons in all of the subgroups can be induced during antiviral responses, with rainbow trout IFN1, a group I subgroup a interferon, known to be up-regulated following immunostimulation with polyinosinic-polycytidylic acid (poly I:C), a synthetic dsRNA molecule [73, 77].The ISGs found in teleosts to date are relatively similar to those in mammals, and seem to play similar roles in the establishment of the antiviral response [68, 78, 79]. For example, while the exact functions of the three identified Mx proteins (Mx1, Mx2, and Mx3) have yet to be identified in rainbow trout, Mx proteins from the barramundi have been shown to interfere with RNA-dependent RNA polymerase activity to inhibit viral transcription as has been seen in some cases with mammals [80-83]. Overall, it appears that teleosts are also able to sense dsRNA and induce ISGs via the production and secretion of type I IFNs to create a cellular antiviral state.

1.5 EAPP

One important adaptive antiviral pathway is the endogenous antigen presentation pathway (EAPP), the focus of this thesis. The EAPP (**Figure 1.4**) in mammals involves the presentation of peptide fragments derived from intracellular sources in the context of major histocompatibility complex (MHC) class I receptors to cytotoxic CD8+ T cells. Peptides are generated in the cytosol by the proteasome and transported into the endoplasmic reticulum (ER) by the transporter associated with antigen processing (TAP), where aminopeptidases trim the peptide to 8-10 amino acids, which is the length required for MHC class I association [84]. Meanwhile, the early folding of the MHC class I α heavy chain along the ER lumen is promoted by calnexin, until the β2-microglobulin (β2m) subunit of the MHC

class I heterodimer can be bound. At this point, calnexin is released, and the complex enters the peptide-loading complex (PLC), which is composed of ERp57, tapasin, calreticulin, and TAP [84-86]. Tapasin is an EAPP-specific chaperone and facilitates the loading of peptides from TAP into the peptide binding groove of the MHC class I receptor [86]. Upon binding of a high-affinity peptide, the rest of the PLC is released, and the MHC class I-peptide complex is trafficked to the cell surface, where it can be presented to cytotoxic T cells [84-86]. When the T cell receptor of a cytotoxic T cell recognizes a specific peptide presented in the context of MHC class I, the T cell is activated, causing it to induce apoptosis in the presenting cell to attempt to stop the spread of infection [87].

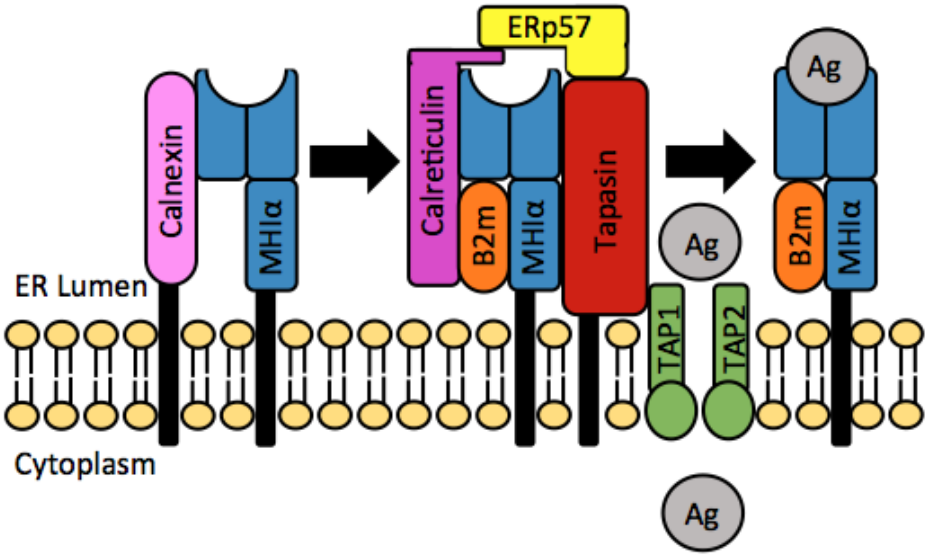

Figure 1.4 Endogenous antigen presentation pathway. Along the ER lumen, folding of the nascent MH class I α heavy chain is promoted by calnexin. When the β2m subunit is bound, calnexin is released, and replaced with calreticulin, ERp57, and tapasin, which allows for association of the receptor-chaperone complex with TAP, forming the peptide-loading complex (PLC). Peptides generated from intracellular sources by the proteasome are transported by TAP from the cytosol into the ER lumen, where tapasin facilitates loading of the peptides into the peptide-binding groove of the MH class I receptor. Once a high-affinity peptide has been bound, the rest of the PLC is released, and the MHC class I-peptide complex is be trafficked to the cell surface to present the bound peptide to cytotoxic T cells.

As with the induction of type I IFNs following recognition of dsRNA, the EAPP of teleosts appears to be relatively similar to that of mammals with some exceptions. One major difference is that teleosts are the only vertebrate group in which MHC class I and II genes are not located in a single genetic complex, and as such, are referred to as major histocompatibility (MH) genes [88]. Additionally, there are two classical MH class I α genes in rainbow trout (UAA and UBA), and at least three or four in walleye, compared to three in humans [89, 90]. Furthermore, while the coding sequences of MH class I α, β2m, tapasin, ERp57, calreticulin, and calnexin have been identified in both rainbow trout and walleye, there are multiple paralogs for some of these genes, with rainbow trout possessing two versions of calnexin and walleye having two calreticulin genes [89, 91-98]. The role of tapasin however appears to be well conserved between teleosts and mammals, as the protein has been shown to interact with MH class I α, ERp57, and TAP in rainbow trout [95]. All of the members of the EAPP are known to be ISGs in mammals, but this has only been studied and confirmed to be true for MH class I α in one teleost, the grass carp [62, 99]. However, protein levels of β2m and tapasin, in addition to MH class I α, were up-regulated following infection of RTS-11, a rainbow trout macrophage/monocyte-like cell line, with VHSV suggesting that these members of the EAPP may also be ISGs [100].

1.6 EAPP and Temperature

In both mammals and teleosts, evidence suggests that suboptimal temperatures negatively regulate EAPP function. At 26°C, a suboptimal temperature for the murine lymphoma RMA-S cell line, MHC class I-β2m complexes can be trafficked to the cell surface, but they do not contain bound peptides, and therefore cannot present antigens to

cytotoxic T cells [101]. Carp provided the first evidence of a similar phenomenon in teleosts, where cell surface MH class I receptors were completely abolished at 6°C, due to a decrease in β2m expression [102]. Furthermore, expression of β2m, MH class I, and tapasin were down-regulated in walleye skin fibroblast cells after 5 d at 4°C [94]. Conversely, in Atlantic salmon and rainbow trout, more cold-adapted fish species, β2m was still constitutively produced and trafficked to the cell surface with MH class I at 4°C [103]. In the rainbow trout spleen macrophage/monocyte-like cell line RTS-11 however, inducible protein production of β2m, MH class I, and tapasin was impaired at 2°C relative to 14°C following infection with VHSV, suggesting that suboptimal temperatures may affect constitutive and inducible expression of EAPP members differently, and in a species-dependent manner [100].

1.7 Thesis Structure

Temperature plays an important role in the host-pathogen relationship, particularly for poikilothermic species such as rainbow trout and walleye. Current research tends to focus on the effects of temperatures above thermal optimums due to the impacts of global warming, but fish species still regularly experience suboptimal temperatures, particularly in Canada. Research consistently shows that these low temperatures cause delays and/or decreases in the function of most immune pathways in teleosts but attempts to discern the effect on the EAPP have been inconsistent between species. Furthermore, the relationship between type I IFNs and the EAPP has not been completely elucidated in teleosts, particularly at low temperature.

The overall goal of this thesis was to better characterize the effect of suboptimal temperatures on the EAPP at the cellular level using rainbow trout and walleye cell lines as models. I hypothesized that suboptimal temperatures would result in delayed induction of the

EAPP in both species, and that delayed type I IFN activity would be involved in this phenomenon. Thus, the first specific objective of this study was to examine how suboptimal temperatures impact constitutive and inducible EAPP member transcript levels, using poly(I:C) and VHSV IVb to induce EAPP transcript up-regulation. The second specific objective was to explore the effects of low temperature on type I IFNs, a potential up-stream regulator of the pathway, to further elucidate the mechanism behind differences in inducible EAPP mRNA up-regulation. Finally, the third specific objective of this thesis was to compare the effects of suboptimal temperature on EAPP regulation between rainbow trout and walleye in order to ascertain whether these responses differ between divergent teleost species. Together, results from this research will provide insight into the host-pathogen relationship at suboptimal temperatures and indicate whether these important species may be more susceptible to disease at colder water temperatures.

This thesis summarizes my research by presenting studies of the impacts of suboptimal temperature on the EAPP and IFN1 in rainbow trout fibroblast cells, and on the EAPP in walleye skin fibroblast cells. Chapter 2 describes the results of studies using the rainbow trout hypodermal fibroblast cell line RTHDF as a model. Chapter 3 describes the results of studies using the walleye skin fibroblast cell line WESk-11 as a model. Chapter 4 presents conclusions, significance of research, and proposes future research directions.

Chapter 2: Effect of Suboptimal Temperature on the Regulation of Endogenous Antigen Presentation in Rainbow Trout Hypodermal Fibroblasts

2.1 Introduction

Rainbow trout are an economically important teleost species widely distributed across North America and are a species model of interest for studying how the teleost EAPP is impacted by suboptimal temperatures [12, 17]. While rainbow trout prefer temperatures of 16°C, they are capable of surviving between 0°C and 27°C, which is important since they have been shown to experience temperatures below 5°C on average in the Great Lakes region and at an aquaculture facility in British Columbia over the winter months [7, 12]. The chronic exposure to suboptimal temperatures that rainbow trout face has made them a common choice for previous studies examining suboptimal temperature impacts on the teleost EAPP. For example, a study of rainbow trout peripheral blood leukocytes found that the constitutive β2m transcript and protein levels were maintained at 2°C relative to 14°C [102, 103]. However, a separate study showed that inducible protein production of β2m, MH class I α, and tapasin was impaired at 2°C relative to 14°C in RTS-11 cells infected with VHSV, suggesting that the effects of suboptimal temperature on the EAPP are not uniform in this species [100].

Based on the previous *in vivo* and *in vitro* studies, the overall effects of suboptimal temperatures on the EAPP are somewhat unclear in rainbow trout. To investigate these effects further, the rainbow trout hypodermal fibroblast cell line RTHDF was chosen as an *in vitro* model, since the skin has been implicated in the viral life cycle of VHSV in rainbow trout, and this cell line has previously been shown to be immunocompetent [36, 104, 105].

The hypothesis was that inducible, and not constitutive, EAPP transcript levels would be impaired at low temperatures in rainbow trout, and that IFN1 signalling would be involved in this impairment. To test this hypothesis, constitutive and inducible EAPP mRNA levels were measured in the RTHDF cell line at different temperatures, using the synthetic dsRNA molecule poly(I:C) and VHSV IVb to induce transcript up-regulation. Furthermore, ISREs were searched for in the promoter regions of the EAPP genes, in order to implicate IFN1 in the regulation of these genes. Finally, the effects of suboptimal temperatures on IFN1 transcript levels and secretion were examined to see if this could be a potential explanation for impairments in inducible EAPP transcript levels.

2.2 Materials and Methods

2.2.1 Maintenance of Cell Lines

Rainbow trout hypodermal fibroblast (RTHDF), an adherent fibroblast cell line [105], and epithelioma papulosum cyprini (EPC), an adherent epithelial cell line derived from the skin of a fathead minnow [106], were maintained at 20°C in 75 cm^2 plug-seal, tissue culture treated-flasks (Biolite) containing 10 mL of complete media comprised of Leibovitz's L-15 medium (L-15; Lonza) supplemented with 100 U/mL penicillin (HyClone), 100 μg/mL streptomycin (HyClone), and 10% fetal bovine serum (FBS; Gibco). Cells were subcultured via washing with phosphate buffered saline (PBS; Lonza) followed by detachment with 0.25% trypsin-EDTA (HyClone) and split 1:2 every 14 days for RTHDF, and 7 days for EPC.

2.2.2 Propagation of VHSV IVb

Viral haemorrhagic septicaemia virus (VHSV) IVb (CEFAS strain U13653; obtained by Dr. Niels Bols at the University of Waterloo from Dr. John Lumsden at the University of Guelph) was propagated on confluent EPC cultures at 14°C in 75 cm^2 tissue culture flasks [42]. EPC cells were infected with virus from a previous stock diluted to 1% in 12 mL of infection media comprised of L-15 media (Lonza) supplemented with 100 U/mL penicillin (HyClone), 100 μg/mL streptomycin (HyClone), and 2% fetal bovine serum (FBS; Gibco) After 2 h, the media was replaced with 12 mL of fresh infection media. At 10 d post-infection, media from infected cells was collected and centrifuged at 4500 ×*g* for 5 min at 4°C. The supernatant was passed through a 0.22 μm filter (Millex), aliquotted, and stored at -80°C until use. The $TCID_{50}$/mL was determined to be 5.53×10^7 based on the viral titreing method described in *Section 2.2.3*, and was converted to 3.87×10^7 pfu/mL by multiplying by 0.7, based on the Poisson distribution [107].

2.2.3 Titration of VHSV IVb

Viral titres were determined in 96 well plates as described by Pham et al. [108]. Briefly, approximately 1.5×10^5 EPC cells were seeded per well in 96 well tissue culture plates (Thermo Scientific) for viral titration and allowed to adhere for 48 h at room temperature. The propagated virus was prepared as a ten-fold serial dilution ranging from 10^{-1} to 10^{-8} in infection media, and for each dilution, four replicate wells of EPC cells were infected with 200 mL of the diluted virus. Plates were sealed with parafilm, and after 10 d of incubation at 14°C, cell monolayers were scored for cytopathic effects and used to calculate the viral titre, which was expressed as tissue culture infectious dose ($TCID_{50}$/mL).

2.2.4 Exposure of RTHDF Cells to Suboptimal Temperatures

Approximately 1×10^6 RTHDF cells in 1 mL of complete media were seeded into six well tissue culture plates and parafilmed. After being allowed to adhere for 24 h at 20°C, an additional 1 mL of complete media was added to each well, and the plates were moved to either 20°C, 14°C, or 4°C incubators. After 1 d, 3 d, and 7 d, RNA was isolated and used to synthesize cDNA as described in *Section 2.2.7*. Four independent trials were conducted, utilizing RTHDF cells between passages 65 and 75 and a separate 6-well plate at each time point.

2.2.5 Stimulation of RTHDF Cells with Poly(I:C)

RTHDF cells were seeded and allowed to adhere as described in *Section 2.2.4*, at which point plates were moved to either 20°C or 4°C incubators and acclimated for either 1 d or 5 d. Following acclimation, media was removed, and cells were either stimulated with 10 μg/mL of poly(I:C) in 2 mL of complete media, or the same volume of media alone. Cells were then incubated at the acclimated temperature for 3 h, 6 h, 24 h, or 48 h, at which point RNA was extracted and synthesized into cDNA as described below in *Section 2.2.7*. Three independent trials were conducted, utilizing RTHDF cells between passages 5 and 15 a separate 6-well plate at each time point.

2.2.6 Infection of RTHDF Cells with VHSV IVb

RTHDF cells were seeded and allowed to adhere as described in *Section 2.2.4*. Following acclimation for 1 d at 20°C or 4°C, cells were either infected with 2.5×10^6

$TCID_{50}$/mL of VHSV IVb (MOI = 3.5) in 2 mL of infection media or 2 mL of infection media alone. After 2 h, infection media was removed and replaced with 2 mL of complete media. At 36 h, 48 h, 72 h, and 96 h post-infection, media from one infected and one control well at each temperature was collected, and RNA extracted for cDNA synthesis, as described below in *Section 2.2.7.* At 8 d and 12 d post-infection, only media was collected. Four independent trials were conducted, utilizing RTHDF cells between passages 22 and 32 and a separate 6-well plate at each time point. Viral titres were determined for each collected media sample as described in *Section 2.2.3.*

2.2.7 RNA Isolation and cDNA Synthesis

At each time point, media was removed from one well at each temperature for each sample type and replaced with 2 mL of incubation temperature PBS. The PBS was then aspirated and replaced with 600 μL of RLT buffer (Qiagen), and RNA was extracted using the Qiagen RNeasy Mini Kit according to the manufacturer's instructions. An on-column DNase I digestion step was performed, but with the addition of 30 μL of Thermo Fisher Scientific DNAse I solution (1 × DNAse, 1 × DNAse buffer, and 8 × water by volume) to each column instead. Sub-samples of the extracted total RNA from randomly selected samples were electrophoresed on a 2% TAE gel to check the integrity of the RNA. The extracted total RNA was quantified using a Nanodrop 2000c Spectrophotometer (Thermo Scientific), and 500 ng was used to synthesize cDNA using the qScript cDNA Supermix Kit (Quanta Biosciences), according to the manufacturer's instructions. Synthesis reactions with no reverse transcriptase were also randomly performed and used in RT-PCR to verify the effectiveness of the DNase I treatment. Synthesized cDNA was stored at -80°C until all

samples were collected, and then analyzed by quantitative reverse-transcriptase PCR (qRT-PCR) (described below in *Section 2.2.9*).

2.2.8 qRT-PCR Primer Validation

qRT-PCR primers used in this study are listed in **Table 2.1**. Primer efficiency was calculated from the slope of a standard curve made from serially diluted RTHDF cDNA using the reaction conditions from *Section 2.2.9*. Only primer sets with efficiency between 90% and 105%, and with an r^2 value of greater than 0.995 for the standard curve were used.

Primer specificity was verified by a melt curve with a single peak, and through the cloning and sequencing of amplicons. Briefly, qRT-PCR products were ligated into the pGEM T-Easy Vector (Promega) at an insert to vector ratio of 3:1 and transformed into XL-1 Blue chemically competent cells. Next, 100 μL of the transformed cells were plated on LB plates with 50 μg/mL of ampicillin and incubated overnight at 37°C. Transformed cells were detected by blue-white screening, and insert presence verified via colony PCR. Colonies containing an insert were used to inoculate overnight LB broth cultures. Plasmid DNA was extracted from 1 mL of overnight culture using the Preparation of Plasmid DNA by Alkaline Lysis and SDS: Miniprep protocol [109], and then sent for sequencing at the Centre for Applied Genomics at Sick Kids Hospital (Toronto). Insert sequences were then verified using the BLASTn tool [110]. At least ten clone sequences positive for the variant without any negatives were required to confirm specificity of the calnexin variant primer sets. The primers for MH class I α recognize the UBA allele, while the primers for β2m recognize all six predicted β2m genes in the rainbow trout genome.

Table 2.1 qRT-PCR primers used in Chapter 2. Dir is the direction of the primer, with S and AS representing sense and antisense primers respectively. Eff% is the percent efficiency of the specified primer set.

Gene	Dir	Sequence 5'-3'	Accession Number	Slope	R^2	Eff%
18S rRNA	S	TTAGTTGGTGGAGCGATTTGTCT	AF308735	-3.37	0.997 [111]	98.04
	AS	CGCCACTTGTCCCTCTAAGAA				
ef1a	S	CCCTGAAGGCCGGTATGAT	AF498320	-3.385	0.997	97.43
	AS	AGGCATGGCCGATTCCA				
b-actin	S	GAGACGAGGCTCAGAGCAAGA	AF157514	-3.31	0.999	100.509
	AS	TGTAGAAGGTGTGATGCCAGATCT				
tfr	S	GCCCATGAAGATGGAAGACTCT	HM190266	-3.538	0.997	91.696
	AS	TCAAGCGAGGTGCCGTAGTA				
gapdh	S	CCAGCATGACCATCGTCAGTAA	NM_001124246	-3.413	0.998	96.339
	AS	CGGTGTAGGCGTGGACTGT				
tapasin	S	GCTGAAGTGCGCCACACA	DQ092322.1	-3.355	0.998	98.63
	AS	AGGGACGGAGGCTCTACAATC				
crt	S	GCCAGGATGCCCGTTTCTAT	AY372389.1	-3.261	0.998	102.589
	AS	TTCTGCTCGTGTTTGACAGTGA				
erp57	S	CCTGGAACCCAAGTGGAAAG	JX441982.1	-3.325	0.998	99.884
	AS	CGTATTGAGATGGCACGTCATT				
b2m	S	CAGACAGACCTGGCCTTCGA	AY217450.1	-3.247	0.998	103.22
	AS	GGCGGACTCTGCAGGTGTAC				
mhIa	S	AAAGTCCGTCCCTCAGTGTCTCT	FR688119.1	-3.419	0.991	96.11
	AS	ATGCTGTTCTTGTCCGTCTTTCT				
cnx 1	S	CAGACACACCACCGGGAC	N/A	-3.350	0.995	98.846
	AS	AAGGACTCGGCGAAGAAGTG				
cnx 2	S	GGTGGAGGCAGACATGCC	N/A	3.501	0.999	93.033
	AS	GTCAAAGGACTCGGCGAAAA				
ifn1	S	AAAACTGTTTGATGGGAATATGAAA	[112]	-3.382	0.997	97.569
	AS	CGTTTCAGTCTCCTCTCAGGTT				
mx3	S	TGAGGCCATTAAGCAGGTGA	[77]	-3.249	0.996	103.118
	AS	TGGTAAGGGTCGGTCGTCT				

2.2.9 qRT-PCR

qRT-PCR was performed using a Quant Studio 5 thermocycler (Applied Biosystems) and SYBR Green chemistry (Applied Biosystems). Each reaction consisted of 2.5 μL of

cDNA template diluted 1:40 in molecular grade water, 5 μL of Power Up SYBR Green Master Mix (Applied Biosystems), and 2.5 μL of a 2 μM primer stock containing sense and antisense primers (Sigma). The run protocol consisted of a UDG activation step of 50°C for 2 min, followed by an initial denaturation step of 95°C for 2 min, and 40 cycles of 95°C for 1 s, and 60°C for 30 s. A melt curve step was added following thermocycling, and involved ramping from 60°C to 95°C at 3°C every 30 s.

To determine the most stable reference gene for each experiment, a pooled sample for each sample type was produced using the corresponding replicate samples, with a 1:40 final dilution of cDNA. These pooled samples were then run in triplicate for each reference gene. The candidate reference gene that produced the lowest m-value using the Relative Quantification Analysis application (Applied Biosystems) was used as an endogenous control, with a maximum acceptable m-value of 0.5 [113].

All samples were run in triplicate for target and control genes. For each set of trials, the control sample from the earliest time point at 20°C was used as a calibrator.

2.2.10 Identification of Promoter Elements in Rainbow Trout EAPP Genes

ISREs (GAAANNGAAA[G/C][T/C]), NF-κB binding sites (GGGAAACTCC), and c-Jun/ATF-2 (AP-1; TGACGTCA) binding sites were identified in promoter regions from rainbow trout genes of interest. Promoter regions from each gene were extracted from the corresponding RefSeq entry on NCBI (accession numbers listed in **Table 2.2**). Putative promoter elements in the extracted sequences were then identified and mapped using the AliBaba2.1 program on the Transfac database. Presence of the putative elements was confirmed using the Match program on the same database. The elements were mapped relative to the start site of the predicted transcript for each respective RefSeq entry.

2.2.11 Determination of Viral Attachment/Entry at Suboptimal Temperatures

RTHDF cells were seeded, allowed to adhere, and acclimated at 20°C or 4°C for 1 d, as described in *Section 2.2.3*. Following acclimation, cells were either infected with 2.5×10^6 $TCID_{50}$/mL of VHSV IVb (MOI = 3.5) in 2 mL of infection media, or 2 mL of infection media alone. After 2 h, media was removed, cells were washed with 2 mL of PBS, and lysed with 300 μL NP-40 lysis buffer (Roche) with protease inhibitors. Lysates were collected and passed through a 25 gauge needle six times, before being centrifuged at 12000 × *g* for 20 min at 4°C. The resulting supernatants were stored at -80°C until all samples were collected, and then analyzed by western blotting (described in *Section 2.2.13*). Three independent trials were conducted, utilizing RTHDF cells between passages 24 and 34 and a separate 6-well plate at each time point.

2.2.12 Production and Purification of Recombinant IFN1 and IFN1 Antisera

A single colony of BL-21 cells containing the recombinant rainbow trout IFN1 (rtIFN1) construct in the pRSET A expression vector (Thermo Fisher Scientific) was inoculated into 50 mL of Super Optimal Broth (SOB) supplemented with 0.01 M $MgCl_2$, 50 μg/mL ampicillin, and 35 μg/mL chloramphenicol, and incubated at 37 °C with shaking at 200 rpm for 18-24 h. The initial 50 mL culture was seeded into flasks containing 1 L of SOB media supplemented 0.01 M $MgCl_2$ and no antibiotics. These bacterial cultures were incubated at 37 °C with shaking at 200 rpm until they reached an optical density (OD) of 0.40-0.60, as measured by a cell density metre (Fisher Scientific). Isopropyl β-D-1-thiogalactopyranoside (Thermo Fisher Scientific) was added to a final concentration of 1 mM to induce protein production, and the bacterial cultures were then incubated for a further 3 h at 37 °C with shaking at 200 rpm. Bacterial pellets were then centrifuged at 14000 ×*g* for 10

min at 4 °C, and the resulting bacterial pellets were stored at -20 °C until recombinant protein purification.

E. coli cell pellets were mixed with 5 mM imidazole lysis buffer at a ratio of 5 mL of buffer for every 1 g of cell pellet, as per the instructions for preparation of *E. coli* lysates under native conditions in the QIAexpressionist handbook (Qiagen). Cells were then lysed using a tissue homogenizer (Omni International) with six 10 s bursts of homogenization on ice and a 10 s cooling period between each burst. Lysates were centrifuged at 15000 ×g for 30 min at 4 °C, and the supernatant collected. For every 1 mL of lysate supernatant, 0.25 mL of Ni-NTA beads (Qiagen) were added, and then the bead-supernatant mixture was incubated at 4 °C for 18-24 h on an orbital shaker. Beads were stored in 30% ethanol and washed three times with 5 mM imidazole lysis buffer prior to use. Then, 30 mL of supernatant lysate was added to a 2.5 cm × 10 cm low-pressure chromatography column (BioRad) and the recombinant rainbow trout IFN1 (rtIFN1) was purified following the protocol for batch purification of 6×His-tagged proteins from *E. coli* under native conditions from the QIAexpressionist handbook (Qiagen), with the following changes to the washing and elution steps: one wash with 20 mL of 5 mM imidazole lysis buffer, ten washes with 20 mL of 30 mM imidazole wash buffer, and ten washes with 2 mL of 250 mM imidazole elution buffer. Elution fractions containing the recombinant rtIFN1 were then dialyzed in 2 L phosphate buffered saline (PBS) overnight at 4 °C. The dialyzed recombinant rtIFN1 was aliquotted and stored at -80°C.

Purified and dialyzed recombinant rtIFN1 was injected into a rabbit and a chicken by Cedarlane, Canada. Boosters were administered to the injected animals until titres of rabbit immunoglobulin G and chicken immunoglobulin Y from test bleeds indicated a sufficient

antibody response to the injected recombinant protein, as determined by indirect ELISA. Serum from the rabbit was then collected, and IgG was purified by agarose A purification and affinity purification, while immunoglobulin Y was harvested from chicken eggs and affinity purified. All purification was performed by Cedarlane, Canada.

2.2.13 Western Blotting

Protein concentrations were determined via BCA assay (Thermo Fisher Scientific), and 20 μg of protein from each sample was then mixed with 4 ×Laemmli sample buffer (BioRad) with β-mercaptoethanol. After boiling for 10 min, samples were loaded and separated on a 10% Mini-PROTEAN TGX Gel (BioRad) for 45 min at 200 V and imaged on a ChemiDoc MP Imager (BioRad) using the Stain-Free Gel application. Proteins were transferred to PVDF membranes (BioRad) using the Mixed MW protocol (7 min at 2.5 A and up to 25 V) on a TransBlot Turbo Transfer System (BioRad) and imaged again using the Stain-Free Blot application. Blots were then blocked with 5% skim milk in tris-buffered saline with Tween-20 (TBS-T; 2 mM Tris, 30 mM NaCl, pH 7.5 with 0.1% Tween-20) for 1 h at room temperature on a platform shaker, and probed with mouse anti-VHSV nucleocapsid protein antibody (IP5B11) [114] at a 1:1000 dilution in 5% skim milk in TBS-T overnight on a rotating shaker at 4°C. In between each blocking and probing step, blots were washed three times with TBS-T. Membranes were subsequently probed with a 1:10000 dilution of goat anti-mouse IgG conjugated to horseradish peroxidase (BioRad), developed with ECL Clarity substrate (BioRad), and imaged using the Chemi Hi Sensitivity application. The 20°C infected sample from the first trial was run on each blot as an inter-blot normalizer.

The same protocol was followed for the blotting of IFN1, except that 50 μg of RTHDF cell supernatants was mixed with loading buffer and loaded into the gel, and a 1:500

dilution of rabbit anti-rtIFN1 (Cedarlane) was used as the primary antibody. Additionally, following overnight incubation with the primary antibody, blots were probed with a 1:20000 dilution of goat anti-rabbit IgG conjugated to biotin, and finally a 1:2000 dilution of streptavadin conjugated to horseradish peroxidase (BioRad).

For IFN1 antisera blocking experiments, duplicate blots were prepared containing 75 μg of a positive sample from *Section 2.2.15*. The blots were probed overnight on a rotating shaker at 4°C with a 1:500 dilution of rabbit anti-rainbow trout IFN1 antibodies in 5% skim milk in TBS-T that were either unblocked or blocked with recombinant rtIFN1 at a 3:1 mass ratio of recombinant rtIFN1 to antibody for 1 h on a shaker at room temperature prior to use for probing the membrane. These steps were repeated for the chicken anti-rainbow trout IFN1 antibody.

2.2.14 RT-PCR for VHSV IVb N Gene and Transcript Levels

RT-PCR amplification of the VHSV N gene from the cDNA samples obtained in *Section 2.2.6* was performed in 20 μL reactions containing 2 μL of 10× reaction buffer (New England Biolabs), 0.4 μL of 10 mM dNTPs (Thermo Scientific), 0.1 μL of Taq DNA polymerase (New England Biolabs), 2.5 μL of primer stock containing 2 μM of each primer (S - 5’ AGGACCCCAGACTGTGCAAGC 3’; AS - 5’ TCCGCCTGGCTGACTCAACA 3’) [115], and 0.5 μL of cDNA, RNA, or water on a T100 Thermocycler (BioRad). The conditions for the PCR were an initial denaturation step of 95°C for 4 min, followed by 35 cycles of 95°C for 30 s, 65°C for 30 s, and 68°C for 60 s, and a final elongation step of 68°C for 4 min. *ef1a* (primer sequences in **Table 2.1**) was also amplified in the same samples under the same thermocycling conditions, but with only 25 cycles. Due to the cDNA

synthesis reactions performed, both the viral N gene and the N gene transcripts should be amplified by the primers used.

After mixing with 6× loading dye, 15 μL from each reaction was loaded onto a 2% TAE gel with 0.03% Gel Red (manufacturer) and electrophoresed for 60 min at 150 V. Gels were imaged using the Gel Red application on a ChemiDoc MP Imager (BioRad).

2.2.15 IFN1 Protein Levels in Cell Supernatants Following Stimulation with Poly(I:C)

RTHDF cells were seeded, allowed to adhere, acclimated, and stimulated with poly(I:C) as described in *Section 2.2.5*. At 3 h, 6 h, 12 h, 24 h, and 48 h post-stimulation, media was collected from one stimulated and one control well at each temperature and stored at -80°C until all samples were collected. Three independent trials were conducted, utilizing RTHDF cells between passages 34 and 44 and a separate 6-well plate at each time point. IFN1 levels in the supernatants were analyzed by western blotting and quantitative enzyme-linked immunosorbent assay (qELISA) as described in *Section 2.2.13* and *Section 2.2.16* respectively.

2.2.16 qELISA

Immulon 4HBX flat bottom 96 well microtiter plates (Fisher Scientific) were coated with 100 μL of 2 μg/mL rabbit anti-rtIFN1 antibodies prepared in pH 7.4 sodium carbonate/sodium bicarbonate coating buffer and incubated for 4 h at room temperature. Plates were next blocked with 300 μL of 5% skim milk in tris-buffered saline (TBS) for 1 h at 37°C, and then 100 μL of either serially diluted recombinant rtIFN1 (from 1600 pg/mL to 50 pg/mL) or supernatant samples were loaded into each well and incubated overnight at 4°C. The next day, plates were acclimated at room temperature for 30 min, and then 100 μL of 0.5 μg/mL chicken anti-rtIFN1 antibodies diluted in 5% skim milk in TBS-T was added to

each well and incubated for 1 h at room temperature. Following addition of 100 μL of a 1:2,000 dilution of anti-chicken IgG conjugated with biotin (Cedarlane) per well, plates were incubated for 1 h at room temperature in the dark. Next, 100 μL of a 1:1,000 dilution of streptavidin conjugated to horseradish peroxidase (Cedarlane) in 5% skim milk in TBS was added to each well and incubated for 45 min at room temperature in the dark. In between each step, plates were washed four times with TBS-T, with the final three washes lasting 5 min each. Finally, detection was performed by adding 100 μL of TMB-sens substrate (Cedarlane) to each well and incubating for 30 min at room temperature in the dark, before stopping the reaction by addition of 100 μL of 0.3 M H_2SO_4 to each well. Absorbance was read at 450 nm on a Synergy H1 Hybrid Reader (BioTek).

2.2.17 Data Analysis

qRT-PCR data from *Section 2.2.3*, *Section 2.2.5*, and *Section 2.2.6* were analyzed statistically with a Poisson-lognormal generalized mixed model and a Markov Chain Monte Carlo procedure using the MCMC.qPCR package [116] implemented in R, which infers changes in transcript levels of all genes from the joint posterior distributions of parameters. The determined control gene for each set of experiments was specified as an endogenous control and data was shown as mean $\log_2$ (fold change) with 95% credible intervals. The 95% credible intervals are the Bayesian equivalent of frequentist confidence intervals, and represent the interval containing the true value of the parameter with 95% probability. Effects were deemed to be statistically significant between groups where credible intervals did not overlap.

Viral titre data from *Section 2.2.6* was analyzed statistically by two-way analysis of variance with Bonferroni post hoc test for comparison of means using GraphPad Prism

(GraphPad Software, Inc.). Data was shown as mean ± standard error, and differences were considered significant between times at a specific temperature when $P < 0.05$

Relative densitometry analysis was performed using the BioRad ImageLab software (BioRad) on the blots from the viral entry samples described in *Section 2.2.11* using the 20°C infected sample from the first trial as an inter-blot normalizer. Data was shown as mean ± standard error and analyzed statistically with a paired students t-test using GraphPad Prism (GraphPad Software, Inc.). Differences were considered significant when $P < 0.05$.

Secreted IFN1 concentrations in *Section 2.2.15*were determined by comparing the absorbance in each sample to a standard curve of recombinant rainbow trout IFN1 run on the same plate. Concentration values below 50 pg/mL, the lower limit of detection on the standard curve, were recorded as non-detectable (nd), and counted as 0 pg/mL for the purpose of calculating means when necessary.

2.3 Results

2.3.1 Effect of Suboptimal Temperatures on Constitutive EAPP Transcript Levels

To first assess whether suboptimal temperatures have an effect on the constitutive transcript levels of EAPP members, RTHDF cells were placed at 20°C, 14°C, and 4°C for 1 d, 3 d, and 7d (**Figure 2.1**). After 1 d at each temperature condition, no significant differences in mRNA levels were observed for any of the target genes. After 3 d and 7 d, *mhIa* (**Figure 2.1F**) and *tapasin* (**Figure 2.1G**) both tended to have higher transcript levels at 4°C than at the other temperatures, although the mRNA levels at these two time points were usually not significantly different. However, there was no difference in mRNA levels between any temperature and time point for *b2m* (**Figure 2.1E**), the other EAPP-specific

member. The pattern of transcript levels for the two calnexin variants were similar (**Figure 2.1A-B**), with differences in relative mRNA levels between temperatures that were not statistically significant, except between 14°C and 4°C at 3 d post temperature change. For the other two non-pathway specific genes, *calreticulin* (**Figure 2.1C**) and *erp57* (**Figure 2.1D**), no significant differences in transcript levels were seen for either gene, with the exception of *calreticulin* (**Figure 2.1C**), which was significantly down-regulated at 14°C after 3 d post temperature shift. Overall, the magnitudes of the observed differences in mRNA levels between temperatures were less than 2 fold, with a couple of exceptions in some of the 14°C samples. This implies that there may not be a biologically relevant difference in constitutive transcript levels of EAPP genes in response to suboptimal temperatures, particularly between 20°C and 4°C.

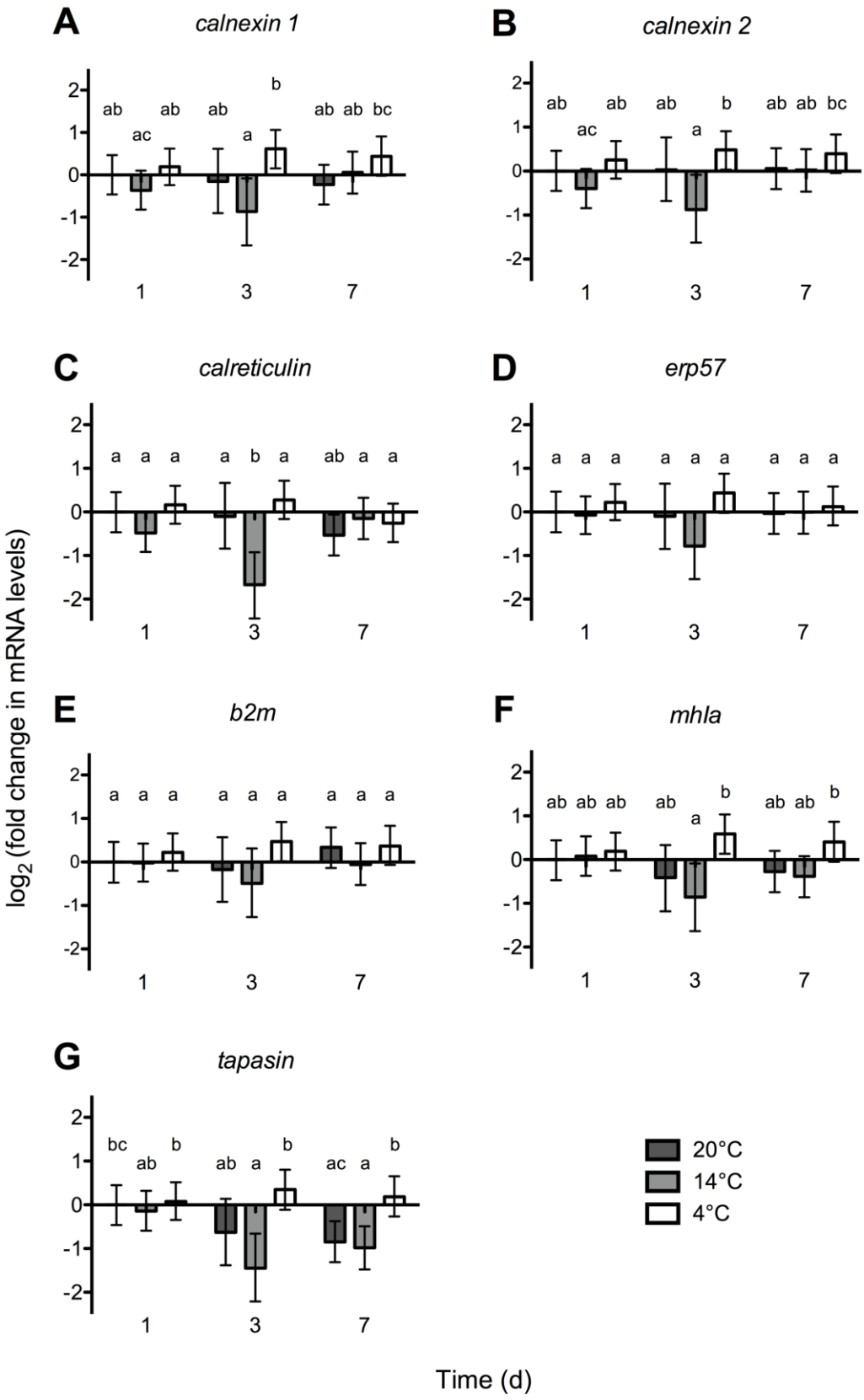
A
calnexin 1
B
calnexin 2
C
calreticulin
D
erp57
E
b2m
F
mhla
G
tapasin
log2 (fold change in mRNA levels)
Time (d)
20°C
14°C
4°C

Figure 2.1 Relative transcript levels of EAPP members in RTHDF cells over time in response to temperature. RTHDF cells were incubated for 1 d, 3 d, or 7d at 20°C, 14°C, or 4°C, at which point transcript levels for *calnexin 1* (A), *calnexin 2* (B), *calreticulin* (C), *erp57* (D), *b2m* (E), *mhIa* (F), and *tapasin* (G) were evaluated by qRT-PCR. Data was analyzed statistically via a Poisson-lognormal generalized mixed model with a Markov-chain Monte Carlo procedure and *gapdh* (m-value = 0.261) specified as a stable endogenous control. Data is shown as mean $\log_2$ (fold change) relative to the 1 d at 20°C group with 95% credible intervals (n = 4), and values are statistically significant between groups where credible intervals do not overlap, or where letters are different.

2.3.2 Promoter Element Analysis of EAPP Genes and Mx3

Next, to try to predict whether the members of the EAPP are also ISGs in rainbow trout, as they are in mammals [62], the promoter regions of the genes of interest in this study were analyzed for the presence of binding sites for transcription factors known to be activated or induced following poly(I:C) stimulation or IFN1 signalling (**Table 2.2**). All of the pathway-specific members of the EAPP (*b2m*, *mhIa*, and *tapasin*), as well as *mx3*, a known rainbow trout ISG [77, 81], had predicted ISREs within a range of 50 bp to 200 bp upstream from the predicted start of the transcript, while only *tapasin* and *mx3* had predicted NF-κB binding sites within 20 bp of this predicted transcript start site (Table 2). Furthermore, only two of the six *b2m* genes predicted in rainbow trout, *b2m b* and *b2m d*, have a predicted ISRE in their promoter (Table 2). None of the non-pathway-specific members of the EAPP (*i.e. calreticulin*, *erp57*, and the two calnexin variants) had predicted ISRE or NF-κB binding sites (Table 2).

Table 2.2 Promoter elements for dsRNA- and IFN1-inducible transcription factors in rainbow trout genes. ISREs, NF-κB binding sites, and c-Jun/ATF-2 binding sites were mapped relative to the start of the transcript for the RefSeq entry on NCBI associated with each accession number. Elements from -200 bp to +100 bp are shown. ND indicates the binding site was not detected.

Gene	Accession Number	ISRE	NF-κB Binding Site	c-Jun/ATF-2 Binding Site
ifn1	NM_001124531	-53 to -42	-101 to -91 -73 to -64	ND
calnexin1	XM_021561370	ND	ND	-133 to -127
calnexin 2	XM_021584082	ND	ND	+25 to +31
calreticulin	XM_021603624	ND	ND	ND
erp57	NM_001281398	ND	ND	ND
b2m a	XM_021565711	ND	ND	ND
b2m b	XM_021565714	-91 to -80 -85 to -74	ND	ND
b2m c	XM_021565716	ND	ND	ND
b2m d	XM_021565717	-50 to -39 -44 to -33	-122 to -113	ND
b2m e	XM_021565718	ND	ND	ND
b2m f	XM_021565719	ND	ND	+26 to +35
mhIa (UBA)	NM_001270412	-180 to -169	ND	ND
tapasin	NM_001124553	-50 to -38 -43 to -32	-14 to -5	ND
mx3	XM_021569609	-88 to -79	+9 to +18	ND

2.3.3 Temperature-Dependent Inducible EAPP Transcript Levels Following Poly(I:C) Stimulation

I next sought to ascertain the effect of suboptimal temperature on inducible EAPP transcript levels following stimulation of RTHDF cells with poly(I:C). mRNA levels of *ifn1* and the pathway-specific members of the EAPP (*b2m*, *mhIa*, and *tapasin*) were measured at 3 h, 6 h, 24 h, and 48 h post-stimulation, as these were the only three EAPP members found to have predicted ISREs in their promoters that would allow them to respond to IFN1 signalling (**Figure 2.2**). Additionally, we tested 1 d (**Figure 2.2A-D**) and 5 d (**Figure 2.2E-H**)

temperature acclimation periods prior to stimulation to assess the impact of acclimation time on our results. Following a 1 d acclimation period, inducible *ifn1* transcript levels were highest at 3 h post-stimulation at 20°C with approximately 1000-fold up-regulation relative to the time- and temperature-matched control, but at 4°C, the same level of induction was delayed to 24 h post-stimulation (**Figure 2.2A**). Temperature-dependent delays were also observed for the pathway-specific members of the EAPP, with the pattern of mRNA regulation for *tapasin* (**Figure 2.2D**) being distinct from the shared pattern of transcript levels for *b2m* (**Figure 2.2B**) and *mhIa* (**Figure 2.2C**). Up-regulation of *tapasin* transcript levels (**Figure 2.2D**) relative to the time- and temperature-matched control was first observed at 3 h post-stimulation at 20°C, with peak up-regulation of approximately 10-fold at 6 h post-stimulation. However, at 4°C, up-regulation of *tapasin* transcript levels was delayed until 48 h post-stimulation and was also approximately 10-fold. For *b2m* (**Figure 2.2B**) and *mhIa* (**Figure 2.2C**), up-regulation at 20°C did not occur until 6 h post-stimulation, with up-regulation first observed at 48 h post-stimulation at 4°C. Peak up-regulation of both genes at 20°C was approximately 5-fold and did not occur until 24 h post-stimulation. Meanwhile, following a 5 d acclimation period, the same pattern of transcript regulation was observed for *ifn1* (**Figure 2.2E**) as was seen after a 1 d acclimation (**Figure 2.2A**) but the EAPP members studied (*b2m*, *mhIa*, and *tapasin*; **Figure 2.2F-H**) all showed reduced or delayed up-regulation at 20°C following the 5 d acclimation, with little to no up-regulation at 4°C.

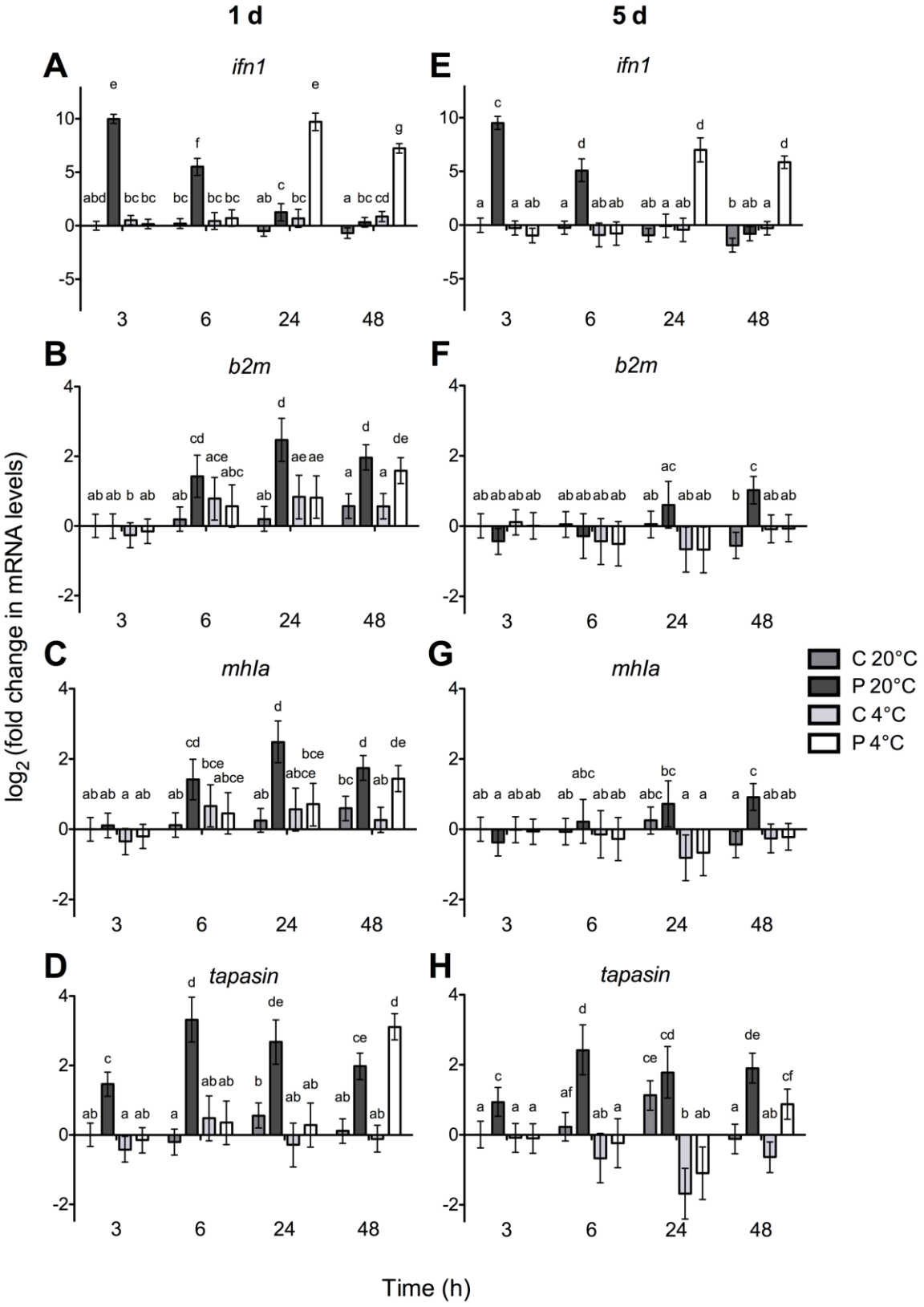
1 d
5 d
A
ifn1
E
ifn1
B
b2m
F
b2m
C
mhla
G
mhla
D
tapasin
H
tapasin
log2 (fold change in mRNA levels)
Time (h)
C 20°C
P 20°C
C 4°C
P 4°C

Figure 2.2 Relative transcript levels of IFN1 and EAPP members in RTHDF cells in response to poly(I:C) stimulation at different temperatures over time. Cells were acclimated for 1 d (A-D) or 5 d (E-H) at either 20°C or 4°C, and then stimulated with 10 µg/mL poly(I:C), or an equal volume of media alone (control). Transcript expression of ifn1 (A,E), *b2m* (B,F), *mhIa* (C,G), and *tapasin* (D,H) was evaluated at 3 h, 6 h, 24 h, and 48 h post-stimulation via qRT-PCR. Data was analyzed statistically via a Poisson-lognormal generalized mixed model with a Markov-chain Monte Carlo procedure and *ef1a* (m-value = 0.336) specified as an endogenous control. Data is shown as mean $\log_2$ (fold change) relative to the unstimulated 20°C group at 3 h post-stimulation with 95% credible intervals (n = 3), and values are statistically significant between groups where credible intervals do not overlap, or where letters are different.

To compare the patterns of transcript regulation of the pathway-specific members of the EAPP to a known rainbow trout ISG, *mx3* mRNA levels were also measured following stimulation of RTHDF cells with poly(I:C) (**Figure 2.3**). Only a 1 d temperature acclimation period was used for this experiment, and for all subsequent experiments, due to the relative lack of response of the EAPP-specific genes at both temperatures following the 5 d acclimation period (**Figure 2.2F-H**). In particular, the decreased response at 20°C suggests that the cells may be starting to become quiescent over the longer acclimation schedule, and thus, the 1 d acclimation period was used to ensure the cells were capable of responding to stimuli and/or infection. Following a 1 d acclimation period, *mx3* (**Figure 2.3**) shared a similar pattern of inducible transcript levels to that of *tapasin* (**Figure 2.2H**), with up-regulation relative to the time- and temperature-matched control first observed at 3 h post-stimulation at 20°C and peak up-regulation of approximately 6-fold reached at 6 h post-stimulation. Meanwhile, at 4°C, up-regulation of *mx3* mRNA levels was also delayed until 48 h post-stimulation (**Figure 2.3**).

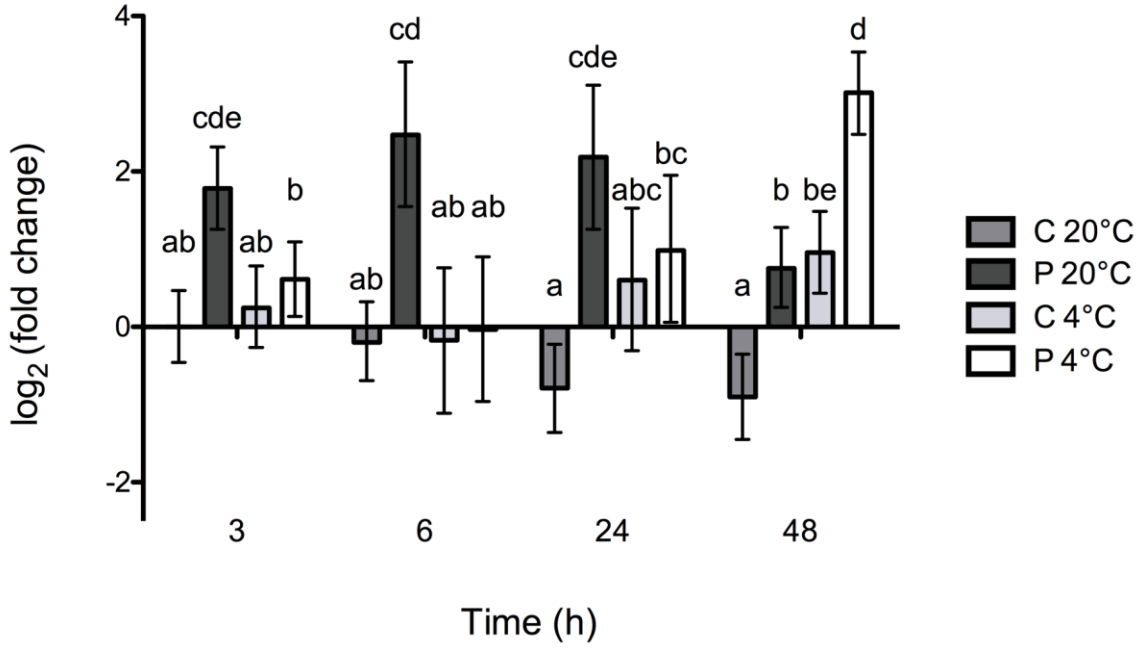

Figure 2.3 Relative *mx3* transcript levels in RTHDF cells in response to poly(I:C) stimulation at different temperatures over time. Cells were acclimated for 1 d at either 20°C or 4°C, and then stimulated with 10 µg/mL poly(I:C), or an equal volume of media alone (control). Transcript levels of *mx3* were evaluated at 3 h, 6 h, 24 h, and 48 h post-stimulation via qRT-PCR. Data was analyzed statistically via a Poisson-lognormal generalized mixed model with a Markov-chain Monte Carlo procedure and *ef1a* (m-value = 0.336) specified as an endogenous control. Data is shown as mean $\log_2$ (fold change) relative to the unstimulated 20°C group at 3 h post-stimulation with 95% credible intervals (n = 3), and values are statistically significant between groups where credible intervals do not overlap, or where letters are different.

2.3.4 IFN1 Secretion in RTHDF Cells at Suboptimal Temperatures

We then sought to examine the effect of suboptimal temperatures on the secretion of IFN1 in RTHDF cells following stimulation with poly(I:C) to determine if delayed production of IFN1 could be a possible contributor to the delays in EAPP transcript level up-regulation following stimulation. First we needed to validate the antisera raised against recombinant rtIFN1. Following nickel column affinity chromatography, both anti-His antisera (**Supplemental Figure S1A**) and rabbit antisera raised against the recombinant

rtIFN1 (**Supplemental Figure S1B**) were specifically able to detect a protein of approximately 22 kDa. Furthermore, the rabbit anti-recombinant rtIFN1 IgG was able to detect a protein of approximately the same size in supernatants of RTHDF cells stimulated with poly(I:C) (**Figure 2.4C**). Importantly, blocking of the rabbit (**Figure 2.4A)** and chicken (**Figure 2.4B**) anti-recombinant rtIFN1 antibodies with recombinant IFN1 protein eliminated detection of the bands from one of the positive supernatant samples and the recombinant protein, including what might be dimers and trimers of the protein due to the high concentration of the recombinant protein used in this experiment.

Secretion of IFN1 into RTHDF cell supernatants at suboptimal temperatures was then evaluated via western blotting and qELISA using the anti-recombinant rtIFN1 antibodies. The pattern of IFN1 secretion and the relative IFN1 levels between samples at the same temperature were consistent between western blot and qELISA (**Figure 2.4C**, **Figure 2.4D**). Similar to what was observed for inducible IFN1 mRNA up-regulation at suboptimal temperatures following poly(I:C) stimulation, the start of IFN1 secretion was delayed at 4°C relative to 20°C, from approximately 6 h to 24 h post-stimulation. After comparison to a standard curve generated from serially diluted recombinant rainbow trout IFN1 run on the same qELISA plate (**Supplemental Figure S2**), the peak levels of secreted IFN1 in RTHDF cell supernatants was determined to be approximately 150 pg/mL at 20°C, and this was also the highest level of secreted IFN1 at 4°C during the time points examined (**Figure 2.4D**).

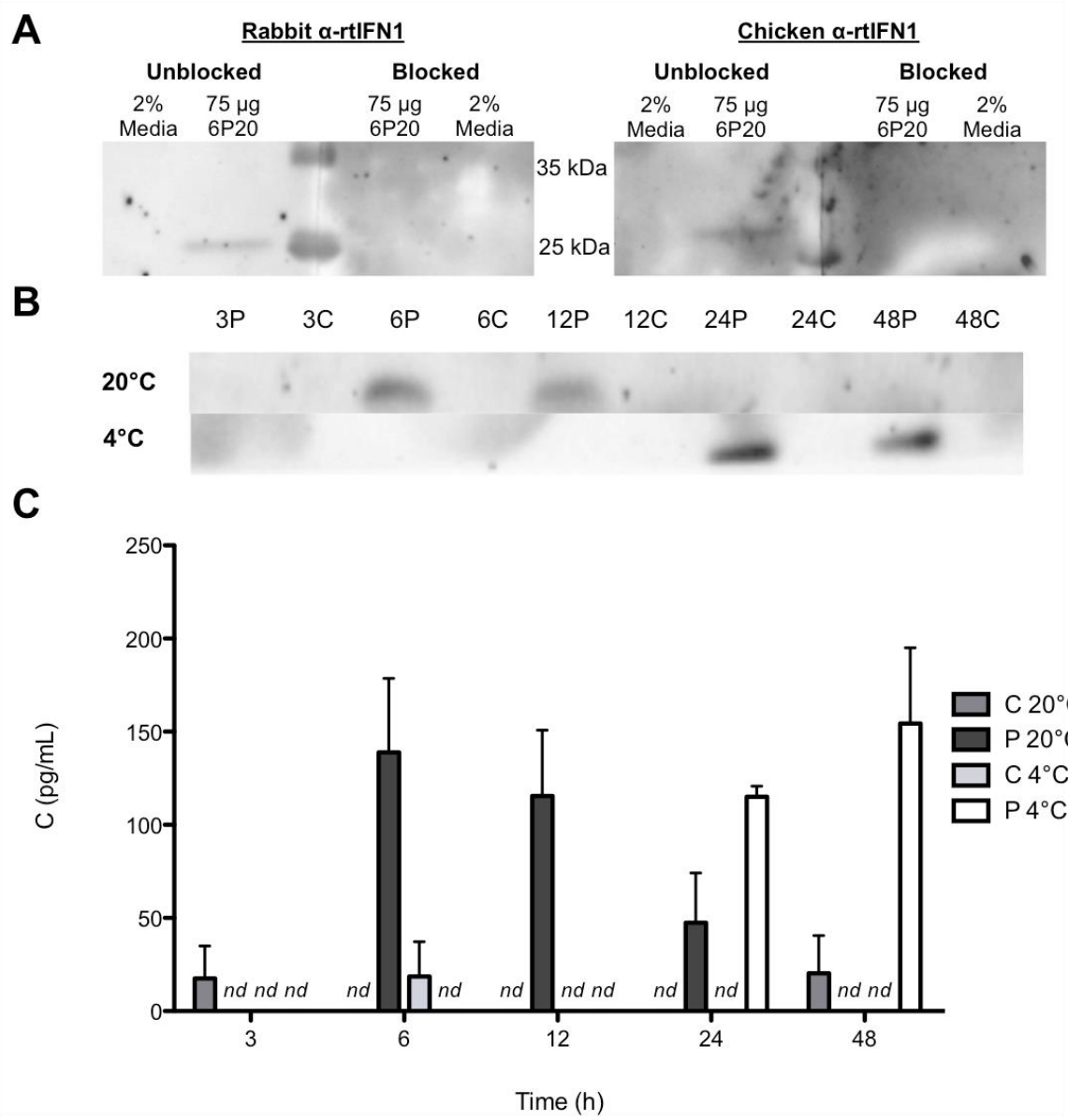
A
Rabbit α-rtIFN1
Chicken α-rtIFN1
Unblocked
Blocked
2% Media
75 µg 6P20
75 µg 6P20
2% Media
35 kDa
25 kDa
B
3P
3C
6P
6C
12P
12C
24P
24C
48P
48C
20°C
4°C
C
C (pg/mL)
250
200
150
100
50
0
nd nd nd
nd
nd
nd
nd nd
nd
nd
nd nd
3
6
12
24
48
Time (h)
C 20°C
P 20°C
C 4°C
P 4°C

Figure 2.4 IFN1 secretion in RTHDF cells at suboptimal temperatures following poly(I:C) stimulation. (A) Blocking of rabbit and chicken anti-recombinant rainbow trout IFN1 (rtIFN1) antibodies with recombinant IFN1 was performed. Duplicate blots with 2% FBS media alone, or 75 µg of RTHDF cell supernatant from cells at 20°C stimulated with 10 µg/mL poly(I:C) for 6 h were probed with a 1:500 dilution of the respective anti-recombinant rtIFN1 antibody that was either unblocked, or blocked with a 3:1 mass ratio of the recombinant protein for 1 h at room temperature. (B) Secreted IFN1 was detected in supernatants from RTHDF cells stimulated with 10 µg/mL poly(I:C) at 20°C or 4°C at 3 h, 6 h, 12 h, 24 h, and 48 h post-stimulation via western blot. P signifies a poly(I:C) stimulated sample, while C denotes an unstimulated control sample. (C) Secreted IFN1 in the supernatant samples described above was measured via a quantitative sandwich ELISA for rainbow trout IFN1. Concentrations below the limit of detection of 50 pg/mL were recorded as nd and counted as 0 pg/mL for the purpose of calculating means when necessary. Data is shown as mean plus standard error (n=3).

2.3.5 Effect of Suboptimal Temperatures on the Infection of RTHDF Cells with VHSV IVb

VHSV IVb attachment/entry, replication, and release of viable virus from RTHDF cells was assessed by nucleocapsid protein levels in cell lysates, N gene transcript levels, and viral titres respectively, in order to determine the suitability of VHSV IVb infection of RTHDF cells as a model at low temperature. Higher nucleocapsid protein levels were observed in lysates from cells at 4°C than at 20°C at 2 h post-infection (**Figure 2.5A**, **Figure 2.5B**). However, no increase in N gene and mRNA levels was observed at either temperature studied (**Figure 2.5C**). Viral titres from cell supernatants exhibited a similar pattern at each temperature, with a significant increase ($P < 0.05$) of less than 10-fold by 4 d post-stimulation at 20°C and 8 d post-stimulation at 4°C, and then returning to earlier levels (**Figure 2.5D**).

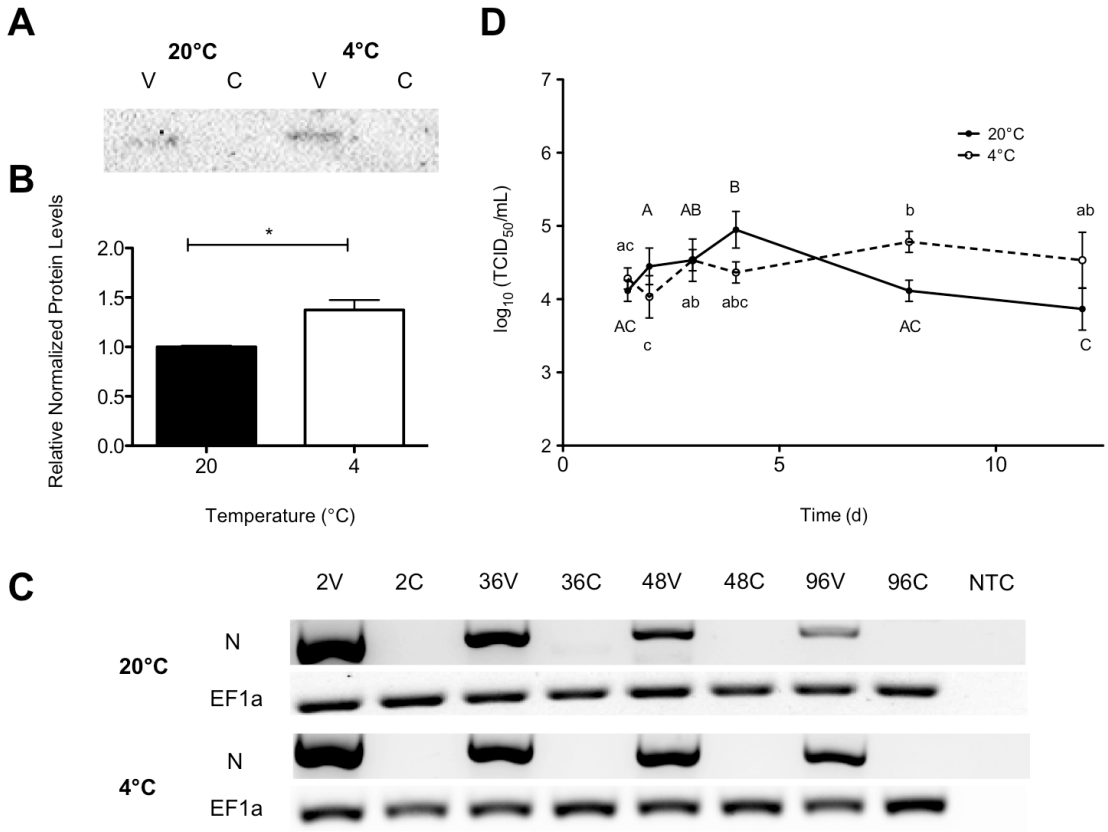

Figure 2.5 Effect of temperature on VHSV IVB attachment/entry, and replication in RTHDF. (A) VHSV N protein levels were evaluated in cells acclimated at either 20°C or 4°C at 2 h post-infection with 3.5× 106 TCID50/mL of VHSV IVb via western blot. V indicates a sample from infected cells, while C indicates a control sample. (B) Target protein levels from each blot were normalized relative to total protein loaded, and data was analyzed statistically by paired t-test. Data is shown as mean plus standard error (n = 3), and values are statistically significant ($P < 0.05$) where letters are different. (C) N gene and transcript levels were studied in cells infected at either 20°C or 4°C at 2 h, 36 h, 48 h and 96 h post-infection with the virus. (D) Viral titres from VHSV-infected RTHDF cell supernatants at either 20°C or 4°C at 1.5 d, 2 d, 3 d, 4 d, 8 d, and 12 d post-infection were measured. Differences in viral titres over time for each temperature were analyzed by two-way ANOVA with Bonferroni post-hoc test. Data is shown as mean log10 ($TCID_{50}$/mL) ± standard error (n = 4) and values are statistically significant ($P < 0.05$) over time where letters are different (capitalized for 20°C, uncapitalized for 4°C).

2.3.6 Temperature-Dependent Inducible EAPP Transcript Levels Following VHSV IVb Infection

Finally, I examined the effect of suboptimal temperature on inducible EAPP transcript up-regulation following infection with VHSV IVb to try to determine how environmental temperature impacts the host-pathogen relationship, and how this response differs from the response to a non-infective stimulant, such as poly(I:C). Transcript levels of *ifn1*, *mx3*, and the pathway-specific EAPP members (*b2m*, *mhIa*, and *tapasin*) in response to infection with VHSV IVb at 36 h, 48 h, 72 h, and 96 h post-infection were measured following a 1 d acclimation to either 20°C or 4°C (**Figure 2.6**). Approximately 5- to 10-fold up-regulation of *ifn1* gene expression at 20°C was observed at all time points studied. At 4°C, infection up-regulated *ifn1* transcript levels at all time points, but peak-upregulation of the gene was higher, with an increase of about 30- to 40-fold, at 36 h and 48 h post-infection (**Figure 2.6A**). At the later time points, the up-regulation was similar in magnitude to what was seen at 20°C (**Figure 2.6A**). In contrast to the observations following poly(I:C) stimulation, no delay was observed in induction of *mx3*, with up-regulation occurring at both temperatures at the time points examined (**Figure 2.6B**). Meanwhile, the pattern of transcript level up-regulation for *tapasin* was more similar to that following stimulation with poly(I:C), with up-regulation at 36 h and 48 h post-infection at 20°C, and delayed induction at 4°C until 72 h post-infection (**Figure 2.6E**). *mhIa* mRNA levels showed a similar temperature-related delay to tapasin, but with 2-fold less up-regulation at both temperatures (**Figure 2.6D**). No changes were observed in *b2m* transcript levels in response to infection, temperature, or time (**Figure 2.6C**).

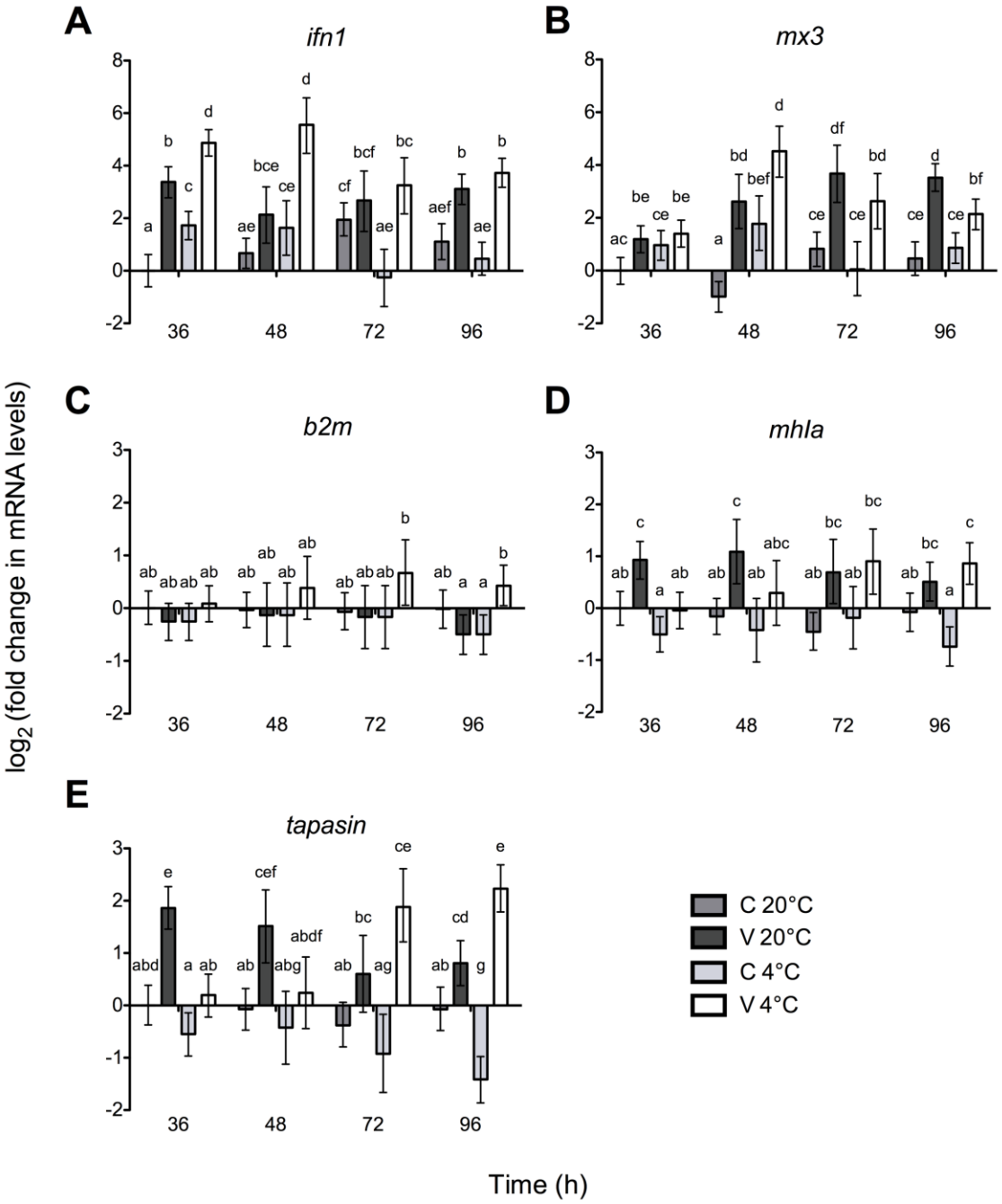
A
ifn1
B
mx3
C
b2m
D
mhla
E
tapasin
log2 (fold change in mRNA levels)
Time (h)
36
48
72
96
C 20°C
V 20°C
C 4°C
V 4°C

Figure 2.6 Relative transcript levels of IFN1, Mx3, and EAPP members in RTHDF cells following infection with VHSV IVb at different temperatures over time. Cells were acclimated for 1 d at either 20°C or 4°C, and then infected with VHSV IVb at an MOI of 3.5, or an equal volume of media alone (control). Transcript levels of *ifn1* (A), *mx3* (B), *b2m* (C), *mhIa* (D), and *tapasin* (E) were evaluated at 36 h, 48 h, 72 h, and 96 h post-stimulation via qRT-PCR. Data was analyzed statistically via a Poisson-lognormal generalized mixed model with a Markov-chain Monte Carlo procedure and *ef1a* (m-value = 0.324) specified as an endogenous control. Data is shown as mean $\log_2$ (fold change) relative to the non-stimulated 20°C group at 36 h post-stimulation with 95% credible intervals (n = 4), and values are statistically significant between groups where credible intervals do not overlap, or where letters are different.

2.4 Discussion

2.4.1 Suboptimal Temperatures Do Not Impair Constitutive EAPP Transcript Levels in RTHDF Cells

No impairment in EAPP transcript levels was observed in RTHDF cells following exposure to suboptimal temperatures, which is consistent with results from other salmonid species. For example, constitutive β2m expression and production in rainbow trout and Atlantic salmon tissues and peripheral blood leukocytes is stable at 4°C, as are MH class I α and β2m protein levels at 1°C in the Arctic charr bulbus arteriosus cell line, ACBA [103, 117]. However, this may not be true for teleosts in other families, as carp experience decreases in β2m production at 6°C relative to 24°C, resulting in the loss of functional MH class I α-β2m complexes [102]. The ability of these salmonid species to constitutively express EAPP genes at suboptimal temperatures without impairment may be an adaptation that allows these species to live at lower temperatures, as rainbow trout, Atlantic salmon, and Arctic charr all have thermal preferences of less than 16°C, while carp prefer 23°C [12, 118, 119].

2.4.2 Role of Promoter Elements in Induction of EAPP Transcript Up-regulation by Poly(I:C)

While ISREs have been identified in the promoter regions of the *mhIa* genes of Atlantic salmon and grass carp, this is the first study in teleosts to identify them in the promoter regions of genes for *b2m* and *tapasin*, the other two pathway-specific members of the EAPP, suggesting that IFN1 is involved in the regulation of these genes [99, 120]. However, no ISREs were found in the promoter regions of the non-pathway-specific members (*calnexin 1*, *calnexin 2*, *calreticulin*, and *erp57*), unlike in mammals, which implies that only the pathway-specific members are involved in the induction of endogenous antigen presentation in rainbow trout [62]. Furthering this hypothesis, NF-κB binding sites were also not found in the promoters of the non-pathway-specific members, with NF-κB activation known to occur directly following dsRNA sensing, as well as indirectly via IFN1 [58, 60]. There is evidence that the lack of dsRNA- or IFN1-inducible promoter elements in the non-pathway specific genes eventually impacts the ability of cells to up-regulate production of these proteins, as ERp57 and calreticulin levels remain unchanged following VHSV infection or poly(I:C) stimulation in RTS-11 cells [100]. Taken together, these results suggests that the ability to induce expression of the non-pathway specific members of the EAPP following sensing of dsRNA arose at some later point in evolutionary history, or in the lineage leading from lobe-finned fishes to tetrapods.

The location of the NF-κB binding sites also appears to be important in the regulation of EAPP members and *mx3* following poly(I:C) stimulation. Only genes with NF-κB binding sites within 20 bp of the start of the transcript (*tapasin* and *mx3*) reached peak up-regulation at 6 h post-stimulation at 20°C and the same magnitude at 48 h post-stimulation at 4°C.

Meanwhile, *b2m b* and *b2m d*, which each have a NF-κB binding site just over 100 bp upstream of the transcript start site, and *mhIa*, which does not have a putative NF-κB element, do not reach peak up-regulation until 24 h post-stimulation at 20°C, indicating that the more proximal element may be necessary for the earlier induction following stimulation with dsRNA, perhaps through the direct signalling pathway for NF-κB [58].

Due to two extra whole genome duplications relative to non-teleosts, salmonids are predicted to have multiple β2m gene copies [121]. Interestingly, only two of the six predicted β2m genes, *b2m b* and *b2m d*, contain an ISRE in their promoter, and as such, the up-regulation of β2m transcript levels following stimulation with poly(I:C) is likely due to an increase in expression of these paralogs. This suggests that *b2m b* and *b2m d* are inducible paralogs, perhaps illustrating a subfunctionalization from the ancestral gene [122]. Due to the highly conserved nature of the sequence, we were not able to develop a primer set that could distinguish between the transcript levels of each predicted β2m gene. Additionally, these predicted β2m genes do not seem to align with the β2m gene locus described by Magor et al. [96], suggesting that further study into their regulation and expression is required.

2.4.3 Inducible EAPP Transcript Level Up-regulation Delayed at 4°C

While constitutive EAPP transcript levels do not seem to be impaired at suboptimal temperatures, the same does not appear to be true for inducible transcript levels. In this study, up-regulation of all the pathway-specific EAPP genes was delayed following exposure to either poly(I:C) or VHSV IVb at the suboptimal temperature of 4°C relative to 20°C, with the exception of *b2m* following viral infection, which was not up-regulated at either test temperature. These findings are consistent with results from another rainbow trout cell line, the spleen macrophage-monocyte-like RTS-11, in which the inducible protein production of

all the pathway-specific members following VHSV infection was impaired at 2°C relative to 14°C, although the up-regulation of β2m at 14°C suggests that either transcription and translation of β2m is uncoupled during infection with the virus, or that the virus induces a different response in the different cell types [100]. However, in the Arctic charr cell line, ACBA, which has an optimal growth temperature of 20°C, no up-regulation of MH class I α or β2m protein levels was observed at 14°C following stimulation with poly(I:C) [117]. One potential explanation for this difference may be that the protein levels were only measured at 24 h post-stimulation. This time point may be too early to see any changes in protein production, since the transcript levels of these genes were not up-regulated until or after that time point in this study, even at the cell line's optimal growth temperature. At the very least, it appears that the induction of EAPP transcript level up-regulation in rainbow trout is impaired at suboptimal temperatures.

The effect of suboptimal temperatures on the transcript level up-regulation and secretion of IFN1 provides a potential explanation for the delay in inducible EAPP mRNA level up-regulation. *ifn1* transcript levels were highest at 3 h post-stimulation with poly(I:C) at 20°C and still up-regulated at 6 h post-stimulation, which is consistent with findings in the rainbow trout gonad cell line RTG-2 [77]. However, peak up-regulation of *ifn1* was not reached until 24 h post-stimulation at 4°C, with a prolonged response as increased transcript levels were still observed at 48 h post-stimulation. Furthermore, using a quantitative ELISA for rainbow trout IFN1, it is clear that IFN1 secretion is also delayed at the suboptimal temperature, which would result in delays in ISG expression, including for the EAPP-specific members due to the ISREs in their promoters. Similar effects on ISG expression have also been observed in Atlantic salmon injected with poly(I:C) at 6°C relative to 14°C, where the

peak magnitude of Mx expression is unchanged, but its occurrence is delayed and prolonged at the lower temperature [123]. Overall, it appears likely that the delays in the induction of ISGs, including the pathway-specific members of the EAPP, at suboptimal temperatures following poly(I:C) stimulation are at least partially due to the delayed transcript level up-regulation and secretion of IFN1.

It is less clear whether this is the case during VHSV IVb exposure, as a delay in IFN1 transcript level up-regulation was not observed at the time points studied. One potential explanation for this is that peak mRNA levels at 20°C may be reached at a point before 36 h post-infection, and therefore was not captured in this study. Alternatively, the known ability of the virus to suppress IFN1 induction, in addition to NF-κB activation, may have influenced the transcript level pattern, particularly at 20°C [45, 46]. Either way, it is likely that the delayed EAPP transcript level up-regulation at 4°C during viral infection is due partly to suppression of other immune signalling pathways in the cold, since suboptimal temperatures are known to generally suppress or delay most aspects of the immune system in teleosts [1].

2.4.4 Interaction of VHSV IVb with RTHDF at Suboptimal Temperatures

VHSV IVb appears to be able to attach/enter RTHDF cells at 4°C, but not transcribe genes or replicate at the suboptimal temperature. At 2 h post-infection, there was significantly more nucleocapsid protein in cell lysates at 4°C than at 20°C, with the protein levels hypothesized to act as a proxy for virions that have attached to and/or entered the cells. While this may indicate increased entry of VHSV IVb at the lower temperature, another possible explanation is that more virions have already uncoated at 20°C and subsequently, the nucleocapsid proteins for these virions have begun to be degraded [124]. However, the

virus does not seem to be capable of replicating effectively inside the cell, as no increase in N gene and transcript levels was seen over time at either temperature studied, which is in contrast to other studies in teleost cell lines [115, 125]. Additionally, the viral titres only increased by just under one order of magnitude at both temperatures, furthering the idea that viral replication is at most only occurring at low levels, especially when compared to results from other studies [115, 125]. Overall, these results suggest that the RTHDF cell line is non-permissive to VHSV IVb at both temperatures studied, indicating that the cellular immune response at both temperatures is sufficient to impair or inhibit viral replication, even with the delays in IFN1 transcript level up-regulation and secretion, and inducible EAPP mRNA levels, seen at 4°C. One potential explanation for this phenomenon might be that even though the initiation of the response seems to be delayed at 4°C, up-regulation of *ifn1* transcript levels seems to persist longer at the lower temperature, perhaps due to delays in shutting down the response. This would imply that rainbow trout cells are able to mount a delayed, albeit effective, antiviral response to VHSV IVb at 4°C. However, suboptimal temperature-induced delays may still compromise the host in some situations, such as when temperatures are closer to the thermal optimum for VHSV IVb, 14°C, or during infection with other pathogens [125], although further research will be required to elucidate whether this is the case.

Chapter 3: Impact of Suboptimal Temperatures on the EAPP in Walleye Skin Fibroblasts

3.1 Introduction

Walleye are an economically and ecologically important teleost species in Canada that evolutionarily diverged from rainbow trout approximately 206 million years ago, providing another interesting species model for studying the effects of suboptimal temperature on the EAPP in teleosts [10, 17, 18, 21]. There are a number of differences between the two divergent teleost species, including how walleye are a strictly freshwater species while salmonids such as rainbow trout have evolved to be anadromous, and that walleye fry have optimal growth at temperatures between 12°C and 29°C but rainbow trout fry grow optimally between 6°C and 12°C [13, 18]. Furthermore, the final temperature preferendum of adult walleye is 22.5°C which is approximately 6°C higher than that of rainbow trout, making walleye a warmer-water fish species compared to the salmonid, even though both species are capable of surviving at environmental temperatures as low as 0°C and face average winter water temperatures of approximately 2°C over the winter months in the Great Lakes [7, 12, 19]. As a result, there may be different evolutionary adaptations as to the regulation of the EAPP due to the different pressures exerted by temperature and life history on these two divergent teleost species.

WDSV, a positive-sense single-stranded RNA retrovirus, causes randomly distributed dermal sarcomas in infected walleye that appear and regress along a seasonal cycle and negatively impact fish value due to their unappetizing appearance [27, 29, 31]. WDSV tumours are composed of interwoven bundles of skin fibroblast cells, and the development

and regression of these tumours follow a seasonal cycle, with observation of tumours only occurring from late fall to spring, when environmental temperatures are lowest [27, 29, 31-33]. Furthermore, experimental studies have shown that the greatest amount of tumour development and regression occurs at temperatures below 10°C and above 15°C respectively, although such studies must use purified virus from tumours due to the lack of an *in vitro* system for propagation of the virus [27, 29, 32]. In addition, walleye that have been previously exposed to the virus are resistant to subsequent infection, implicating the adaptive immune system in the cycle of tumour development and regression [27, 31]. Due to the role of skin fibroblasts in the pathology of WDSV the walleye skin fibroblast cell line WESk-11 (Vo and Bols, unpublished) is an optimal *in vitro* model for further examining the temperature-EAPP relationship in walleye. The EAPP is one candidate pathway to be involved in the tumour development cycle, as constitutive transcript levels of pathway members β2m, MH class I α, and tapasin were all down-regulated in WESk-11 cells after 5 d at 4°C (Katzenback, Kellendonk and Dixon, unpublished). However, the effect of suboptimal temperature on inducible EAPP transcript levels remains to be studied in this species. My hypothesis was that suboptimal temperatures would delay induction of EAPP genes in the WESk-11 cell line. To test this hypothesis, inducible EAPP transcript levels were measured in the WESk-11 cell line at different temperatures, using poly(I:C), a synthetic dsRNA molecule, and VHSV IVb, which was used instead of WDSV due to the inability to propagate WDSV *in vitro* [27, 29, 32], to induce up-regulation.

3.2 Materials and Methods

3.2.1 Maintenance of Cell Lines

Walleye skin fibroblast (WESk-11), an adherent fibroblast cell line (Vo et al., unpublished), was maintained at 26°C in 75 cm^2 plug-seal, tissue culture treated flasks (Biolite, Fisher Scientific) containing complete media comprised of Leibovitz's L-15 medium (L-15; Lonza) supplemented with 100 U/mL penicillin (HyClone), 100 μg/mL streptomycin (HyClone), and 15% fetal bovine serum (FBS; Gibco). Cells were subcultured by washing cells with phosphate buffered saline (PBS; Lonza) followed by trypsin treatment using 0.25% trypsin-EDTA (HyClone). Cells were split 1:4 every 5-7 days and trypsin was inactivated with complete media to a total volume of 10 mL in each flask. Epithelioma papulosum cyprini (EPC), an adherent epithelial cell line derived from the skin of a fathead minnow [126] was maintained as described in *Section 2.2.1*.

3.2.2 Propagation and Titration of VHSV IVb

Viral haemorrhagic septicaemia virus (VHSV) IVb (CEFAS strain U13653) was propagated as described in *Section 2.2.2* [42] and titred as described in *Section 2.2.3*. The viral tire was calculated and expressed as tissue culture infectious dose ($TCID_{50}$/mL). The $TCID_{50}$/mL was determined to be 5.53×10^7 based on the titreing method described in *Section 2.2.3*, and was converted to 3.87×10^7 pfu/mL by multiplying by 0.7, based on the Poisson distribution [107].

3.2.3 Assessment of Poly(I:C)-Induced Loss of Adherence in WESk-11 Cells

Approximately 1×10^6 WESk-11 cells in 2 mL of complete media were seeded into six well tissue culture plates and parafilmed. After being allowed to adhere for 24 h at 26°C,

the plates remained at 26°C or were moved to 4°C incubators and acclimated for 1 d. Following acclimation, media was removed, and cells were either stimulated with 10 μg/mL, 1 μg/mL, 100 ng/mL, or 10 ng/mL of poly(I:C) in 2 mL of complete media, or the same volume of media without poly(I:C). Cells were incubated at the acclimated temperature for 72 h and phase contrast digital images were taken at 6 h, 24 h, 48 h, and 72 h post-stimulation.

3.2.4 Stimulation of WESk-11 Cells with Poly(I:C) for Transcript Level Studies

WESk-11 cells were seeded, allowed to adhere, and acclimated as described in *Section 2.2.4*. Following acclimation, media was removed, and cells were either stimulated with 25 ng/mL of poly(I:C) in 2 mL of complete media, or the same volume of media without the stimulant was added. Cells were then incubated at the acclimated temperature for 3 h, 6 h, 24 h, or 48 h, at which point RNA was extracted and synthesized into cDNA for use as a template in qRT-PCR, as described below in *Section 3.2.7* and *Section 3.2.9*, respectively. Four independent trials were conducted, utilizing WESk-11 cells between passages 12 and 22 and a separate 6-well plate at each time point.

3.2.5 Infection of WESk-11 Cells with VHSV IVb

WESk-11 cells were seeded and allowed to adhere as described in *Section 3.2.3*, and then acclimated for 1 d at either 20°C or 4°C. Following acclimation, cells were either infected with 2.5×10^6 $TCID_{50}$/mL of VHSV IVb (MOI = 3.5) in 2 mL of infection media, comprised of Leibovitz's L-15 medium (L-15; Lonza) supplemented with 100 U/mL penicillin (HyClone), 100 μg/mL streptomycin (HyClone), and 2% fetal bovine serum (FBS; Gibco), or 2 mL of infection media alone. After 2 h, infection media was removed and

replaced with 2 mL of complete media. At 36 h, 48 h, 72 h, and 96 h post-infection, media from one infected and one control well at each temperature was collected, and RNA extracted from adherent cells for use in cDNA synthesis (*Section 3.2.6*) and qRT-PCR (*Section 3.2.8*). At 8 d post-infection, only media was collected for use in determining $TCID_{50}$/mL. Viral titres were determined for each collected media sample as described in *Section 2.2.3.* Three independent trials were conducted, utilizing WESk-11 cells between passages 15 and 25 and a separate 6-well plate at each time point.

3.2.6 RNA Isolation and cDNA Synthesis

At each time point, media was removed from one well at each temperature for each sample type and replaced with 2 mL of incubation temperature PBS. The PBS was then aspirated and replaced with 600 μL of RLT buffer (Qiagen), and RNA was extracted using the Qiagen RNeasy Mini Kit according to the manufacturer's instructions. An on-column DNase I digestion step was performed, but with the addition of 30 μL of Thermo Fisher Scientific DNase I solution (1 × DNase, 1 × DNase buffer, and 8 × water by volume) to each column instead. Sub-samples of the extracted total RNA from randomly selected samples were electrophoresed on a 2% TAE gel to check the integrity of the RNA. The extracted total RNA was quantified using a Nanodrop 2000c Spectrophotometer (Thermo Scientific), and 500 ng was used to synthesize cDNA using the qScript cDNA Supermix Kit (Quanta Biosciences), according to the manufacturer's instructions. Synthesis reactions with no reverse transcriptase were also randomly performed and used in RT-PCR to verify the effectiveness of the DNase I treatment. Synthesized cDNA was stored at -80°C until all samples were collected, and then analyzed by quantitative reverse-transcriptase PCR (qRT-PCR) (described below in *Section 3.2.8*).

3.2.7 qRT-PCR Primer Validation

Quantitative real-time PCR (qRT-PCR) primers used in this study are listed in **Table 3.1**. Primer efficiency and validation was previously performed using the same methods as described in *Section 2.2.8* (Katzenback, Kellendonk, and Dixon, unpublished).

Table 3.1 qRT-PCR primers used in Chapter 3. Dir is the direction of the primer, with S and AS representing sense and antisense primers respectively. Eff% is the percent efficiency of the specified primer set. All primer sequences and sets were previously designed and validated (Katzenback, Kellendonk and Dixon, unpublished).

Gene	Dir	Sequence 5'-3'	Slope	R^2	Eff%
ef1a	S	GTCAGAGTCTCGTGGTGCAT	-3.485	0.999	93.62
	AS	GTATGGTCGTCACCTTCGCT			
b2m	S	AGCCCTGGTAGCTGTCTCAT	-3.348	0.998	93.97
	AS	TCCCGTACTCTCCTGGATGG			
mhIa	S	GAGGGACGATCTGTTCTCAGCA	-3.436	0.993	95.45
	AS	GACAAAGCTTGGATAGCTCAGAGT			
tapasin	S	ACTATTACGCGTGCTCCCAC	-3.395	0.999	97.04
	AS	AACCCAGAAGCTGCAATCCA			

3.2.8 qRT-PCR

qRT-PCR was performed using a Quant Studio 5 thermocycler (Applied Biosystems) and SYBR Green chemistry (Applied Biosystems). Each reaction consisted of 2.5 μL of cDNA template diluted 1:40 in molecular grade water, 5 μL of Power Up SYBR Green Master Mix (Applied Biosystems), and 2.5 μL of a 2 μM primer stock containing sense and antisense primers (Sigma). The run protocol consisted of a UDG activation step of 50°C for 2 min, followed by an initial denaturation step of 95°C for 2 min, and 40 cycles of 95°C for 1 s, and 60°C for 30 s. A melt curve step was added following thermocycling, and involved ramping from 60°C to 95°C at 3°C every 30 s.

Candidate reference gene selection was performed as described in *Section 2.2.9*. The candidate reference gene that produced the lowest m-value using the Relative Quantification Analysis application (Applied Biosystems) was used as an endogenous control, with a maximum acceptable m-value of 0.5 [113]. Chosen candidate reference genes are listed with their respective m-values in the figure legend for each set of experiments.

All samples were run in triplicate for target and control genes. For each set of trials, the control sample from the earliest time point at 26°C or 20°C was used as a calibrator, depending on the experiment.

3.2.9 RT-PCR for VHSV IVb N Gene and Transcript Levels

RT-PCR amplification of the VHSV N gene (S - 5' AGGACCCCAGACTGTGCAAGC 3'; AS - 5' TCCGCCTGGCTGACTCAACA 3') [115] was performed as described in *Section 2.2.13* using the cDNA samples obtained in *Section 3.2.6*. *ef1a* (primer sequence in **Table 3.1**) was used as a control gene.

3.2.10 Data Analysis

qRT-PCR data from *Section 3.2.4* and *Section 3.2.5* were analyzed statistically with a Poisson-lognormal generalized mixed model and a Markov Chain Monte Carlo procedure using the MCMC.qPCR package [116] implemented in R, which infers changes in transcript levels of all genes from the joint posterior distributions of parameters. The determined control gene for each set of experiments was specified as an endogenous control and data was shown as mean $\log_2$ (fold change) with 95% credible intervals. The 95% credible intervals are the Bayesian equivalent of frequentist confidence intervals, and represent the interval containing the true value of the parameter with 95% probability. Effects were

deemed to be statistically significant between groups where credible intervals did not overlap.

Viral titre data from *Section 3.2.5* was analyzed statistically by two-way analysis of variance with Bonferroni post hoc test for comparison of means using GraphPad Prism (GraphPad Software, Inc.). Data was shown as mean ± standard error, and differences were considered significant between times at a specific temperature when $P < 0.05$.

3.3 Results

3.3.1 WESk-11 Cell Adherence Following Poly(I:C) Stimulation

First, to assess whether stimulation with poly(I:C) would negatively impact cell adherence at 4°C, WESk-11 cells were stimulated with the synthetic dsRNA at both 26°C (**Figure 3.1 and 3.2**) and 4°C (**Figure 3.3 and 3.4**), and observed via phase contrast microscopy over 72 h. At 26°C, no loss of adherence was observed over the 72 h window (**Figure 3.1 and 3.2**). However, at 4°C, WESk-11 cells lost adherence in a dose-dependent manner following stimulation with poly I:C (**Figure 3.3 and 3.4**). By 24 h post-stimulation with 10 μg/mL of poly I:C, a concentration used in studies with rainbow trout cells (**Figure 3.3**), most WESk-11 cells had lost adherence, and this was true at 48 h following stimulation with 1 μg/mL and 100 ng/mL of poly(I:C) (**Figure 3.4**). Following stimulation with 10 ng/mL of poly(I:C), cells began to lose adherence at 48 h post-stimulation, but most cells appeared to remain adherent at 72 h post-stimulation (**Figure 3.4**).

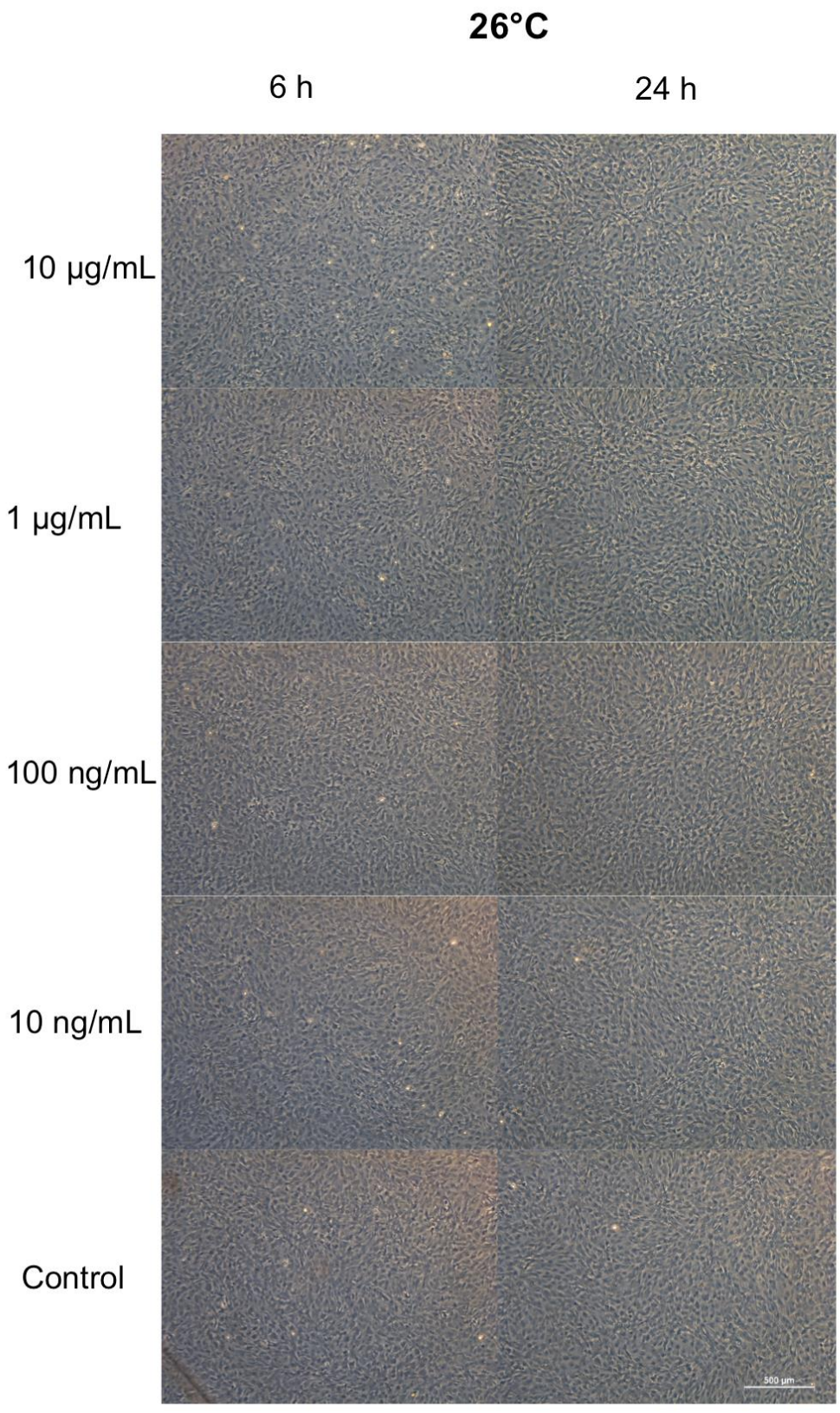
26°C
6 h
24 h
10 µg/mL
1 µg/mL
100 ng/mL
10 ng/mL
Control
500 µm

Figure 3.1 Poly(I:C)-induced loss of adherence in WESk-11 cells after 6 h and 24 h at 26°C. Cells were acclimated for 1 d at 26°C, and then stimulated with 10 μg/mL, 1 μg/mL, 100 ng/mL, or 10 ng/mL poly(I:C), or an equal volume of media alone (control). Phase contrast digital images (50× magnification) were taken from one well at each concentration at 6 h and 24 h post-stimulation. Scale bar = 500 μm.

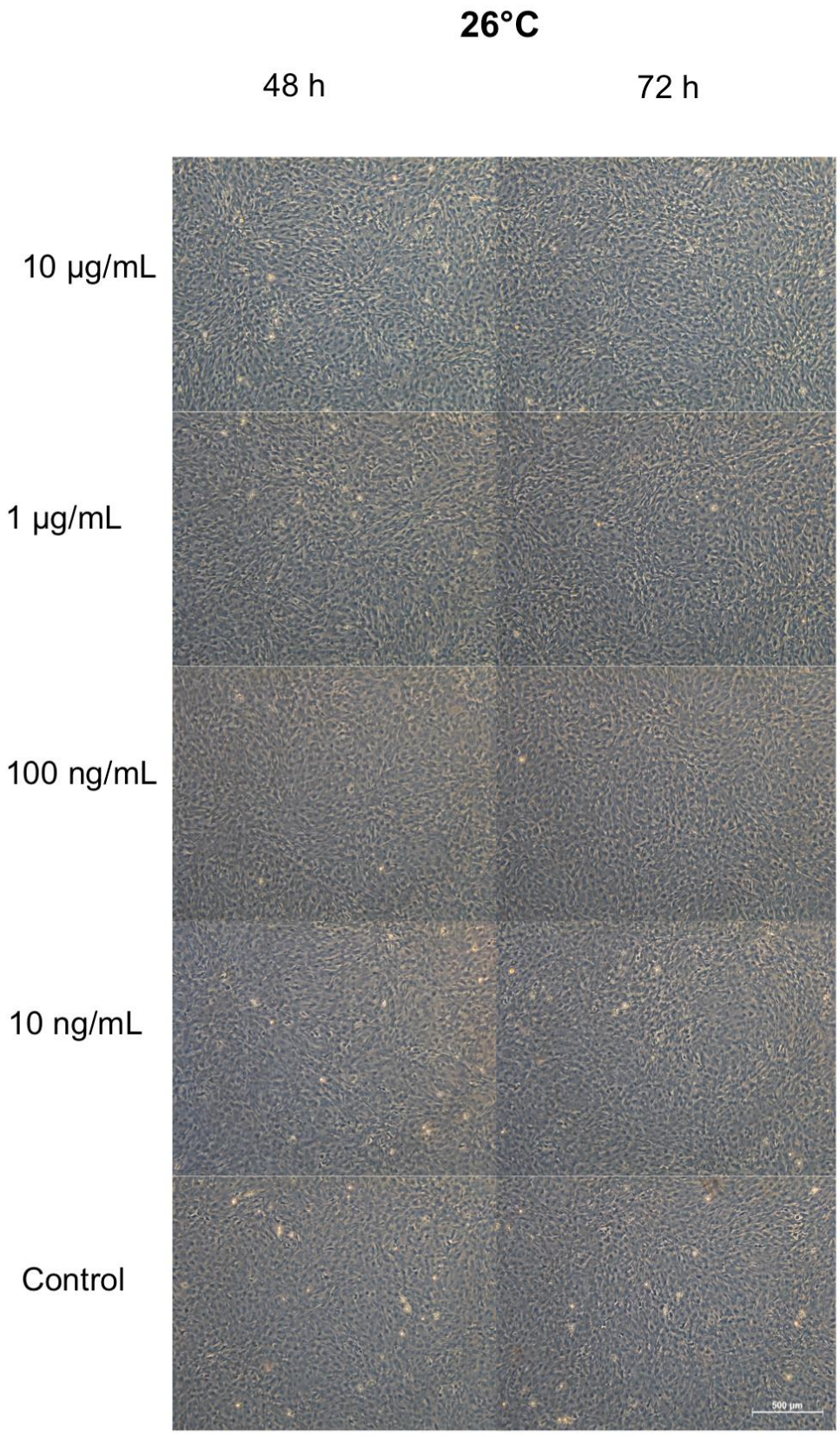
26°C
48 h
72 h
10 µg/mL
1 µg/mL
100 ng/mL
10 ng/mL
Control
500 µm

Figure 3.2 Poly(I:C)-induced loss of adherence in WESk-11 cells after 48 h and 72 h at 26°C. Cells were acclimated for 1 d at 26°C, and then stimulated with 10 μg/mL, 1 μg/mL, 100 ng/mL, or 10 ng/mL poly(I:C), or an equal volume of media alone (control). Phase contrast digital images (50× magnification) were taken from one well at each concentration at 48 h and 72 h post-stimulation. Scale bar = 500 μm.

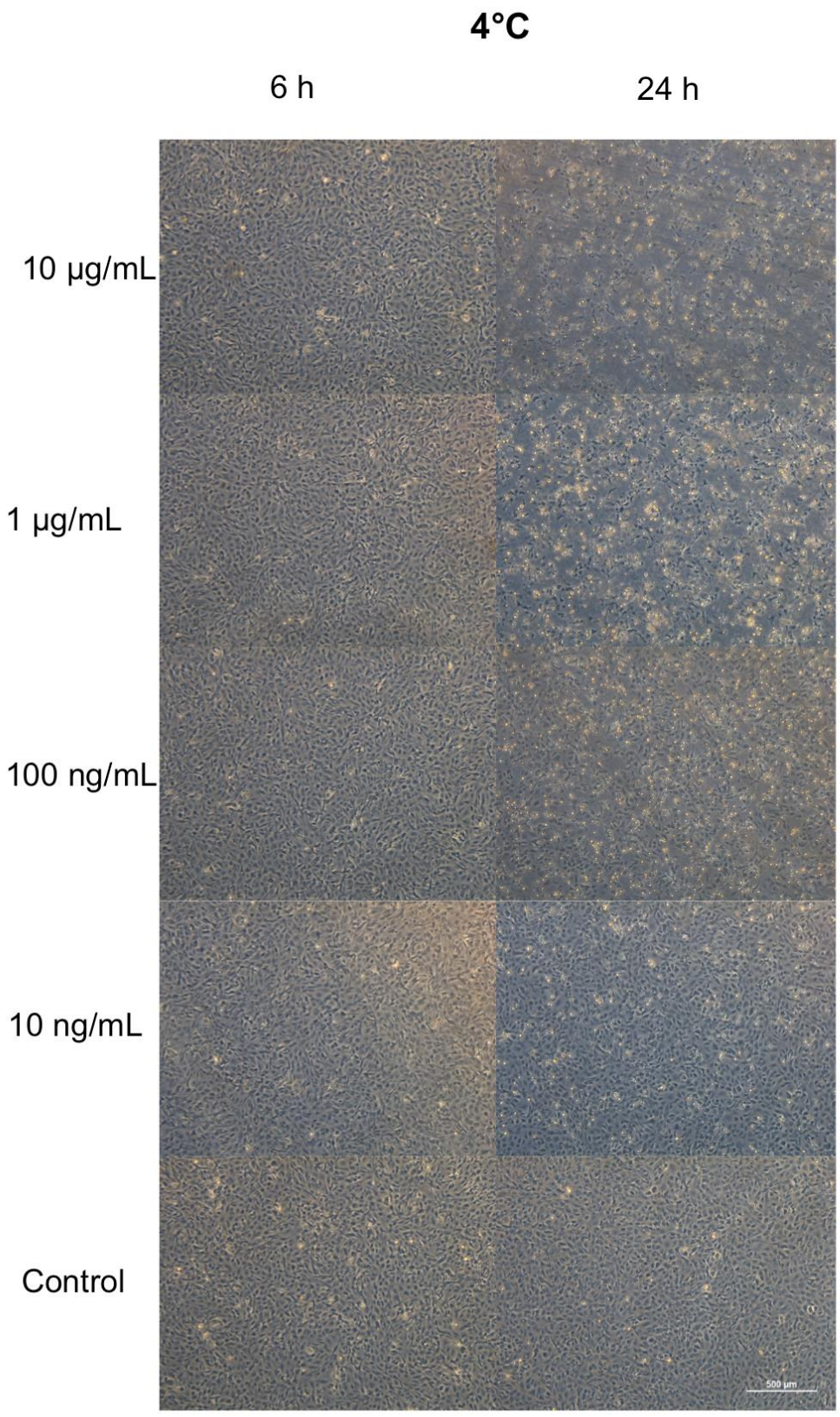
4°C
6 h
24 h
10 µg/mL
1 µg/mL
100 ng/mL
10 ng/mL
Control
500 µm

Figure 3.3 Poly(I:C)-induced loss of adherence in WESk-11 cells after 6 h and 24 h at 4°C. Cells were acclimated for 1 d at 4°C, and then stimulated with 10 μg/mL, 1 μg/mL, 100 ng/mL, or 10 ng/mL poly(I:C), or an equal volume of media alone (control). Phase contrast digital images (50× magnification) were taken from one well at each concentration at 6 h and 24 h post-stimulation. Scale bar = 500 μm.

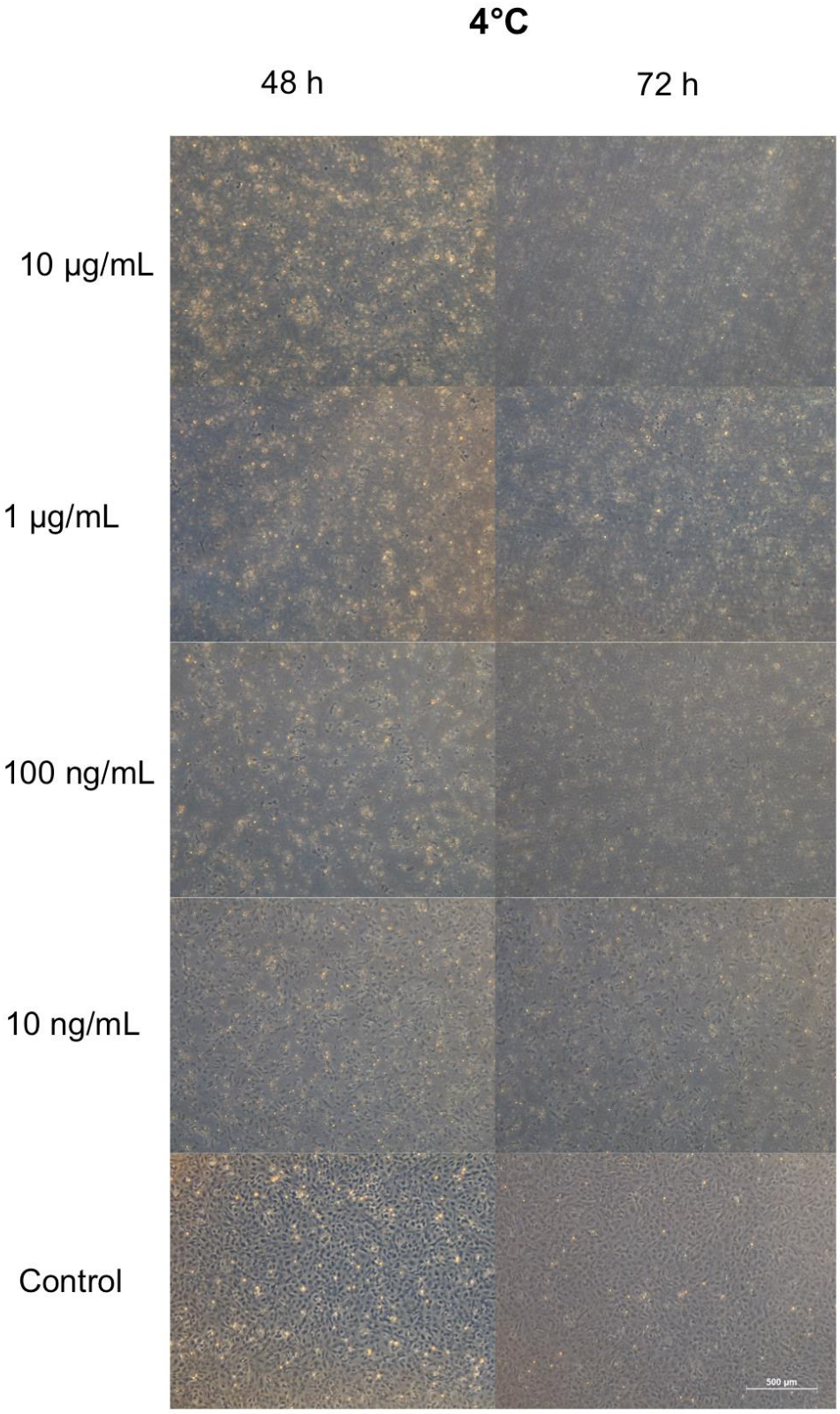
4°C
48 h
72 h
10 µg/mL
1 µg/mL
100 ng/mL
10 ng/mL
Control
500 µm

Figure 3.4 Poly(I:C)-induced loss of adherence in WESk-11 cells after 48 h and 72 h at 4°C. Cells were acclimated for 1 d at 4°C, and then stimulated with 10 μg/mL, 1 μg/mL, 100 ng/mL, or 10 ng/mL poly(I:C), or an equal volume of media alone (control). Phase contrast digital images (50× magnification) were taken from one well at each concentration at 48 h and 72 h post-stimulation. Scale bar = 500 μm.

3.3.2 Effect of Temperature on Inducible EAPP Transcript Levels Following Poly(I:C) Stimulation

Next, the effect of suboptimal temperature on inducible EAPP transcript levels following stimulation with 25 ng/mL of poly(I:C) was examined. This dose was chosen to maximize the stimulation of the cells while simultaneously minimizing loss of adherence in the majority of the cells at 4°C over 72 h, based upon the results from **Figure 3.4** where most cells appeared to remain adherent over this time frame at the suboptimal temperature. mRNA levels of the pathway-specific members of the EAPP (*b2m*, *mhIa*, and *tapasin*) were measured at 3 h, 6 h, 24 h, 48 h, and 72 h post-stimulation with poly(I:C) following a 1 d acclimation to either 26°C or 4°C (**Figure 3.5**). The genes *b2m* (**Figure 3.5A**) and *mhIa* (**Figure 3.5B**) shared a similar pattern of regulation, where the transcript levels were significantly higher relative to the 26°C unstimulated samples, but not the 4°C samples, from 24 h to 72 h post-stimulation, with peak up-regulation of approximately 4-fold. No differences in transcript levels were observed at any time point for either gene at 4°C. However, this pattern was not shared for *tapasin* (**Figure 3.5C**), as significant up-regulation relative to the controls at both study temperatures was seen at 26°C from 6 h onwards, reaching a peak up-regulation of approximately 10-fold and then beginning to fall at 72 h post-stimulation. Furthermore, up-regulation of *tapasin* at 4°C was delayed until 72 h post-stimulation (**Figure 3.5C**).

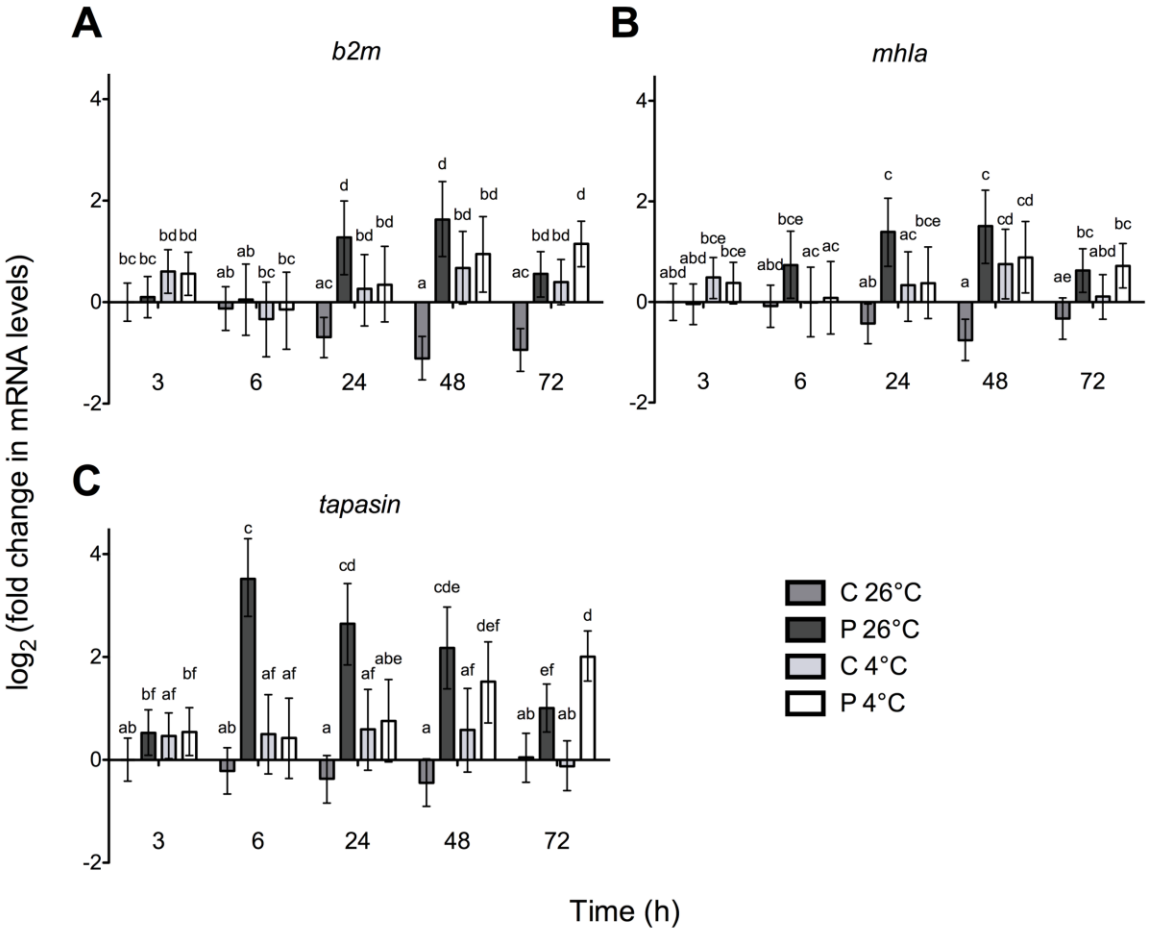

Figure 3.5 Relative mRNA levels of EAPP members in WESk-11 cells in response to poly(I:C) stimulation at different temperatures over time. Cells were acclimated for 1 d at either 26°C or 4°C, and then stimulated with 25 ng/mL poly(I:C), or an equal volume of media alone (control). Transcript levels of *b2m* (A), *mhIa* (B), and *tapasin* (C) were evaluated at 3 h, 6 h, 24 h, 48 h, and 72 h post-stimulation via qRT-PCR. Data was analyzed statistically via a Poisson-lognormal generalized mixed model with a Markov-chain Monte Carlo procedure and *ef1a* (m-value = 0.210) specified as an endogenous control. Data is shown as mean $\log_2$ (fold change) relative to the unstimulated 26°C group at 3 h post-stimulation with 95% credible intervals (n = 4), and values are statistically significant between groups where credible intervals do not overlap, or where letters are different.

3.3.3 Impact of Suboptimal Temperature on the Infection of WESk-11 Cells with VHSV IVb

Analysis of the transcript and gene levels of the VHSV IVb nucleocapsid (N) gene and viral titres of supernatants from infected WESk-11 cells were performed to assess the ability of the virus to replicate in the WESk-11 cell line at 20°C and 4°C in order to determine the suitability of this infection model for studies of the EAPP at suboptimal temperatures (**Figure 3.6**). For these experiments, 20°C was used as the control temperature instead of 26°C since the virus does not appear to be able to replicate in cells at the higher temperature [125]. N gene and transcript levels increased over time at 20°C, but only a small increase in these levels, if any, was observed at 4°C (**Figure 3.6A**). However, significant increases in viral titres were seen over time at both study temperatures, with an increase of approximately two orders of magnitude by 2 d post-infection at 26°C, and one order of magnitude by 8 d post-infection at 4°C (**Figure 3.6B**).

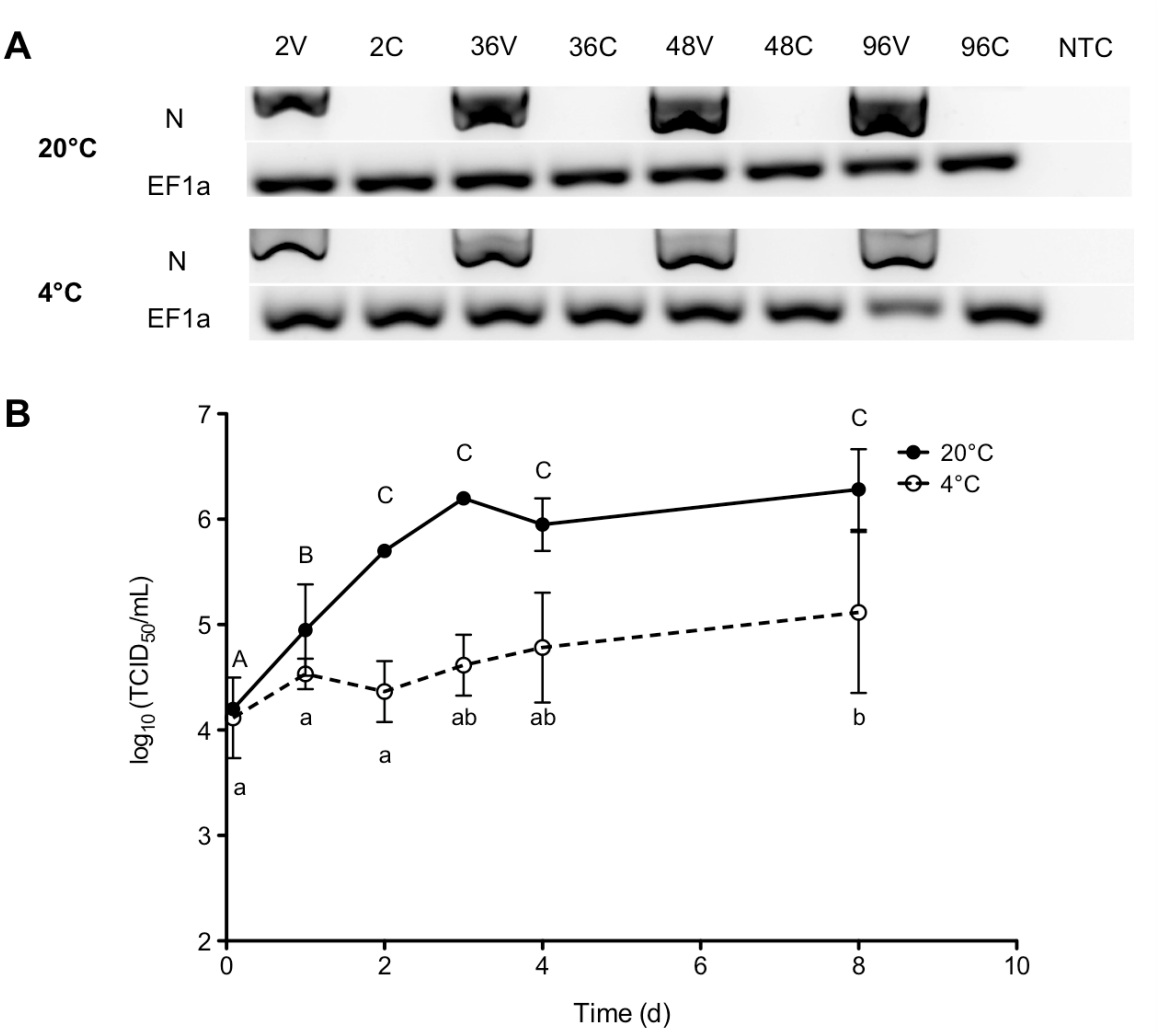

Figure 3.6 Effect of temperature on VHSV IVB attachment/entry, and replication in WESk-11. (A) N gene and transcript levels were studied in cells infected at either 20°C or 4°C at 2 h, 24 h, 48 h and 96 h post-infection with the virus. (B) Viral titres from VHSV-infected WESk-11 cell supernatants at either 20°C or 4°C at 2 h, 1 d, 2 d, 3 d, 4 d and 8 d post-infection were measured. Differences in viral titres over time for each temperature were analyzed by two-way ANOVA with Bonferroni post-hoc test. Data is shown as mean log10 ($TCID_{50}$/mL) ± standard error (n = 3) and values are statistically significant ($P < 0.05$) over time where letters are different (capitalized for 20°C, uncapitalized for 4°C).

3.3.4 Inducible EAPP Transcript Level Up-regulation Following VHSV IVb Infection

Finally, the effect of suboptimal temperature on inducible EAPP transcript levels following infection with live VHSV IVb was examined to see how this response differs from the response to poly(I:C). mRNA levels of the pathway-specific members of the EAPP (*b2m*, *mhIa*, and *tapasin*) were measured at 24 h, 48 h, 72 h, and 96 h post-infection with VHSV IVb following a 1 d acclimation to either 20°C or 4°C (**Figure 3.7**). As was the case following stimulation with poly(I:C), *b2m* (**Figure 3.7A**) and *mhIa* (**Figure 3.7B**) shared a similar pattern of regulation, whereby at 20°C the mRNA levels of *b2m* and *mhIa* were higher relative to the time- and temperature-matched control at all time points, with a peak up-regulation of approximately 4-fold, but only at 96 h post-infection relative to the 4°C samples. In addition, there was no difference in mRNA levels of b2m (**Figure 3.7A**) and *mhIa* (**Figure 3.7B**) between infected and control cells at 4°C at any time point. The pattern of mRNA levels for *tapasin* (**Figure 3.7C**) was again different from that of *b2m* and *mhIa* following infection at 20°C, with up-regulation at all time points studied, and peak up-regulation of approximately 9-fold. However, *tapasin*, like *b2m* and *mhIa*, was not up-regulated at any time post-infection at 4°C (**Figure 3.7C**).

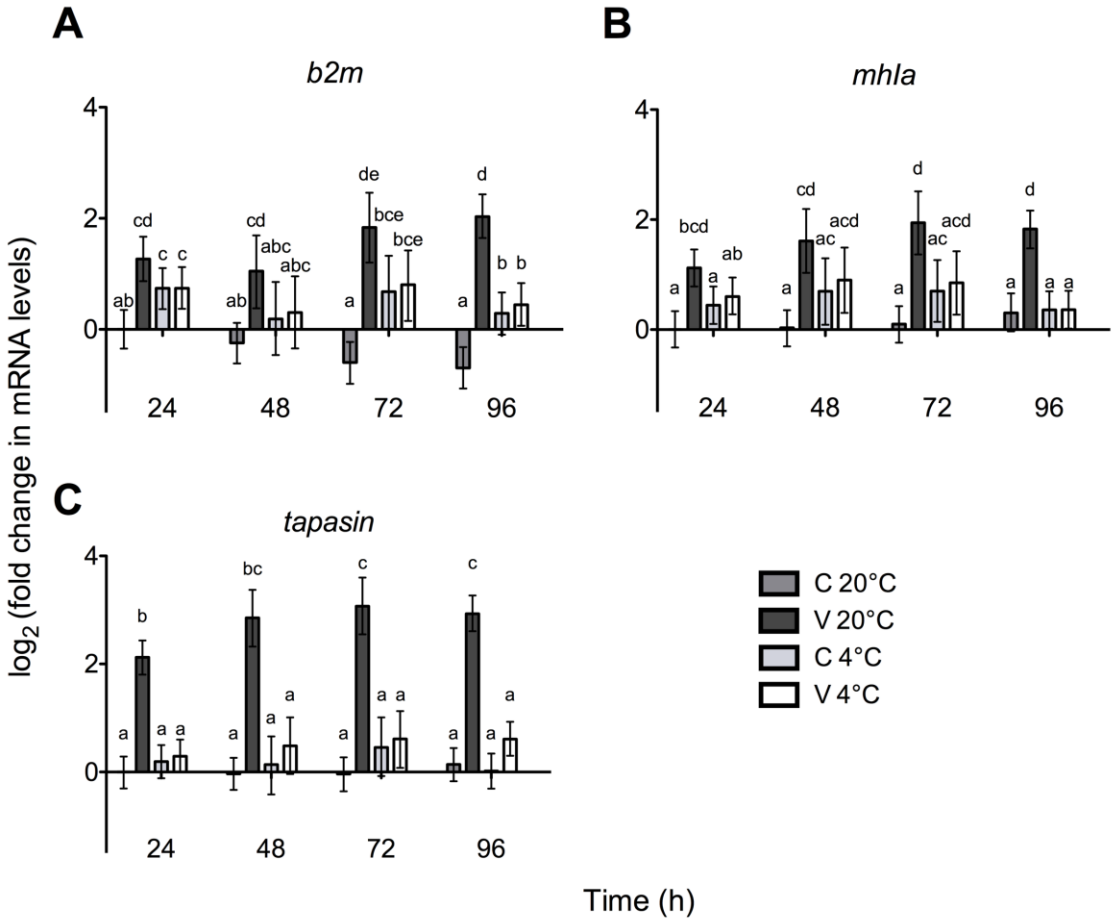

Figure 3.7 Relative transcript levels of EAPP members in WESk-11 cells following infection with VHSV IVb at different temperatures over time. Cells were acclimated for 1 d at either 20°C or 4°C, and then infected with VHSV IVb at an MOI of 3.5, or an equal volume of media alone (control). Transcript levels of *b2m* (A), *mhIa* (B), and *tapasin* (C) were evaluated at 24 h, 48 h, 72 h, and 96 h post-stimulation via qRT-PCR. Data was analyzed statistically via a Poisson-lognormal generalized mixed model with a Markov-chain Monte Carlo procedure and *ef1a* (m-value = 0.272) specified as an endogenous control. Data is shown as mean $\log_2$ (fold change) relative to the non-stimulated 20°C group at 24 h post-stimulation with 95% credible intervals (n = 3), and values are statistically significant between groups where credible intervals do not overlap, or where letters are different.

3.4 Discussion

3.4.1 Inducible EAPP Transcript Up-regulation Impaired at 4°C in WESk-11 Cells

Suboptimal temperature appears to impair inducible EAPP transcript level up-regulation in WESk-11 cells, as no increase in transcript levels of the pathway-specific members (*b2m*, *mhIa*, and *tapasin*) were seen at 4°C at any time point following poly(I:C) stimulation or VHSV IVb infection, with the exception of *tapasin* following poly(I:C) stimulation, where up-regulation was delayed at 4°C from 6 h to 72 h post-stimulation relative to 26°C. Since inducible *tapasin* transcript levels at 26°C occurred earlier than for *b2m* and *mhIa* following stimulation, it is possible that increased mRNA levels of these genes were also delayed at 4°C, but to a time point beyond 72 h post-stimulation. Interestingly, the cells do appear to be able to respond to poly(I:C), as evidenced by the eventual loss of adherence at 4°C (**Figure 3.4**), which also supports the idea that increases of *b2m* and *mhIa* mRNAs might be delayed at 4°C to a time point beyond 72 h post-stimulation. However, there was no evidence of any up-regulation in any of the EAPP-specific members at 4°C following infection with VHSV IVb. These results are consistent with those from the rainbow trout spleen macrophage-monocyte like cell line RTS-11, where inducible protein production of the EAPP-specific members was impaired at 2°C relative to 14°C following VHSV infection, and the arctic charr bulbous arteriosus cell line ACBA, where no up-regulation of MH class I α or β2m protein levels was observed at the suboptimal temperature of 14°C following stimulation with poly(I:C) [100, 117]. However, only one time point was used for the aforementioned experiments with RTS-11 and ACBA so it is unclear whether delayed induction at the suboptimal temperature would have occurred at a later point in these

cell lines. On the whole though, it appears that the induction of EAPP transcript level up-regulation is impaired at suboptimal temperatures in walleye, as it is for other teleost species.

3.4.2 Interaction of VHSV IVb with WESk-11 at Suboptimal Temperatures

WESk-11 cells appear to be permissive to VHSV IVb at both 20°C and 4°C. N gene and transcript levels increased over time at 20°C, suggesting that early transcription of viral genes and/or viral genome replication is occurring at this temperature, but little to no increase in these levels was observed at 4°C. However, the pattern of transcript and gene levels at the suboptimal temperature was similar to that of the walleye caudal fin fibroblast cell line WE-cfin11f, and N protein levels did increase over time at 4°C in this cell line, suggesting that N gene expression may also be occurring in infected WESk-11 cells at 4°C but at a slower rate than at 20°C [44]. Furthermore, viral titres increased over time at both study temperatures in WESk-11, but at different rates, with an increase of one order of magnitude taking 1 d at 20°C but 8 d at 4°C, implying that while the WESk-11 cells are permissive to VHSV IVb at both 20°C and 4°C, viral replication is slower at the suboptimal temperature. The decreased rate of viral replication is not necessarily indicative of a less problematic infection, as increases in viral titres were similarly delayed in the WE-cfin11f cell line, but the levels did not plateau over the time course assayed at 4°C as they did after 14 d at 14°C, steadily increasing over 28 d post-infection, suggesting that viral titres might have also increased further in this study if later time points were studied [44]. These results suggest that at suboptimal temperatures, VHSV IVb has a reduced replication rate in walleye cells but might be capable of sustaining a longer-lasting infection than at more optimal temperatures for the host. The potentially longer-lasting infections at the suboptimal temperature would coincide with the complete inability to up-regulate EAPP transcript levels over the first 96 h post-

infection at 4°C, indicating the cellular antiviral response may be impaired at this temperature. Additionally, the impairment of EAPP transcript level regulation following viral infection lends support to the idea that this pathway may be involved in the etiology of walleye dermal sarcoma virus tumourigenesis. As a retrovirus, WDSV could integrate into the genome and remain latent after infecting walleye in the spring, until temperatures have decreased sufficiently in the late fall to impair regulation of endogenous antigen presentation [27, 29, 32, 34]. At this time, the virus would be able to replicate with less opposition from the immune system of the fish, allowing for development of the dermal tumours. On the whole, further research regarding the role of the walleye EAPP in WDSV etiology at suboptimal temperatures will be needed to substantiate this hypothesis, but regulation of the walleye EAPP does seem to be impaired at suboptimal temperatures.

Chapter 4: General Discussion and Future Directions

Suboptimal temperatures have been shown to generally impact immune pathways in teleosts negatively by causing delays and/or decreases in the functions of these pathways, potentially leading to increased disease susceptibility at lower temperatures [1]. Previous studies in teleosts attempting to discern the effect of such temperatures on the EAPP have been inconsistent between species. In this thesis, the rainbow trout hypodermal fibroblast cell line RTHDF and the walleye skin fibroblast cell line WESk-11 were used as models to further ascertain the effects of suboptimal temperature on the teleost EAPP and the potential role of IFN1 in regulating this pathway. While suboptimal temperatures impaired regulation of inducible EAPP transcript levels in both cell lines, this impairment was more pronounced for the WESk-11 cells. Moreover, IFN1 was implicated in the regulation of the pathway-specific members of the EAPP (*b2m*, *mhIa*, and *tapasin*) in rainbow trout, and as such, the delays in transcript level up-regulation and secretion of IFN1 at 4°C in the RTHDF cell line may provide a partial explanation for the observed delays in inducible EAPP transcript levels at the suboptimal temperature. Finally, the permissiveness of the cell lines to VHSV IVb infection differed at both temperatures studied, providing an interesting perspective with which to examine the potential repercussions of the impairments in EAPP gene regulation at suboptimal temperatures in the two different species. These findings and their larger-scale implications are discussed in the following subsections of Chapter 4, along with proposed future directions to expand upon the results of this thesis.

4.1 Suboptimal Temperature Impairs Regulation of EAPP Genes

Suboptimal temperatures caused greater impairment of the regulation of inducible EAPP transcript levels in the WESk-11 cell line than the RTHDF cell line, suggesting that

rainbow trout may be better adapted evolutionarily to respond to pathogen challenges than walleye at such temperatures. Furthering this idea, while constitutive levels of EAPP transcripts were not effected by suboptimal temperature in RTHDF cells, previous work in the WESk-11 cell line showed that these temperatures caused decreases in mRNA levels of the pathway-specific members of the EAPP (*b2m*, *mhIa*, and *tapasin*) over time at 4°C (Katzenback, Kellendonk, and Dixon, unpublished). Looking at similar studies in other teleosts, it appears that regulation of constitutive EAPP transcript levels is not affected in other members of the salmonids (Atlantic salmon and Arctic charr), but is also impaired in the common carp, a member of the cyprinids [102, 103, 117]. These results suggest that salmonids may have adapted to be able to regulate EAPP transcript levels at suboptimal temperatures more effectively than other teleosts, which could help them maintain presentation of endogenous antigens when exposed to low temperatures over the winter months and during extreme cold weather events, potentially decreasing their relative susceptibility to infection during these periods. Perhaps this improved ability to regulate EAPP mRNA levels at suboptimal temperatures arose as a consequence of the environmental temperatures experienced by these species, as the three salmonid species mentioned all prefer water temperatures of less that than 16°C, while walleye and carp prefer 23°C and 32°C respectively, allowing the salmonids to fulfill ecological niches with lower water temperatures [12, 118, 119]. Another complementary explanation may come from the life history of these species, as salmonids have evolved to be anadromous while walleye and carp are strictly freshwater species [13, 18]. Anadromous fish have to transition from freshwater to saltwater during smoltification and then be tolerant of marine conditions that include surface sea temperatures ranging from approximately 7°C to 13°C on average over the course

of a year along Canadian coasts [127, 128]. During this exposure to suboptimal temperatures that can last multiple years, the ability to maintain endogenous antigen presentation would be important for fighting off challenges from pathogens in the marine environment.

Moving forward, it will be important to further validate the transcript level results regarding the EAPP and suboptimal temperatures at the protein level, *in vivo*, and in other species. Transcription and translation are not always coupled, and therefore similar experiments examining the regulation of EAPP proteins at suboptimal temperatures should be performed to corroborate these transcriptional results at a more functional level, either through FACS analysis as described by Rodrigues et al. [102] or western blotting as shown by Sever et al. [100]. Furthermore, these results should be verified *in vivo* to determine the relevance of these findings, as the results from a single cell type may not be reflective of the integrated physiological response at the organismal level. However, constitutive transcript levels of β2m have been previously examined in rainbow trout peripheral blood leukocytes *in vivo* at suboptimal temperatures, and levels were stable at 4°C as was seen in the RTHDF cell line, lending confidence that these *in vitro* results will correlate to the level of a whole fish. It would also be interesting to examine the impacts of suboptimal temperatures in other species, both within and outside of Teleostei. Like teleosts, amphibians are poikilothermic and cannot regulate their internal body temperature [129]. While there is also evidence of impaired immune function and response to pathogen challenge at suboptimal temperatures in amphibians, no one has examined this in the context of the EAPP, which would be useful in ascertaining whether suboptimal temperature impairs regulation of the EAPP in all poikliothermic vertebrates or only in teleosts [130, 131].

4.2 Role of IFN1 in the Regulation of the Rainbow Trout EAPP

The impairment in inducible EAPP transcript up-regulation at suboptimal temperatures following stimulation with poly(I:C) in rainbow trout might be partially explained by the delayed transcript level up-regulation and secretion of IFN1 seen in RTHDF cells at 4°C. All of the pathway-specific members of the EAPP in rainbow trout were found to have ISREs in their promoters, suggesting that these genes may be regulated by type I IFN signalling [61, 78]. Interestingly, since the non-pathway specific members did not have ISREs, it appears that the regulation of these genes has been uncoupled from that of the pathway-specific members, unlike in mammals where all of the members of the EAPP are known to be ISGs [62]. The speculated differences in regulation between rainbow trout and mammals are supported by previous studies in rainbow trout cells that have shown that *calreticulin* is not up-regulated under the same conditions as in mammals, including following stimulation with poly(I:C) [93]. Perhaps this set-up is more efficient for rainbow trout, whereby they only have to up-regulate levels of the pathway-specific members during infection to induce more endogenous antigen presentation. Alternatively, increasing levels of the non-pathway-specific members may have adverse effects due to their roles in other pathways in the ER, although further study would be needed to determine if either of these potential explanations is correct. On the whole, these results suggest that the delays in IFN1 transcript level up-regulation and secretion in the rainbow trout cells may be involved in the impairment in inducible EAPP transcript levels. This impairment in IFN1 up-regulation also portends larger issues for teleosts at suboptimal temperatures, as it implies that the entire antiviral response, including the EAPP, will be compromised when they are exposed to such temperatures, such as over the winter months and during extreme low temperature events.

Experimentally, this concept has been shown in rainbow trout fry where viral replication of infectious pancreatic necrosis virus increased and *ifn1* transcript levels decreased with decreasing temperature, implying that it will be easier for viruses to establish infection in fish at suboptimal temperatures [132].

In order to lend more support to these claims it will be important to verify that IFN1 regulates the EAPP, and to examine this relationship in walleye and other species. One potential way to confirm that IFN1 regulates the EAPP would be to stimulate RTHDF cells with purified recombinant rainbow trout IFN1 and measure EAPP mRNA levels to see if the recombinant cytokine can induce up-regulation of the EAPP genes. Then, electrophoretic mobility shift assays could be performed to show that activated transcription factors are binding specifically to the ISRE. In addition, NF-κB also appears to play a role in the regulation of the EAPP genes as only *tapasin* has an NF-κB binding site within 20 bp of the start of the transcript, as does *mx3*, a typical rainbow trout ISG. The presence of the NF-κB binding site correlates with the earlier up-regulation of *tapasin* and *mx3* relative to *b2m* and *mhIa* following poly(I:C) stimulation, suggesting that NF-κB might be responsible for early ISG up-regulation following sensing of dsRNA, and as such offers another candidate pathway to be examined at suboptimal temperature. It would also be important to examine the effect of suboptimal temperature on IFN1 in other species, including walleye, although the analogous type I IFN sequence in walleye would first need to be identified. There was a large difference in sensitivity to poly(I:C) between the two cell lines, as evidenced by the ability to induce similar up-regulation in transcript levels of EAPP genes at a dose that was almost three orders of magnitude smaller in the WESk-11 cells than the RTHDF cells. Perhaps differences in the abundance and function of different surface and intracellular

sensors of dsRNA between the two cell lines might account for this increased sensitivity to poly(I:C), although it is unclear if such differences would impact regulation of IFN1 in the cells or at an organismal level. In addition, the pattern of regulation of the EAPP-specific genes following poly(I:C) stimulation resembled the pattern in the RTHDF cell line, whereby *tapasin* reached peak up-regulation earlier than *b2m* and *mhIa* at 26°C. This correlation implies that transcriptional regulation of the EAPP genes following sensing of dsRNA has been conserved between these two teleost species that diverged 206 million years ago [10]. Therefore, it is likely that IFN1 regulation may also be impaired at suboptimal temperatures in this species, and perhaps to a greater degree than in rainbow trout, a more cold-adapted species. Moreover, colder temperatures have also been implicated in impairment of antiviral responses in mice, where they allow for infection in the extremities, suggesting that the issue of suboptimal temperatures impacting antiviral responses may extend beyond the Teleostei, providing further avenues of study for this complex issue [133].

4.3 Role of Suboptimal Temperature in Viral Infections

Suboptimal temperatures had differing effects on permissiveness to VHSV IVb in the RTHDF and WESk-11 cell lines, underscoring the complexities of the effect of suboptimal temperature on host-pathogen interactions. VHSV IVb appeared to be able to cause infection over a more prolonged period of time in the WESk-11 cell line at 4°C relative to 20°C, perhaps taking advantage of impairments in the cellular antiviral response that could prevent clearance of viral pathogens in the cold, as evidenced by the complete impairment of inducible EAPP transcript levels at 4°C. The prolonged infection model at low temperature is also consistent with results from the walleye caudal fin fibroblast cell line WE-cfin11f where titres and N protein levels steadily increased over 28 d post-infection at 4°C, lending further

evidence that the cellular antiviral response, including the EAPP, may be impaired in walleye at suboptimal temperatures [134]. These results also support the idea that the EAPP might be involved in the seasonal tumour development and regression cycle of WDSV, as after infecting walleye in the spring, the virus could integrate into the genome and remain latent until the late fall when temperatures have decreased sufficiently to impair regulation of endogenous antigen presentation [27, 29, 32, 34]. In this way, the virus could avoid detection by the immune system until the ability of the host to clear the infection has been compromised, allowing the virus to induce development of the dermal tumours. On the other hand, the RTHDF cell line did not appear to be permissive to VHSV IVb at 4°C at the time points examined, underscoring the potential for differences in pathogenicity of a virus in different models from different teleost species. However, VHSV subtype IVb is known to be less virulent than subtype IVa in rainbow trout *in vivo* and *in vitro*, and therefore subtype IVa or another pathogen might be better able to take advantage of the delayed inducible EAPP gene up-regulation in the RTHDF cell line and potentially *in vivo* [36, 115].

If the impaired regulation of the EAPP pathway and IFN1 at suboptimal temperatures is indicative of impaired cellular antiviral responses in rainbow trout, walleye and other teleosts, then there are a number of larger implications of this research with regards to climate change, and the recreational fishing and aquaculture industries. Firstly, global climate change will lead to increased acute exposure to suboptimal temperatures for teleosts, due to the increasing frequency and magnitude of extreme weather events such as cold snaps [5, 6, 8]. During these periods, if the antiviral responses of teleosts are compromised, they will be more susceptible to viral infection and less effective in clearing these infections. Furthermore, the same challenge will be faced by fish over the winter months, particularly in

northern climates such as Canada where the average winter water temperatures experienced by teleosts are usually less than 5°C [7, 14]. The potential for increased and persistent viral infections would be problematic for fisheries and aquaculture industries in Canada. Maintaining stable stocks of target fish populations in lakes and other water bodies is important for recreational fisheries, and over 1 billion walleye are stocked in lakes across North America for this purpose every year [18]. To ensure the survival of these stocked fish, predicted seasonal water temperatures should be considered when deciding when and where to stock fish to minimize the impact of antiviral response impairment at low temperatures. In aquaculture settings, impairments in the antiviral responses of the farmed fish at suboptimal temperatures could result in increased mortalities and/or decreased fillet quality, both of which result in economic losses for the industry and reduced food production for a constantly growing consumer population [9]. Of particular concern is the potential for persisting viral infections at low temperatures, as feed intake and specific growth rate are impaired during viral infection, and if mortalities do eventually occur, more resources have been wasted on these individuals [135]. The estimated percent mortality due to disease in aquaculture industries has been estimated to be 15%, which suggests that approximately 4 million dollars was lost in the Ontario rainbow trout aquaculture industry alone in 2015 [17, 136, 137]. While suboptimal temperatures do not account for all of this mortality directly, they can also indirectly contribute through practices such as vaccination. The results from this thesis suggest that vaccination at low temperatures may not be effective at initiating a sufficient immune response to induce immunological memory against the pathogen being vaccinated against, or alternatively that memory against the pathogen would develop over a longer time frame at a suboptimal temperature. In either case, the effectiveness of the vaccine would be

impaired at low temperatures, and this is consistent with results from bacterial vaccines in rainbow trout, as a vaccine for *Yersinia ruckerii*, the causative agent of enteric red mouth disease, conferred protection when trout were vaccinated at 15°C but not when they were vaccinated at 5°C [138]. Changes in practices to ensure fish are vaccinated at temperatures closer to their thermal optimum could increase the effectiveness of the vaccination process, thereby reducing the approximately 4 million dollars lost in the Ontario aquaculture industry annually. In addition, land-based aquaculture operations that must set and maintain water temperatures in their facilities may wish to use set temperature points that are higher than 4°C to minimize disease risks, although further research would be required to determine an ideal temperature for this purpose. Overall, the impairments in EAPP and IFN1 regulation at a cellular level, and the likely compromised antiviral response that results, could prove challenging for fishery and aquaculture industries, particularly in the face of global climate change.

Bibliography

[**1**] Q.H. Abram, B. Dixon, B.A. Katzenback, Impacts of low temperature on the teleost immune system, Biol (Basel) 6(4) (2017).
[**2**] T.J. Bowden, Modulation of the immune system of fish by their environment, Fish Shellfish Immunol 25(4) (2008) 373-383.
[**3**] C. Le Morvan, D. Troutaud, P. Deschaux, Differential effects of temperature on specific and nonspecific immune defences in fish, J Exp Biol 201(Pt 2) (1998) 165-168.
[**4**] M. Marcos-Lopez, P. Gale, B.C. Oidtmann, E.J. Peeler, Assessing the impact of climate change on disease emergence in freshwater fish in the United Kingdom, Transbound Emerg Dis 57(5) (2010) 293-304.
[**5**] Managing the risks of extreme events and disasters to advance climate change adaptation, I.P.C.C. Cambridge University Press, Cambridge, UK, 2012.
[**6**] H. Hengeveld, B. Whitewood, A. Fergusson, An introduction to climate change: A Canadian perspective, 2005. https://www.cip-icu.ca/Files/Resources/ANINTROENGLISH_EC.
[**7**] C.P. Madenjian, T.A. Hayden, T.B. Peat, C.S. Vandergoot, D.G. Fielder, A.M. Gorman, S.A. Pothoven, J.M. Dettmers, S.J. Cooke, Y.M. Zhao, C.C. Krueger, Temperature regimes, growth, and food consumption for female and male adult walleye in Lake Huron and Lake Erie: a bioenergetics analysis, Can J Fish Aquat Sci 75(10) (2018) 1573-1586.
[**8**] M.P. Tingley, P. Huybers, Recent temperature extremes at high northern latitudes unprecedented in the past 600 years, Nature 496(7444) (2013) 201.
[**9**] FAO, The State of World Fisheries and Aquaculture 2016: Contributing to food security and nutrition for all, (2016).
[**10**] R.R. Betancur, R.E. Broughton, E.O. Wiley, K. Carpenter, J.A. Lopez, C. Li, N.I. Holcroft, D. Arcila, M. Sanciangco, J.C. Cureton Ii, F. Zhang, T. Buser, M.A. Campbell, J.A. Ballesteros, A. Roa-Varon, S. Willis, W.C. Borden, T. Rowley, P.C. Reneau, D.J. Hough, G. Lu, T. Grande, G. Arratia, G. Orti, The tree of life and a new classification of bony fishes, PLoS Curr 5 (2013).
[**11**] S.J. Kerr, R.E. Grant, Ecological impacts of fish introductions: Evaluating the rosk, 2000. https://www.mffp.gouv.qc.ca/faune/peche/ensemencement/Pdf/impacts-ecologiques-en.pdf (Accessed 25.02 2019).
[**12**] S.S. Hasnain, C.K. Minns, B.J. Shuter, Key ecological temperature metrics for Canadian freshwater fishes, 2010.
http://www.climateontario.ca/MNR_Publications/stdprod_088017.pdf.
[**13**] FAO, *Oncorhynchus mykiss* (Walbaum, 1972).
http://www.fao.org/fishery/culturedspecies/Oncorhynchus_mykiss/en. (Accessed 25.02 2019).
[**14**] K.E. Jain, A.P. Farrell, Influence of seasonal temperature on the repeat swimming performance of rainbow trout *Oncorhynchus mykiss*, J Exp Biol 206(Pt 20) (2003) 3569-3579.
[**15**] DFO, Farmed Trout, 2017. http://www.dfo-mpo.gc.ca/aquaculture/sector-secteur/species-especes/trout-truite-eng.htm. (Accessed 03.11 2019).
[**16**] C.A.I.A., Sustainable, Diverse, and Growing: The State of Farmed Seafood in Canada 2017, 2017. http://animalbiosciences.uoguelph.ca/aquacentre/files/misc-

factsheets/The%20State%20of%20Farmed%20Seafood%20in%20Canada%202017~Report.pdf. (Accessed 03.11 2019).
[**17**] R.D.B. Moccia, D.J., AquaStats: Ontario aquaculture production in 2016, 2017. http://animalbiosciences.uoguelph.ca/aquacentre/files/aquastats/Aquastats%202016%20-%20Ontario%20Statistics%20for%202016.pdf. (Accessed 19.01.08 2019).
[**18**] G.F. Hartman, A biological synopsis of walleye (*Sander vitreus*), Can. Manuscr. Rep. Fish Sci. (2009) 2888.
[**19**] T.B. Peat, T.A. Hayden, L.F. Gutowsky, C.S. Vandergoot, D.G. Fielder, C.P. Madenjian, K.J. Murchie, J.M. Dettmers, C.C. Krueger, S.J. Cooke, Seasonal thermal ecology of adult walleye (*Sander vitreus*) in Lake Huron and Lake Erie, J Therm Biol 53 (2015) 98-106.
[**20**] FAO, Survey of recreational fishing in Canada, 2010. http://www.dfo-mpo.gc.ca/stats/rec/can/2010/RECFISH2010_ENG.pdf.
[**21**] S. Hill, $244M ecomomic impact shows importance of Lake Erie commercial fishery, Windsor Star, Windsor, 2015.
[**22**] Z.S.H. Feiner, T.O., Environmental biology of percids, in: P.D. Kestemont, K.; Summerfelt, R.C. (Ed.), Biology and culture of percid fishes: Principles and practices, Springer2015.
[**23**] D.E. Pirhalla, S.C. Sheridan, V. Ransibrahmanakul, C.C. Lee, Assessing cold-snap and mortality events in South Florida coastal ecosystems: Development of a biological cold stress index using satellite SST and weather pattern forcing, Estuar Coast 38(6) (2015) 2310-2322.
[**24**] M. Jobling, Temperature tolerance and the final preferendudm: Rapid methods for the assessment of optimum growth temperatures, J Fish Biol 19 (1981) 439-455.
[**25**] L. Chiaramonte, D. Munson, J. Trushenski, Climate change and considerations for fish health and fish health professionals, Fisheries 41(7) (2016) 396-399.
[**26**] J.A. Guijarro, D. Cascales, A.I. Garcia-Torrico, M. Garcia-Dominguez, J. Mendez, Temperature-dependent expression of virulence genes in fish-pathogenic bacteria, Front Microbiol 6 (2015).
[**27**] J. Rovnak, S.L. Quackenbush, Walleye dermal sarcoma virus: molecular biology and oncogenesis, Viruses 2(9) (2010) 1984-1999.
[**28**] T.K. Yamamoto, R.K.; Nielsen, O., Morphological differentiation of virus-associated skin tumours of walleye (*Stizostedion vitreum* vitreum), Fish Pathol 20(361-372) (1985).
[**29**] P.R. Bowser, M.J. Wolfe, J.L. Forney, G.A. Wooster, Seasonal prevalence of skin tumors from walleye (*Stizostedion vitreum*) from Oneida Lake, New York, 24 (1988) 7.
[**30**] R.G. Getchell, G.A. Wooster, L.G. Rudstam, A.J. Van de Valk, T.E. Brooking, P.R. Bowser, Prevalence of walleye dermal sarcoma by age-class in walleyes from Oneida Lake, New York, J Aquat Anim Health 12(3) (2000) 220-223.
[**31**] R.G. Getchell, G.A. Wooster, P.R. Bowser, Resistance to walleye dermal sarcoma tumor redevelopment, J Aquat Anim Health 13(3) (2001) 228-233.
[**32**] R.G. Getchell, G.A. Wooster, P.R. Bowser, Temperature-associated regression of walleye dermal sarcoma tumors, J Aquat Anim Healt 12(3) (2000) 189-195.
[**33**] P.R. Bowser, G.A. Wooster, S.L. Quackenbush, R.N. Casey, J.W. Casey, Communications: Comparison of fall and spring tumors as inocula for experimental transmission of walleye dermal sarcoma, J Aquat Anim Health 8(1) (1996) 78-81.
[**34**] D.S. Ruelas, W.C. Greene, An Integrated Overview of HIV-1 Latency, Cell 155(3) (2013) 519-529.

[**35**] M.K. Purcell, K.J. Laing, J.R. Winton, Immunity to fish rhabdoviruses, Viruses 4(1) (2012) 140-166.
[**36**] L. Al-Hussinee, P. Huber, S. Russell, V. LePage, A. Reid, K.M. Young, E. Nagy, R.M.W. Stevenson, J.S. Lumsden, Viral haemorrhagic septicaemia virus IVb experimental infection of rainbow trout, *Oncorhynchus mykiss* (Walbaum), and fathead minnow, *Pimphales promelas* (Rafinesque), J Fish Dis 33(4) (2010) 347-360.
[**37**] B.E. Brudeseth, J. Castric, O. Evensen, Studies on pathogenesis following single and double infection with viral hemorrhagic septicemia virus and infectious hematopoietic necrosis virus in rainbow trout (*Oncorhynchus mykiss*), Vet Pathol 39(2) (2002) 180-189.
[**38**] T.B. Yamamoto, W.N.; Winton, J.R., In vitro infection of salmonid epidermal tissues by infectious hematopoietic necrosis virus and viral hemorrhagic septicemia virus, J Aquat Anim Healt 4 (1992) 231-239.
[**39**] R. Kim, M. Faisal, Comparative susceptibility of representative Great Lakes fish species to the North American viral hemorrhagic septicemia virus Sublineage IVb, Dis Aquat Organ 91(1) (2010) 23-34.
[**40**] P.J. Enzmann, M. Konrad, K. Parey, VHS in wild living fish and experimental transmission of the virus, Fish Res 17(1-2) (1993) 153-161.
[**41**] G.H. Groocockl, R.G. Getchell, G.A. Wooster, K.L. Britt, W.N. Batts, J.R. Winton, R.N. Casey, J.W. Casey, P.R. Bowser, Detection of viral hemorrhagic septicemia in round gobies in New York state (USA) waters of lake Ontario and the St. Lawrence river, Dis Aquat Organ 76(3) (2007) 187-192.
[**42**] J.S. Lumsden, B. Morrison, C. Yason, S. Russell, K. Young, A. Yazdanpanah, P. Huber, L. Al-Hussinee, D. Stone, K. Way, Mortality event in freshwater drum *Aplodinotus grunniens* from Lake Ontario, Canada, associated with viral haemorrhagic septicemia virus, type IV, Dis Aquat Organ 76(2) (2007) 99-111.
[**43**] L.M. Hawley, K.A. Garver, Stability of viral hemorrhagic septicemia virus (VHSV) in freshwater and seawater at various temperatures, Dis Aquat Organ 82(3) (2008) 171-178.
[**44**] N.T. Vo, A.W. Bender, L.E. Lee, J.S. Lumsden, N. Lorenzen, B. Dixon, N.C. Bols, Development of a walleye cell line and use to study the effects of temperature on infection by viral haemorrhagic septicaemia virus group IVb, J Fish Dis 38(2) (2015) 121-136.
[**45**] M.S. Kim, K.H. Kim, Effects of NV gene knock-out recombinant viral hemorrhagic septicemia virus (VHSV) on Mx gene expression in Epithelioma papulosum cyprini (EPC) cells and olive flounder (*Paralichthys olivaceus*), Fish Shellfish Immunol 32(3) (2012) 459-463.
[**46**] M.S. Kim, K.H. Kim, The role of viral hemorrhagic septicemia virus (VHSV) NV gene in TNF-alpha- and VHSV infection-mediated NF-kappaB activation, Fish Shellfish Immunol 34(5) (2013) 1315-1319.
[**47**] L.B. Ivashkiv, L.T. Donlin, Regulation of type I interferon responses, Nat Rev Immunol 14(1) (2014) 36-49.
[**48**] B.L. Jacobs, J.O. Langland, When two strands are better than one: the mediators and modulators of the cellular responses to double-stranded RNA, Virol 219(2) (1996) 339-349.
[**49**] C.J. Desmet, K.J. Ishii, Nucleic acid sensing at the interface between innate and adaptive immunity in vaccination, Nat Rev Immunol 12(7) (2012) 479-491.
[**50**] H. Kato, O. Takeuchi, E. Mikamo-Satoh, R. Hirai, T. Kawai, K. Matsushita, A. Hiiragi, T.S. Dermody, T. Fujita, S. Akira, Length-dependent recognition of double-stranded

ribonucleic acids by retinoic acid-inducible gene-I and melanoma differentiation-associated gene 5, J Exp Med 205(7) (2008) 1601-1610.
[**51**] T. Kawai, S. Akira, The role of pattern-recognition receptors in innate immunity: update on Toll-like receptors, Nat Immunol 11(5) (2010) 373-384.
[**52**] S.J. Poynter, S.J. DeWitte-Orr, Understanding viral dsRNA-mediated innate immune responses at the cellular level using a rainbow trout model, Front Immunol 9 (2018) 829.
[**53**] S.J. DeWitte-Orr, S.E. Collins, C.M. Bauer, D.M. Bowdish, K.L. Mossman, An accessory to the 'Trinity': SR-As are essential pathogen sensors of extracellular dsRNA, mediating entry and leading to subsequent type I IFN responses, PLoS Pathog 6(3) (2010) e1000829.
[**54**] S.J. DeWitte-Orr, D.R. Mehta, S.E. Collins, M.S. Suthar, M. Gale, Jr., K.L. Mossman, Long double-stranded RNA induces an antiviral response independent of IFN regulatory factor 3, IFN-beta promoter stimulator 1, and IFN, J Immunol 183(10) (2009) 6545-6553.
[**55**] T. Kawai, S. Akira, The role of pattern-recognition receptors in innate immunity: update on Toll-like receptors, Nat Immunol 11(5) (2010) 373-84.
[**56**] D. Pietretti, G.F. Wiegertjes, Ligand specificities of Toll-like receptors in fish: indications from infection studies, Dev Comp Immunol 43(2) (2014) 205-222.
[**57**] M. Yoneyama, T. Fujita, RNA recognition and signal transduction by RIG-I-like receptors, Immunol Rev 227(1) (2009) 54-65.
[**58**] M.S. Iordanov, J. Wong, J.C. Bell, B.E. Magun, Activation of NF-kappaB by double-stranded RNA (dsRNA) in the absence of protein kinase R and RNase L demonstrates the existence of two separate dsRNA-triggered antiviral programs, Mol Cell Biol 21(1) (2001) 61-72.
[**59**] S. Chattopadhyay, G.C. Sen, dsRNA-activation of TLR3 and RLR signaling: gene induction-dependent and independent effects, J Interferon Cytokine Res 34(6) (2014) 427-436.
[**60**] L.M. Pfeffer, The role of nuclear factor kappaB in the interferon response, J Interferon Cytokine Res 31(7) (2011) 553-559.
[**61**] G.C. Sen, S.N. Sarkar, Transcriptional signaling by double-stranded RNA: role of TLR3, Cytokine Growth Factor Rev 16(1) (2005) 1-14.
[**62**] I. Rusinova, S. Forster, S. Yu, A. Kannan, M. Masse, H. Cumming, R. Chapman, P.J. Hertzog, Interferome v2.0: an updated database of annotated interferon-regulated genes, Nucleic Acids Res 41(Database issue) (2013) D1040-1046.
[**63**] S. Goodbourn, L. Didcock, R.E. Randall, Interferons: cell signalling, immune modulation, antiviral responses and virus countermeasures, J Gel Virol 81 (2000) 2341-2364.
[**64**] S.J. Poynter, A.L. Monjo, S.J. DeWitte-Orr, Identification of three class A scavenger receptors from rainbow trout (*Oncorhynchus mykiss*): SCARA3, SCARA4, and SCARA5, Fish Shellfish Immunol 76 (2018) 121-125.
[**65**] S.J. Poynter, J. Weleff, A.B. Soares, S.J. DeWitte-Orr, Class-A scavenger receptor function and expression in the rainbow trout (*Oncorhynchus mykiss*) epithelial cell lines RTgutGC and RTgill-W1, Fish Shellfish Immunol 44(1) (2015) 138-146.
[**66**] S.L. Semple, N.T.K. Vo, S.J. Poynter, M. Li, D.D. Heath, S.J. DeWitte-Orr, B. Dixon, Extracellular dsRNA induces a type I interferon response mediated via class A scavenger receptors in a novel Chinook salmon derived spleen cell line, Dev Comp Immunol 89 (2018) 93-101.

[**67**] A. Matsuo, H. Oshiumi, T. Tsujita, H. Mitani, H. Kasai, M. Yoshimizu, M. Matsumoto, T. Seya, Teleost TLR22 recognizes RNA duplex to induce IFN and protect cells from birnaviruses, J Immunol 181(5) (2008) 3474-3485.
[**68**] S. Poynter, G. Lisser, A. Monjo, S. DeWitte-Orr, Sensors of infection: viral nucleic acid PRRs in fish, Biol 4(3) (2015) 460-493.
[**69**] M. Samanta, M. Basu, B. Swain, P. Panda, P. Jayasankar, Molecular cloning and characterization of Toll-like receptor 3, and inductive expression analysis of type I IFN, Mx and pro-inflammatory cytokines in the Indian carp, rohu (*Labeo rohita*), Mol Biol Rep 40(1) (2013) 225-235.
[**70**] Z.X. Zhou, B.C. Zhang, L. Sun, Poly(I:C) induces antiviral immune responses in Japanese flounder (*Paralichthys olivaceus*) that require TLR3 and MDA5 and is negatively regulated by Myd88, PLoS One 9(11) (2014) e112918.
[**71**] M. Chang, B. Collet, P. Nie, K. Lester, S. Campbell, C.J. Secombes, J. Zou, Expression and functional characterization of the RIG-I-like receptors MDA5 and LGP2 in Rainbow trout (*Oncorhynchus mykiss*), J Virol 85(16) (2011) 8403-8412.
[**72**] F. Sun, Y.B. Zhang, T.K. Liu, L. Gan, F.F. Yu, Y. Liu, J.F. Gui, Characterization of fish IRF3 as an IFN-inducible protein reveals evolving regulation of IFN response in vertebrates, J Immunol 185(12) (2010) 7573-7582.
[**73**] J. Zou, B. Gorgoglione, N.G. Taylor, T. Summathed, P.T. Lee, A. Panigrahi, C. Genet, Y.M. Chen, T.Y. Chen, M. Ul Hassan, S.M. Mughal, P. Boudinot, C.J. Secombes, Salmonids have an extraordinary complex type I IFN system: characterization of the IFN locus in rainbow trout *Oncorhynchus mykiss* reveals two novel IFN subgroups, J Immunol 193(5) (2014) 2273-2286.
[**74**] M.X. Chang, P. Nie, B. Collet, C.J. Secombes, J. Zou, Identification of an additional two-cysteine containing type I interferon in rainbow trout *Oncorhynchus mykiss* provides evidence of a major gene duplication event within this gene family in teleosts, Immunogenetics 61(4) (2009) 315-325.
[**75**] M.K. Purcell, K.J. Laing, J.C. Woodson, G.H. Thorgaard, J.D. Hansen, Characterization of the interferon genes in homozygous rainbow trout reveals two novel genes, alternate splicing and differential regulation of duplicated genes, Fish Shellfish Immunol 26(2) (2009) 293-304.
[**76**] J. Zou, C. Tafalla, J. Truckle, C.J. Secombes, Identification of a second group of type I IFNs in fish sheds light on IFN evolution in vertebrates, J Immunol 179(6) (2007) 3859-3871.
[**77**] S.J. Poynter, S.J. DeWitte-Orr, Length-dependent innate antiviral effects of double-stranded RNA in the rainbow trout (*Oncorhynchus mykiss*) cell line, RTG-2, Fish Shellfish Immunol 46(2) (2015) 557-565.
[**78**] C. Langevin, E. Aleksejeva, G. Passoni, N. Palha, J.P. Levraud, P. Boudinot, The antiviral innate immune response in fish: evolution and conservation of the IFN system, J Mol Biol 425(24) (2013) 4904-4920.
[**79**] J.C. Leong, G.D. Trobridge, C.H. Kim, M. Johnson, B. Simon, Interferon-inducible Mx proteins in fish, Immunol Rev 166 (1998) 349-363.
[**80**] S.J. Poynter, S.J. DeWitte-Orr, Fish interferon-stimulated genes: The antiviral effectors, Dev Comp Immunol 65 (2016) 218-225.

[**81**] G.D. Trobridge, P.P. Chiou, J.A. Leong, Cloning of the rainbow trout (*Oncorhynchus mykiss*) Mx2 and Mx3 cDNAs and characterization of trout Mx protein expression in salmon cells, J Virol 71(7) (1997) 5304-5311.
[**82**] K. Turan, M. Mibayashi, K. Sugiyama, S. Saito, A. Numajiri, K. Nagata, Nuclear MxA proteins form a complex with influenza virus NP and inhibit the transcription of the engineered influenza virus genome, Nucleic Acids Res 32(2) (2004) 643-652.
[**83**] Y.C. Wu, Y.F. Lu, S.C. Chi, Anti-viral mechanism of barramundi Mx against betanodavirus involves the inhibition of viral RNA synthesis through the interference of RdRp, Fish Shellfish Immunol 28(3) (2010) 467-475.
[**84**] P.A. Wearsch, P. Cresswell, The quality control of MHC class I peptide loading, Curr Opin Cell Biol 20(6) (2008) 624-631.
[**85**] D.C. Chapman, D.B. Williams, ER quality control in the biogenesis of MHC class I molecules, Semin Cell Dev Biol 21(5) (2010) 512-519.
[**86**] D.R. Peaper, P. Cresswell, Regulation of MHC class I assembly and peptide binding, Annu Rev Cell Dev Biol 24 (2008) 343-368.
[**87**] M. Barry, R.C. Bleackley, Cytotoxic T lymphocytes: all roads lead to death, Nat Rev Immunol 2(6) (2002) 401-419.
[**88**] R.J. Stet, C.P. Kruiswijk, B. Dixon, Major histocompatability lineages and immune gene function in teleost fishes: The road not taken, Crit Rev Immunol 23 (2003) 441-471.
[**89**] K. Fujiki, M. Booman, E. Chin-Dixon, B. Dixon, Cloning and characterization of cDNA clones encoding membrane-bound and potentially secreted major histocompatibility class I receptors from walleye (*Stizostedion vitreum*), Immunogenetics 53(9) (2001) 760-769.
[**90**] U. Grimholt, MHC and Evolution in Teleosts, Biology (Basel) 5(1) (2016).
[**91**] K. Aoyagi, J.M. Dijkstra, C. Xia, I. Denda, M. Ototake, K. Hashimoto, T. Nakanishi, Classical MHC class I genes composed of highly divergent sequence lineages share a single locus in rainbow trout (*Oncorhynchus mykiss*), J Immunol 168(1) (2002) 260-273.
[**92**] D. Christie, G. Wei, K. Fujiki, B. Dixon, Cloning and characterization of a cDNA encoding walleye (*Sander vitreum*) beta-2 microglobulin, Fish Shellfish Immunol 22(6) (2007) 727-733.
[**93**] S. Kales, K. Fujiki, B. Dixon, Molecular cloning and characterization of calreticulin from rainbow trout (*Oncorhynchus mykiss*), Immunogenetics 55(10) (2004) 717-723.
[**94**] B.A. Katzenback, C.J.; Dixon, B., Unpublished.
[**95**] E.D. Landis, Y. Palti, J. Dekoning, R. Drew, R.B. Phillips, J.D. Hansen, Identification and regulatory analysis of rainbow trout tapasin and tapasin-related genes, Immunogenetics 58(1) (2006) 56-69.
[**96**] K.E. Magor, B.P. Shum, P. Parham, The beta 2-microglobulin locus of rainbow trout (*Oncorhynchus mykiss*) contains three polymorphic genes, J Immunol 172(6) (2004) 3635-3643.
[**97**] L. Sever, N.C. Bols, B. Dixon, The cloning and inducible expression of the rainbow trout ERp57 gene, Fish Shellfish Immunol 34(2) (2013) 410-419.
[**98**] L. Sever, N.T. Vo, N.C. Bols, B. Dixon, Rainbow trout (*Oncorhynchus mykiss*) contain two calnexin genes which encode distinct proteins, Dev Comp Immunol 42(2) (2014) 211-219.
[**99**] W. Chen, Z. Jia, T. Zhang, N. Zhang, C. Lin, F. Gao, L. Wang, X. Li, Y. Jiang, X. Li, G.F. Gao, C. Xia, MHC class I presentation and regulation by IFN in bony fish determined by molecular analysis of the class I locus in grass carp, J Immunol 185(4) (2010) 2209-2221.

[**100**] L. Sever, N.T.K. Vo, J. Lumsden, N.C. Bols, B. Dixon, Induction of rainbow trout MH class I and accessory proteins by viral haemorrhagic septicaemia virus, Mol Immunol 59(2) (2014) 154-162.
[**101**] H.G. Ljunggren, N.J. Stam, C. Ohlen, J.J. Neefjes, P. Hoglund, M.T. Heemels, J. Bastin, T.N. Schumacher, A. Townsend, K. Karre, et al., Empty MHC class I molecules come out in the cold, Nature 346(6283) (1990) 476-480.
[**102**] P.N. Rodrigues, B. Dixon, J. Roelofs, J.H. Rombout, E. Egberts, B. Pohajdak, R.J. Stet, Expression and temperature-dependent regulation of the beta2-microglobulin (Cyca-B2m) gene in a cold-blooded vertebrate, the common carp (*Cyprinus carpio* L.), Dev Immunol 5(4) (1998) 263-275.
[**103**] S. Kales, J. Parks-Dely, P. Schulte, B. Dixon, Beta-2-microglobulin gene expression is maintained in rainbow trout and Atlantic salmon kept at low temperatures, Fish Shellfish Immunol 21(2) (2006) 176-186.
[**104**] H.C. Ingerslev, C.G. Ossum, T. Lindenstrom, M.E. Nielsen, Fibroblasts express immune relevant genes and are important sentinel cells during tissue damage in rainbow trout (*Oncorhynchus mykiss*), Plos One 5(2) (2010).
[**105**] C.G. Ossum, E.K. Hoffmann, M.M. Vijayan, S.E. Holt, N.C. Bols, Characterization of a novel fibroblast-like cell line from rainbow trout and responses to sublethal anoxia, J Fish Biol 64(4) (2004) 1103-1116.
[**106**] J. Winton, W. Batts, P. deKinkelin, M. LeBerre, M. Bremont, N. Fijan, Current lineages of the epithelioma papulosum cyprini (EPC) cell line are contaminated with fathead minnow, *Pimephales promelas*, cells, J Fish Dis 33 (2010) 701-704.
[**107**] A.T.C.C., ATCC Virology Guide, 2012.
[**108**] P.H. Pham, J. Jung, N.C. Bols, Using 96-well tissue culture polystyrene plates and a fluorescent plate reader as tools to study the survival and inactivation of viruses on surfaces, Cytotechnology 63 (2011) 385-397.
[**109**] M.R. Sambrook, J. Green, Molecular Cloning, Cold Spring Harbor Laboratory Press2012.
[**110**] S.F. Altschul, W. Gish, W. Miller, E.W. Myers, D.J. Lipman, Basic local alignment search tool, J Mol Biol 215(3) (1990) 403-410.
[**111**] S.M. Jørgensen, D.L. Hetland, C.M. Press, U. Grimholt, T. Gjøen, Effect of early infectious salmon anaemia virus (ISAV) infection on expression of MHC pathway genes and type I and II interferon in Atlantic salmon (*Salmo salar* L.) tissues, Fish & Shellfish Immunology 23(3) (2007) 576-588.
[**112**] E. Chaves-Pozo, J. Zou, C.J. Secombes, A. Cuesta, C. Tafalla, The rainbow trout (*Oncorhynchus mykiss*) interferon response in the ovary, Mol Immunol 47(9) (2010) 1757-1764.
[**113**] S. Taylor, M. Wakem, G. Dijkman, M. Alsarraj, M. Nguyen, A practical approach to RT-qPCR-Publishing data that conform to the MIQE guidelines, Methods 50(4) (2010) S1-S5.
[**114**] N.O. Lorenzen, N.J.; Jorgensen, P.E.V.;, Production and characterization of monoclonal antibodies to four Egtved virus structural proteins, Dis Aquat Organ 4 (1988) 35-42.
[**115**] P.H. Pham, J.S. Lumsden, C. Tafalla, B. Dixon, N.C. Bols, Differential effects of viral hemorrhagic septicaemia virus (VHSV) genotypes IVa and IVb on gill epithelial and spleen

macrophage cell lines from rainbow trout (*Oncorhynchus mykiss*), Fish Shellfish Immunol 34(2) (2013) 632-640.
[**116**] M.V. Matz, R.M. Wright, J.G. Scott, No control genes required: Bayesian analysis of qRT-PCR data, PLoS One 8(8) (2013) e71448.
[**117**] S.L. Semple, N.T.K. Vo, A.R. Li, P.H. Pham, N.C. Bols, B. Dixon, Development and use of an Arctic charr cell line to study antiviral responses at extremely low temperatures, J Fish Dis 40(10) (2017) 1423-1439.
[**118**] S. Larsson, Thermal preference of Arctic charr, *Salvelinus alpinus*, and brown trout, *Salmo trutta* – implications for their niche segregation, Environ Biol Fish 73(1) (2005) 89-96.
[**119**] T.K.G. Pitt, E.T.; Hepburn, R.L.;, Temperature selection of the carp (*Cyprinus carpio Linn.*), Can Soc Zoo 34(6) (1956) 555-557.
[**120**] S.M. Jorgensen, B.L. Syvertsen, M. Lukacs, U. Grimholt, T. Gjoen, Expression of MHC class I pathway genes in response to infectious salmon anaemia virus in Atlantic salmon (*Salmo salar* L.) cells, Fish Shellfish Immunol 21(5) (2006) 548-560.
[**121**] U. Grimholt, Whole genome duplications have provided teleosts with many roads to peptide loaded MHC class I molecules, BMC Evol Biol 18(1) (2018) 25.
[**122**] S.M. Glasauer, S.C. Neuhauss, Whole-genome duplication in teleost fishes and its evolutionary consequences, Mol Genet Genomics 289(6) (2014) 1045-1060.
[**123**] I. Salinas, K. Lockhart, T.J. Bowden, B. Collet, C.J. Secombes, A.E. Ellis, An assessment of immunostimulants as Mx inducers in Atlantic salmon (*Salmo salar* L.) parr and the effect of temperature on the kinetics of Mx responses, Fish Shellfish Immunol 17(2) (2004) 159-170.
[**124**] L.A. Byk, N.G. Iglesias, F.A. De Maio, L.G. Gebhard, M. Rossi, A.V. Gamarnik, Dengue virus genome uncoating requires ubiquitination, MBio 7(3) (2016).
[**125**] N.T. Vo, A.W. Bender, J.S. Lumsden, B. Dixon, N.C. Bols, Differential viral haemorrhagic septicaemia virus genotype IVb infection in fin fibroblast and epithelial cell lines from walleye, *Sander vitreus* (Mitchill), at cold temperatures, J Fish Dis 39(2) (2016) 175-188.
[**126**] E. Lorenzen, B. Carstensen, N.J. Olesen, Inter-laboratory comparison of cell lines for susceptibility to three viruses: VHSV, IHNV and IPNV, Dis Aquat Org 37(2) (1999) 81-88.
[**127**] DFO, Data from BC lightstations. http://www.pac.dfo-mpo.gc.ca/science/oceans/data-donnees/lightstations-phares/index-eng.html. (Accessed 03.06 2019).
[**128**] J.D. Reist, F.J. Wrona, T.D. Prowse, M. Power, J.B. Dempson, J.R. King, R.J. Beamish, An overview of effects of climate change on selected arctic freshwater and anadromous fishes, Ambio 35(7) (2006) 381-387.
[**129**] M.A. Sheridan, Regulation of Lipid-Metabolism in Poikilothermic Vertebrates, Comp Biochem Phys B 107(4) (1994) 495-508.
[**130**] G.D. Maniero, C. Carey, Changes in selected aspects of immune function in the leopard frog, *Rana pipiens*, associated with exposure to cold, J Comp Physiol B 167(4) (1997) 256-263.
[**131**] S. Rojas, K. Richards, J.K. Jancovich, E.W. Davidson, Influence of temperature on Ranavirus infection in larval salamanders *Ambystoma tigrinum*, Dis Aquat Org 63(2-3) (2005) 95-100.
[**132**] D.A. Cortes, A.P.R. Zuniga, R.E. Sais, J.S.M. Castaneda, C.O. Santana, Effect of temperature on the expression of IFN-1 (alpha), STAT-1 and Mx-1 genes in *Oncorhynchus*

mykiss (Salmoniformes: Salmonidae) exposed with the virus of the infectious pancreatic necrosis (IPNV), Rev Biol Trop 63(2) (2015) 559-569.
[**133**] N.A. Prow, B. Tang, J. Gardner, T.T. Le, A. Taylor, Y.S. Poo, E. Nakayama, T.D.C. Hirata, H.I. Nakaya, A. Slonchak, P. Mukhopadhyay, S. Mahalingam, W.A. Schroder, W. Klimstra, A. Suhrbier, Lower temperatures reduce type I interferon activity and promote alphaviral arthritis, Plos Pathogens 13(12) (2017).
[**134**] N.T. Vo, A.W. Bender, D.A. Ammendolia, J.S. Lumsden, B. Dixon, N.C. Bols, Development of a walleye spleen stromal cell line sensitive to viral hemorrhagic septicemia virus (VHSV IVb) and to protection by synthetic dsRNA, Fish Shellfish Immunol 45(1) (2015) 83-93.
[**135**] B. Damsgard, A. Mortensen, A.I. Sommer, Effects of infectious pancreatic necrosis virus (IPNV) on appetite and growth in Atlantic salmon, *Salmo salar* L, Aquaculture 163(3-4) (1998) 185-193.
[**136**] T.L.F. Leung, A.E. Bates, More rapid and severe disease outbreaks for aquaculture at the tropics: Implications for food security, J Appl Ecol 50 (2013) 215-222.
[**137**] M. Taveras-Dias, M.L. Martins, An overall estimation of losses caused by diseases in the Brazilian fish farms, 41 (2017) 913-918.
[**138**] M.K. Raida, K. Buchmann, Bath vaccination of rainbow trout (*Oncorhynchus mykiss* Walbaum) against *Yersinia ruckeri*: effects of temperature on protection and gene expression, Vaccine 26 (2008) 1050-1062.

Appendix A: Supplementary Figures

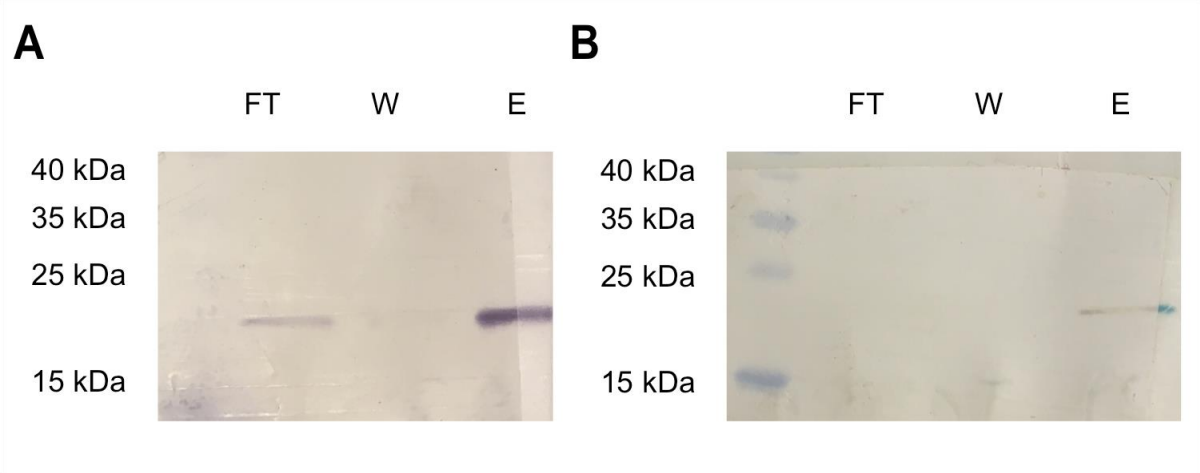

Supplemental Figure S1. Validation of purification of recombinant rainbow trout IFN1. Following nickel column-affinity chromatography, 20 µL of the initial flow-through (FT), the final wash (W), and the eluted protein (E) were loaded and run on duplicate SDS-PAGE gels. After being transferred onto nitrocellulose membranes, the blots were probed with mouse α-polyHis (A), diluted 1:6000 in TBS-T with 5% skim milk, and rabbit anti-rainbow trout IFN1 (B), conjugated to HRP and diluted 1:500 in TBS-T with 5% skim milk, respectively. (A) The blot was then probed with anti-mouse IgG conjugated to alkaline phosphatase that was diluted 1:30000 in TBS-T with 5% skim milk, and bands were detected using alkaline phosphatase detection solution (1.7 mM nitro blue tetrazolium chloride, 3.5 mM 5-bromo-4-chloro-3-indoyl-phosphate). (B) Bands were detected with TMB-sens Elispot substrate (Cedarlane).

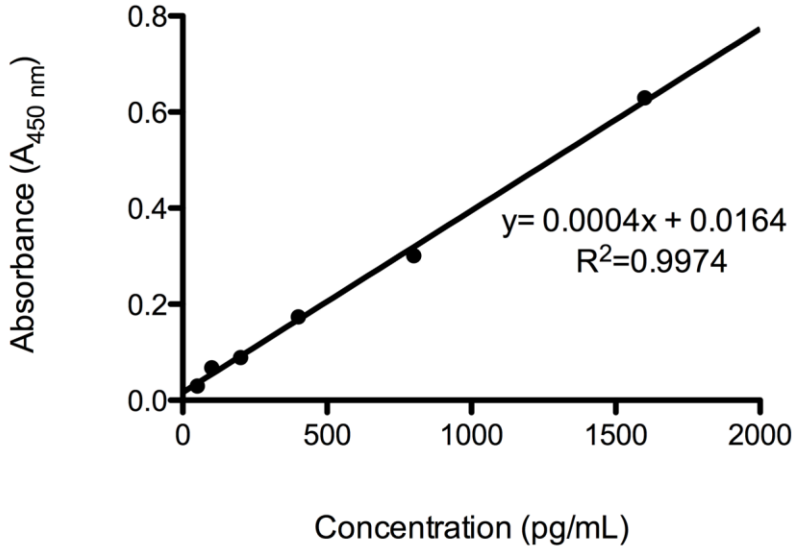

Supplemental Figure S2. Standard curve of recombinant rainbow trout IFN1 on qELISA. A serial doubling dilution from 3200 pg/mL to 50 pg/mL of recombinant rainbow trout IFN1 was performed, and each dilution was then run in triplicate on a qELISA. Average absorbance values for each concentration are shown with standard deviation. A linear regression was performed, and the equation of the resulting line is shown with the corresponding R^2 value.